The AAA-ATPase p97 and its cofactors in regulatory degradation of substrate proteins after DNA damage or replication stress

Inaugural-Dissertation
zur
Erlangung des Doktorgrades

Dr. rer. nat.

der Fakultät für
Biologie

an der

Universität Duisburg-Essen

vorgelegt von

Alina Dressler
aus Bochum
April 2016

Die der vorliegenden Arbeit zugrunde liegenden Experimente wurden am Lehrstuhl für Molekularbiologie I am Zentrum für Medizinische Biotechnologie der Universität Duisburg-Essen bzw. am Institut für medizinische Strahlenbiologie des Universitätsklinikums Essen durchgeführt.

1. Gutachter: Prof. Dr. Hemmo Meyer

2. Gutachter: Prof. Dr. Georg Iliakis

Vorsitzender des Prüfungsausschusses: Prof. Dr. Stefan Westermann

Tag der mündlichen Prüfung: 19.08.2016

Table of contents

List of Figures

List of Tables

Abbreviations

6-4PPs	6-4photoproducts
βTrCP	beta-transducin repeat containing protein
γH2AX	H2A histone family, member X, phosphorylated
AAA	ATPases associated with diverse cellular activities
ADP	adenosine diphosphate
ALS	amyotrophic lateral sclerosis
APC/C	anaphase promoting complex/cyclosome
APH	aphidicolin
ATM	ataxia-telangiectasia-mutated
ATP	adenosine triphosphate
ATR	ataxia-telangiectasia-mutated and Rad3-related
BCA	bicinchoninic acid
BrdU	5-bromo-2’-deoxyuridine
BS1	binding site 1
BSA	bovine serum albumin
CDC25	cell division cycle 25
CDC25A	cell division cycle 25, type A
CDC25B	cell division cycle 25, type B
CDC25C	cell division cycle 25, type C
Cdc48	cell division cycle 48 (yeast p97)
CDC-48	cell division cycle 48 (worm p97)
CDK	cyclin-dependent kinase
CDT1	chromatin licensing and DNA replication factor 1
CDT2	chromatin licensing and DNA replication factor 2
Chk1	checkpoint kinase 1
Chk2	checkpoint kinase 2
CHX	cycloheximide
CMG	CDC45, Mcm2-7, GINS
CPDs	cyclobutane pyrimidine dimers
CRL	cullin-RING ligase
CSA	Cockayne syndrome complementary group A
CSB	Cockayne syndrome complementary group B
Ctrl	control
CUL	cullin
DAPI	4',6-diamidino-2-phenylindole

DBeQ	N^2, N^4-dibenzylquinazoline-2,4-diamine
DDB1	DNA damage binding protein 1
DDB2	DNA damage binding protein 2
DDR	DNA damage response
DMEM	Dulbecco's Modified Eagle Medium
DMSO	dimethyl sulfoxide
DNA	deoxyribonucleic acid
dNTP	deoxyribonucleotide
DSB	double-strand break
DUB	deubiquitinating enzyme
DVC1	DNA damage-targeting VCP/p97 adaptor C1orf124
EerI	eeyarestatin I
EM	electron microscopy
ER	endoplasmic reticulum
ERAD	ER-associated degradation
FA	Fanconi anemia
FAF1	FAS-associated factor 1
FBS	fetal bovine serum
FRT	Flp recombination target
GAPDH	glyceraldehyde 3-phosphate dehydrogenase
GFP	green fluorescent protein
GG-NER	global genome NER
GINS	SLD-5, PSF-1, PSF-2, PSF-3
HA	human influenza hemagglutinin
HCT116	human colon cancer cells
HECT	homologous to the E6-AP C-terminus
HeLa	Henrietta Lacks human cervical carcinoma cell line
HIF1α	hypoxia inducible factor 1 alpha
HR	homologous recombination
HRP	horseradish peroxidase
IBMPFD	Inclusion body myopathy associated with Paget's disease of bone and frontotemporal dementia
IC50	half maximal inhibitory concentration
ID	FANCI/FANCD2
IκBα	NF-κB inhibitor alpha
IR	ionizing radiation
LB	lysogeny broth

luc	luciferase
MCM	minichromosome maintenance
MTS	3-(4,5-dimethylthiazol-2-yl)-5-(3-carboxymethoxyphenyl)-2-(4-sulfophenyl)-2H-tetrazolium
NEDD8	neural precursor cell expressed, developmentally down-regulated 8
NEM	N-ethylmaleimide
NER	nucleotide excision repair
NF-κB	nuclear factor kappa-light-chain-enhancer of activated B-cells
NHEJ	non-homologous end-joining
Npl4	nuclear protein localization 4
NZF	Npl4 zinc finger
ORC	origin recognition complex
PBS	phosphate buffered saline
PBS-T	PBS with Tween 20
PCNA	proliferating cell nuclear antigen
PCR	polymerase chain reaction
RDS	radioresistant DNA synthesis
PEI	polyethylenimine
PFA	(para-)formaldehyde
PI	propidium iodide
PIP	PCNA-interacting protein motif
PLK1	polo-like kinase 1
Pol	polymerase
PSMB5	proteasome subunit beta type-5
Rbx1	RING-box protein 1
RING	really interesting new gene
RNA	ribonucleic acid
RNAi	RNA interference
RPA	replication protein A
Rpb1	RNA polymerase II, subunit b1
SCF	Skp1-Cul1-F-box
s.d.	standard deviation
SDS	sodium dodecyl sulfate
SDS-PAGE	sodium dodecyl sulfate polyacrylamide gel electrophoresis
SIM	SUMO-interacting motif
siRNA	small interfering RNA

Skp1	S phase kinase associated protein 1
SOC	super optimal broth
SUMO	small ubiquitin-like modifier
TAE	Tris/acetic acid/EDTA
TC-NER	transcription-coupled NER
TLS	translesion synthesis
TNFα	tumor necrosis factor alpha
TO	Tet-On
Tub	alpha-tubulin
U2OS	human osteosarcoma cell line
UAS	ubiquitin-associating
Ub	ubiquitin
UBA	ubiquitin-associated
UBX	ubiquitin regulatory X
Ubx5	yeast UBXD7
UBXD7	UBX domain-containing protein 7
UBXD8	UBX domain-containing protein 8
UBX-L	UBX-like
UBZ	ubiquitin-binding zinc finger
Ufd1	ubiquitin fusion degradation 1 protein
UIM	ubiquitin-interacting motif
UT3	Ufd1 truncation 3
UV	ultraviolet
VCP	valosin-containing protein
VHL	von-Hippel-Landau
WEE1	WEE1-like protein kinase
Wss1	weak suppressor of smt3-331
XPC	xeroderma pigmentosum group C

Abstract

The cellular response to radiation is governed by a complex signaling network that is regulated by the ubiquitin-proteasome system in multiple ways. The AAA-type ATPase p97 (also known as VCP or Cdc48) has emerged as a central element of the ubiquitin-proteasome system as it facilitates the degradation of critical substrate proteins by the proteasome. As such, it is involved in replication stress and DNA damage responses, and is currently explored as a cancer drug target in clinical trials. However, its function is still poorly understood. p97 cooperates with protein cofactors, three of which have been linked to the radiation response: the heterodimeric Ufd1-Npl4 ubiquitin adapter, DVC1 and UBXD7 that acts as an adapter to cullin-RING ubiquitin ligases (CRLs).

This work provides insight into three different aspects of the role of p97 and its cofactors in the response to replication stress and DNA damage in human cells. First, we investigated the relevance of p97 for DNA damage checkpoints. Second, we examined the significance of p97 and its cofactors for survival of human cancer cells after replication stress. Third, we explored the role of a novel p97 cofactor, UBXD7 that was linked to DNA-related functions of p97. Analyses of the G1/S and intra S checkpoints showed that $p97^{Ufd1\text{-}Npl4}$ may only play a minor role in these checkpoints. However, DVC1 is crucial for the intra S checkpoint. Importantly, work from this study contributed to demonstrating that the $p97^{Ufd1\text{-}Npl4}$ complex ensures robustness of the G2/M checkpoint by facilitating the degradation of the phosphatase CDC25A (published in Riemer et al, 2014). This study confirmed the relevant target protein of p97, CDC25A, in the checkpoint and contributed to the identification of the cofactors involved in CDC25A degradation, including the novel p97 cofactor UBXD7. Moreover, we could demonstrate that in mammalian cells, unrepaired DNA damage from interphase manifests in mitotic segregation errors in cells depleted of $p97^{Ufd1\text{-}Npl4}$ and that the lack of either of these components decreased cell survival after replication stress. Furthermore, p97 inhibition with the inhibitor NMS-873 showed a synergistic effect with the genotoxic chemotherapeutic agent doxorubicin. Additionally, NMS-873 was able to delay the degradation of CDC25A in the DNA damage response. Finally, by investigating the significance of UBXD7 for diverse p97 substrate proteins, we found that UBXD7 is not generally involved in CRL- and p97-dependent degradation both in the nucleus and the cytoplasm. Moreover, a detailed structure-function analysis revealed that binding to CRLs and p97 is essential for UBXD7 function.

Zusammenfassung

Die zelluläre Strahlenantwort wird von einem komplexen Signalnetzwerk gesteuert, das auf vielfältige Weise vom Ubiquitin-Proteasom-System reguliert wird. Ein zentrales Element des Ubiquitin-Proteasom-Systems stellt die AAA-ATPase p97 (auch bekannt als VCP oder Cdc48) dar, welche die Degradation von kritischen Substratproteinen durch das Proteasom unterstützt. p97 ist involviert in die zelluläre Reaktion auf Replikationsstress und DNA-Schäden und wird gegenwärtig als Wirkstoffziel für Krebsmedikamente in klinischen Studien erforscht. Dennoch ist seine Funktion noch wenig verstanden. p97 kooperiert mit Protein-Kofaktoren, von denen drei mit der zellulären Strahlenantwort in Verbindung gebracht wurden: der heterodimere Ufd1-Npl4-Ubiquitin-Adapter, DVC1 und UBXD7, welches als Adapter für Cullin-RING-Ubiquitin-Ligasen (CRLs) fungiert.

Diese Arbeit bietet Einblick in drei verschiedene Aspekte der Rolle von p97 und seinen Kofaktoren in der Reaktion auf Replikationsstress und DNA-Schäden in menschlichen Zellen. Zunächst wurde die Relevanz von p97 für die Zellzyklus-Kontrollpunkte untersucht. Danach wurde die Bedeutung von p97 und seinen Kofaktoren für das Überleben humaner Krebszellen nach Replikationsstress überprüft. Schließlich wurde der neue p97-Kofaktor UBXD7, der mit Funktionen in Bezug auf DNA in Verbindung gebracht wurde, untersucht. Analysen des G1/S- und des intra-S-Kontrollpunkts haben gezeigt, dass $p97^{Ufd1\text{-}Npl4}$ möglicherweise eine untergeordnete Rolle in diesen Kontrollpunkten spielt. DVC1 jedoch ist entscheidend für den intra-S-Kontrollpunkt. Arbeiten dieser Studie haben zu dem Nachweis beigetragen, dass der $p97^{Ufd1\text{-}Npl4}$-Komplex die Robustheit des G2/M-Kontrollpunkts gewährleistet, indem er die Degradation der Phosphatase CDC25A unterstützt (publiziert in Riemer et al, 2014). Diese Arbeit bestätigt CDC25A als das relevante Zielprotein von p97 im Kontrollpunkt und trug zur Identifikation der an der CDC25A-Degradation beteiligten Kofaktoren bei, einschließlich des neuen p97-Kofaktors UBXD7. Darüber hinaus konnte gezeigt werden, dass sich in Säugerzellen mit herunterreguliertem $p97^{Ufd1\text{-}Npl4}$ unreparierte DNA-Schäden aus der Interphase in der Mitose in Segregationsdefekten manifestieren. Zudem minderte der Mangel an einer dieser Komponenten das Überleben der Zellen nach Replikationsstress. Darüber hinaus wies p97-Inhibition mit dem Inhibitor NMS-873 einen synergistischen Effekt mit dem genotoxischen Chemotherapeutikum Doxorubicin auf. Zusätzlich verzögerte NMS-873 die Degradation von CDC25A in der DNA-Schadenantwort. Durch die Erforschung der Relevanz von UBXD7 für diverse p97-Substratproteine konnte schließlich gezeigt werden, dass UBXD7 nicht generell in CRL- und p97-abhängigem Abbau im Nukleus und Zytoplasma involviert ist. Eine

detaillierte Struktur-Funktionsanalyse hat ergeben, dass die Bindung an CRLs und p97 für die Funktion von UBXD7 essentiell ist.

1 Introduction

1.1 The mammalian cell cycle

The cell cycle or cell division cycle is defined as the sequence of events in a cell that leads to faithful transmission of the whole genetic material to two daughter cells. In mammalian cells, the cell cycle is divided into G1, S, G2 and M phase. During G1, the cell grows and prepares for DNA duplication, which takes place in S phase. In G2, the cell accumulates nutrients and arranges for cell division which finally happens during M phase. Timely and accurate cell cycle progression is controlled by cyclins and cyclin-dependent kinases (CDKs), which belong to the family of serine/threonine kinases. The catalytic activity of CDKs is triggered by complex formation with a cyclin. Upon cyclin binding, CDKs phosphorylate and thereby activate or inactivate target proteins. This orchestrates coordinated entry into the next cell cycle phase. Different cyclin-CDK combinations determine substrate targeting. While CDKs are constitutively expressed in cells, cyclins are synthesized and degraded at specific cell cycle stages to restrict the activity of the different CDK-cyclin complexes to their specific cell cycle phase (Nurse, 2000). Progression through S phase is driven by CDK2-cyclin E and CDK2-cyclin A. In contrast, initiation and progression through mitosis is governed by CDK1-cyclin A and CDK1-cyclin B. Besides cyclin degradation, CDK activity is regulated by reversible inactivation via phosphorylation of two residues within the ATP-binding loop, T14 and Y15, through the WEE1 and myelin transcription factor 1 (MYT1) kinases (Malumbres & Barbacid, 2005). When progression into the next phase of the cell cycle requires CDK activity, cell division cycle (CDC) 25 dual-specific phosphatases remove these inhibitory phosphates, thereby activating the CDK-cyclin complex and promoting cell cycle progression (Donzelli & Draetta, 2003).

1.1.1 DNA replication

DNA replication describes the process in which two identical replicas are produced from one original DNA molecule. For maintenance of genome integrity, it is indispensable that the genome is replicated exactly once per cell cycle. The elucidation of the DNA double helix structure by Watson and Crick in 1953 led to the discovery of semi-conservative replication, meaning that each strand of the double helix serves as a template for synthesis of a new strand (Watson & Crick, 1953; Meselson & Stahl, 1958). Since this finding, many molecular details of DNA synthesis have been revealed. Replication proceeds in three steps: initiation, elongation and termination. The initiation takes place at specific locations in the genome, termed origins of replication, where initiator proteins (DeLaBarre et al, 2006) are recruited to already

during G1 phase (Yardimci & Walter, 2014). In eukaryotes, replication initiation starts with binding of the origin recognition complex (ORC) to DNA. ORC is a hetero-hexamer consisting of the subunits Orc1 to Orc6. ORC in turn recruits the cell division cycle protein 6 (Cdc6) and the chromatin licensing and DNA replication factor 1 (CDT1), which are required to load the minichromosome maintenance (MCM) complex onto chromatin. The MCM complex is a hetero-hexameric ring that encircles DNA and is built of the six homologous AAA (ATPases associated with diverse cellular activities) enzymes Mcm2 to Mcm7. Altogether, this complex of ORC, Cdc6, CDT1 and MCM complex is called the pre-replicative complex (pre-RC) and the assembly of the pre-RC is defined as replication licensing (Bell & Dutta, 2002; Sclafani & Holzen, 2007). Hundreds of thousands of Mcm2-7 complexes are loaded onto DNA in the form of head-to-head double hexamers, but only 30-50 thousand of these are activated per human cell during DNA replication, while the rest stays dormant and is only activated in the case of replication stress (McIntosh & Blow, 2012). Activation of the MCM complex takes place when cells enter S phase and requires phosphorylation via Dbf4-dependent kinase (DDK) and S phase CDKs (Boos et al, 2012; Tanaka & Araki, 2013). This phosphorylation step entails recruitment of two further factors, CDC45 and Go-Ichi-Ni-San (GINS, representative for the subunits SLD-5, PSF-1, PSF-2, and PSF-3), to the MCM complex and hence formation of the CMG (CDC45, Mcm2-7, GINS) helicase complex (Ilves et al, 2010). The two active CMG helicase complexes formed from an inactive Mcm2-7 double hexamer establish bi-directional replication forks by unzipping DNA and moving away from each other (Yardimci et al, 2010). The replication machinery, also termed replisome, is built around the CMG helicase which associates stably with DNA replication forks until the termination of DNA synthesis (Boos et al, 2012). Overall, the replisome consists of about 150 proteins including DNA polymerases α, δ and ε, the sliding clamp proliferating cell nuclear antigen (PCNA), which enhances the processivity of DNA polymerases, and replication protein A (RPA), which prevents re-annealing of single-stranded DNA. During the elongation step, a primase adds RNA primers to template strands, one to the leading strand and several to the lagging strand. Starting from the primers, a high-processivity DNA polymerase extends the strand in 5’ to 3’ direction. When two converging replication forks from neighboring origins encounter, DNA synthesis is terminated locally which leads to a rapid disassembly of the replisomes. MCM complex removal from chromatin is facilitated by the mini-chromosome maintenance complex-binding protein (MCM-BP) and its interacting partner ubiquitin-specific-processing protease 7, or short USP7 (Nishiyama et al, 2011; Jagannathan et al, 2013). Finally, topoisomerase II resolves the daughter DNA molecules (Fachinetti et al, 2010).

1.1.2 Mitosis

Mitosis is the cell cycle phase in which replicated chromatids are equally distributed into two daughter cells. The process needs to be highly regulated to prevent segregation errors that result in chromosomal instability and hence lead to cancer (Kops et al, 2005). At the beginning of mitosis, the chromosomes condense in prophase and the formation of the mitotic spindle is initiated (Fig. 1.1). The nuclear envelope, which separates the nucleus from cytoplasm, breaks down during prometaphase. Protruding microtubules from opposite poles of the mitotic spindle attach stochastically to kinetochores at the centromeres of the chromosomes in a bipolar manner aligning the chromosomes at the center of the cell at the metaphase plate. Erroneous microtubule-kinetochore attachments have to be corrected to ensure faithful chromosome segregation (Lampson et al, 2004). In anaphase, the microtubules contract in order to pull the sister chromatids of each chromosome to opposing sites of the cell. During telophase, a new nuclear envelope forms around the segregated chromatin, before the cell actually divides in cytokinesis.

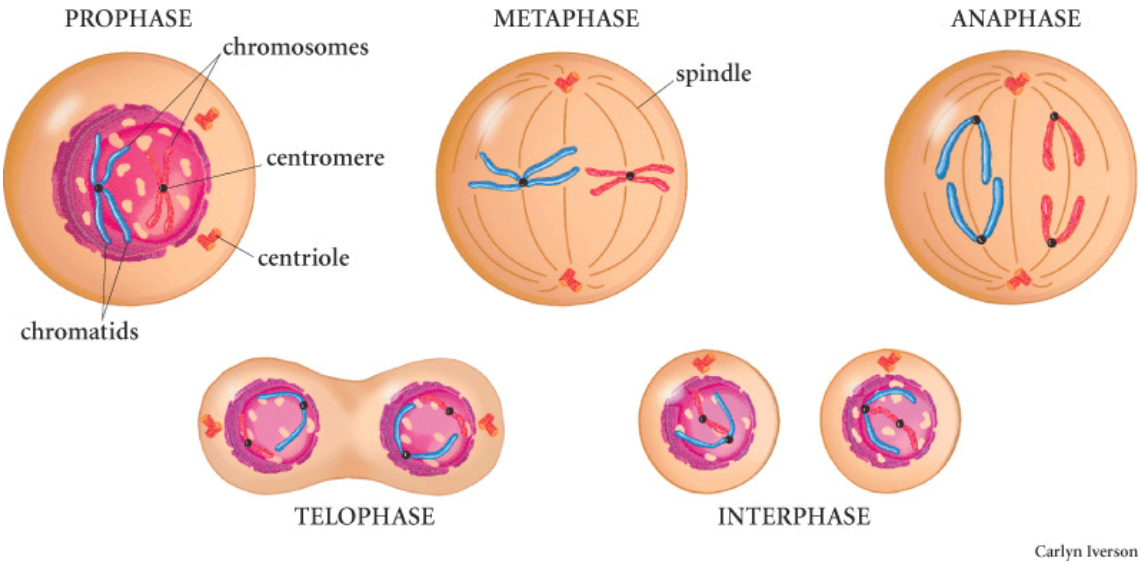

Figure 1.1: The mitotic phases. At the beginning of mitosis, chromatin condenses to form chromosomes in prophase. In metaphase, the replicated chromatids line up along the center of the cell by attaching to the fibers of the mitotic spindle. During anaphase, the chromatid pairs are segregated, with each strand of a pair moving to an opposing site of the cell. Division of the nucleus completes in telophase, when a new membrane forms around each of the two groups of chromosomes (http://www.houghtonmifflinbooks.com/booksellers/press_release/student science/gif/mitosis1.gif).

1.1.3 Cell cycle checkpoints and the DNA damage response

To ensure proper cell cycle progression and thus maintain genomic integrity, the mammalian cell cycle harbors a number of checkpoints that monitor fidelity and completion level of each of the cell cycle phases (Bartek & Lukas, 2007). Upon DNA

damage or incomplete DNA replication, these cell cycle checkpoints are activated, leading to a transient inhibition of cell cycle progression and allowing for repair of any defects. During the DNA damage response (DDR), DNA lesions are sensed as well as defects in chromosome segregation and spindle assembly. Sensing of these errors ultimately leads to a cell cycle arrest by inhibition of the CDKs. Cell cycle checkpoints monitor G1/S transition, intra S phase, G2/M transition and spindle assembly during mitosis.

The key regulators for the response to DNA damage are the ataxia-telangiectasia-mutated (ATM) and Rad3-related (ATR) serine/threonine protein kinases. ATM/ATR accumulate at sites of DNA damage where they are subsequently activated (Shiloh, 2001; Bartek & Lukas, 2007). ATM/ATR transduce the DNA damage signal by phosphorylating the checkpoint kinases Chk1 and Chk2 and the histone variant H2AX (Sancar et al, 2004). Chk1, in turn, phosphorylates the CDC25 family phosphatases, WEE1 kinase and polo-like kinase 1 (PLK1; Fig. 1.2).

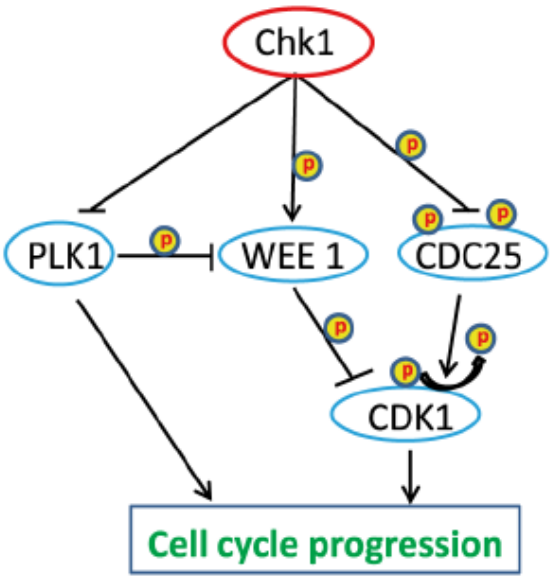

Figure 1.2: Chk1 regulation of cell cycle progression. Chk1 controls cell cycle progression by inhibiting PLK1 and CDC25 phosphatases, and activating WEE1 kinase. WEE1 phosphorylates and thereby inhibits CDK1, whereas CDC25 phosphatases dephosphorylate and thus activate CDK1. PLK1 can activate CDK1 by inhibiting WEE1 and it can directly promote cell cycle progression (adopted from Patil et al, 2013).

CDC25 phosphatases dephosphorylate CDKs in their ATP-binding loop, leading to the activation of CDKs and thus cell cycle progression (Donzelli & Draetta, 2003). However, upon phosphorylation by Chk1, CDC25 phosphatases are inactivated to arrest the cell cycle. In mammalian cells, there are three CDC25 isoforms named CDC25A, CDC25B and CDC25C, all of which are phosphorylated by Chk1 during the

DDR (Fig. 1.3). While CDC25A governs G1/S transition, S phase progression and G2/M transition, CDC25B and CDC25C primarily regulate G2/M transition (Donzelli & Draetta, 2003; Patil et al, 2013).

Upon phosphorylation of S123 by Chk1, CDC25A is targeted for ubiquitin-dependent proteasomal degradation, which leads to the inhibition of CDK1 causing a cell cycle arrest at G1/S transition, S phase and G2/M transition (Patil et al, 2013). Proteasome-targeting ubiquitylation of CDC25A is mediated by the Skp1-Cul1-F-box (SCF) βTrCP ubiquitin ligase in S and G2 phase (Busino et al, 2003). In addition to direct phosphorylation of CDC25A, Chk1 activates the NIMA-related kinase 11 (Nek11), which also phosphorylates CDC25A and thus further amplifies the DDR-induced cell cycle arrest (Melixetian et al, 2009). In contrast to CDC25A, Chk1-mediated phosphorylation of CDC25B and CDC25C leads to their inactivation by spatial translocation instead of degradation. Following their phosphorylation, CDC25B and CDC25C bind to 14-3-3 proteins which results in centrosomal sequestration of CDC25B and nuclear exclusion of CDC25C, respectively (Patil et al, 2013).

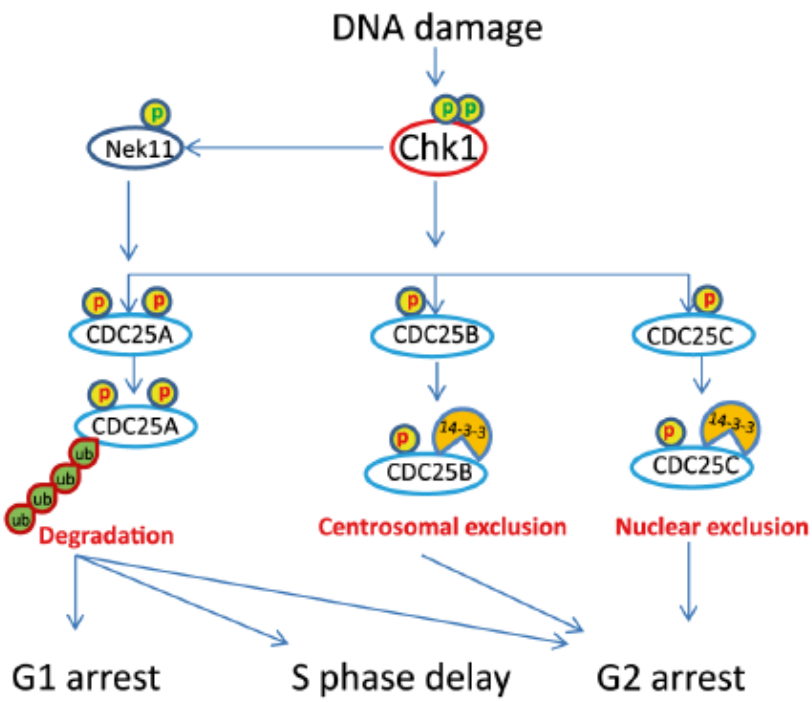

Figure 1.3: Chk1-mediated cell cycle arrest in response to DNA damage. Chk1 phosphorylates CDC25 phosphatases which causes their inhibition. Chk1 can additionally activate Nek11 kinase, which further phosphorylates CDC25A to target it for ubiquitin-dependent degradation. CDC25A governs G1/S transition, S phase progression, and mitotic entry. Thus, its degradation leads to G1 arrest, G2 arrest, and delayed S phase. Phosphorylation of CDC25B induces its binding to 14-3-3 protein and subsequent centrosomal exclusion. Chk1 also phosphorylates CDC25C thereby promoting its association with 14-3-3 protein and nuclear exclusion. CDC25B and CDC25C inhibition mainly results in G2 arrest (adopted from Patil et al, 2013).

Besides the CDC25 phosphatases, Chk1 targets WEE1, the protein kinase which mediates the inhibitory phosphorylation of CDK1 at Y15 (Fig. 1.2). In response to DNA damage, phosphorylation and activation of WEE1 by Chk1 results in the inhibition of CDK1 activity and cell cycle arrest in G2 phase (O'Connell, 1997).

Furthermore, Chk1 negatively regulates PLK1, a mitotic kinase which is involved in centrosome maturation, spindle formation and cytokinesis (Tang et al, 2006). PLK1 phosphorylates WEE1 and targets it for degradation, which causes CDK1-cyclin B complex activation and initiation of the G2/M transition (Watanabe et al, 2005). Upon DNA damage, Chk1-mediated phosphorylation of PLK1 leads to its inhibition, thus WEE1 is stabilized and the cell cycle arrests in G2 phase.

In addition to the activation of the checkpoint kinases, ATM phosphorylates and thereby activates the tumor suppressor p53, which leads to transcription of the CDK inhibitor p21 and a subsequent cell cycle arrest (Löbrich & Jeggo, 2007). This transcription- and translation-dependent pathway is slower than the fast activation of the checkpoint kinases that depends on phosphorylation and dephosphorylation events as well as ubiquitylation.

1.2 The ubiquitin-proteasome system

The covalent attachment of the small modifier protein ubiquitin (8 kDa) to proteins is a major regulatory mechanism for governing protein function and is indispensable for a functional cell cycle. This process called ubiquitylation (or ubiquitination or ubiquitinylation) is essential for the precise spatial and temporal proteolysis of key regulators of the cell cycle, thereby ensuring unidirectionality of the cell cycle.

1.2.1 Ubiquitin ligases

Ubiquitylation is ATP-dependent and requires the sequential action of three classes of enzymes (Fig. 1.4). First, the C-terminus of free ubiquitin is activated by a ubiquitin-activating enzyme (E1). Ubiquitin is then passed to a ubiquitin-conjugating enzyme (E2) and is finally conjugated to a lysine residue of the target protein via an isopeptide bond by an E3 ubiquitin ligase (Hershko & Ciechanover, 1998). This monoubiquitin can be extended to polyubiquitin chains by adding additional ubiquitin moieties to the first one. Ubiquitin itself has seven lysines, which can participate in the formation of polyubiquitin chains (K6, K11, K27, K29, K33, K48 and K63), as well as the N-terminal methionine (Johnson et al, 1995; Peng et al, 2003; Behrends & Harper, 2011). The different ubiquitin linkages which can be linear or branched have diverse topologies and functions. For example, K11- and K48-linked chains usually target proteins for proteasomal degradation (Baboshina & Haas, 1996; Haglund & Dikic, 2005). In

contrast, monoubiquitin and other types of chains have non-degradative functions or target proteins and larger structures to the lysosome by endolysosomal sorting or autophagy. Further modulation of ubiquitin chains occurs by deubiquitinating enzymes (DUBs) which are able to hydrolyze ubiquitin bonds, thereby reversing ubiquitylation of target proteins and recycling ubiquitin (Reyes-Turcu et al, 2009).

Specificity of protein ubiquitylation is conferred by more than 600 different E3 ubiquitin ligases encoded in the human genome (Li et al, 2008). These human E3 ubiquitin ligases are subdivided into two major classes, the homologous to the E6-AP C-terminus (HECT) E3 ligases and the really interesting new gene (RING) E3 ligases (Rotin & Kumar, 2009; Metzger et al, 2012). For HECT E3 ligases, ubiquitin transfer from the E2 enzyme to the substrate involves a thioester intermediate with the active-site cysteine of the E3. In contrast, RING E3s catalyze the direct transfer of ubiquitin from the E2 enzyme to the substrate by bringing them into close proximity (Metzger et al, 2012).

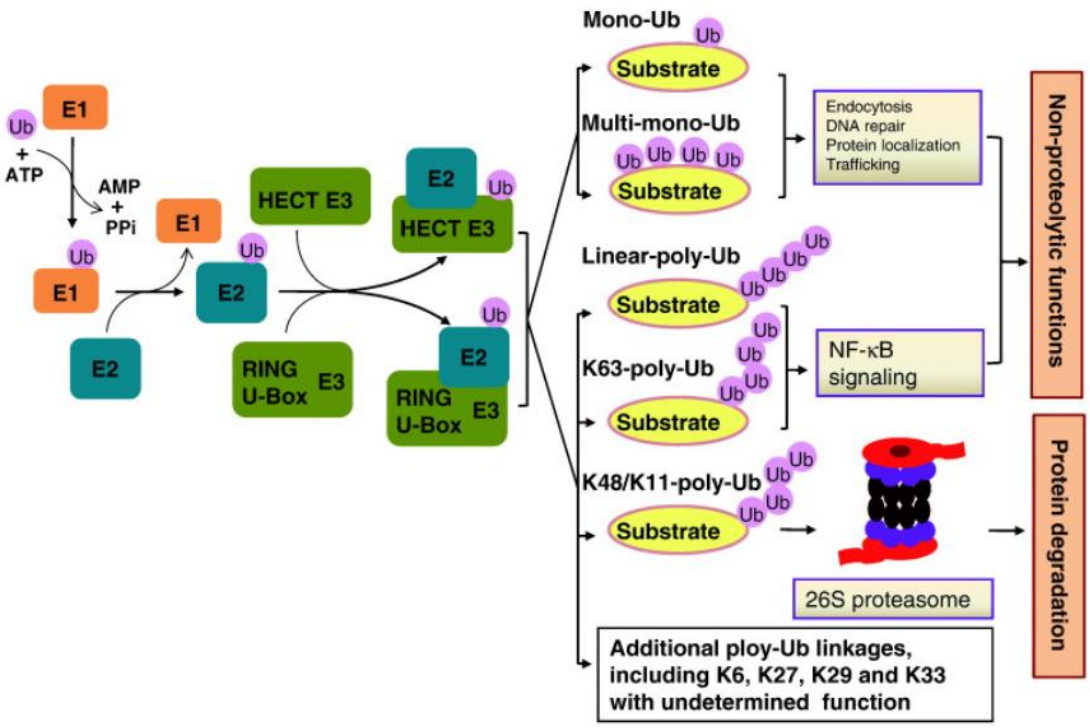

Figure 1.4: Schematic illustration of the ubiquitin-proteasome system. Ubiquitylation requires the sequential action of a ubiquitin-activating enzyme E1, a ubiquitin-conjugating enzyme E2, and an E3 ubiquitin ligase. First, ubiquitin (Ub) is activated and transferred to the E1 in an ATP-dependent manner. Subsequently, the activated ubiquitin is conjugated to the E2. Then the E2-loaded ubiquitin is transferred to a substrate, catalyzed by an E3 ligase. E3 ligases are divided into HECT or RING ligases. Substrates can be mono- or polyubiquitylated with diversely linked ubiquitin chains, which determines the biological outcome ranging from protein degradation to non-proteolytic functions including NF-κB signaling, DNA repair or endocytosis (adopted from Zhang et al, 2014).

The vast majority of human E3 ubiquitin ligases belong to the RING ligases and among them, with up to 240 complexes, cullin-RING ligases (CRLs) constitute the largest group accounting for >40% of all ubiquitin ligases and about 20% of protein degradation via the proteasome (Soucy et al, 2009). CRLs are multisubunit complexes composed of three core components – a RING finger protein that mediates binding to ubiquitin-conjugating enzymes (E2), a cullin that serves as a scaffold, and a cullin-specific adaptor protein (Deshaies & Joazeiro, 2009). Higher eukaryotes express seven different canonical cullins (CUL1, 2, 3, 4A, 4B, 5 and 7) that, with the exception of CUL3 based CRLs, bind to diverse cullin-specific adaptor proteins. The latter, in turn, associate with interchangeable substrate specificity factors, which then recruit substrates for ubiquitination. Activation of CRLs is stimulated by the covalent attachment of a ubiquitin-like molecule, NEDD8, to a conserved lysine residue in the cullin (Duda et al, 2008; Saha & Deshaies, 2008), and continuous neddylation and deneddylation cycles are required for their proper function (Bosu & Kipreos, 2008).

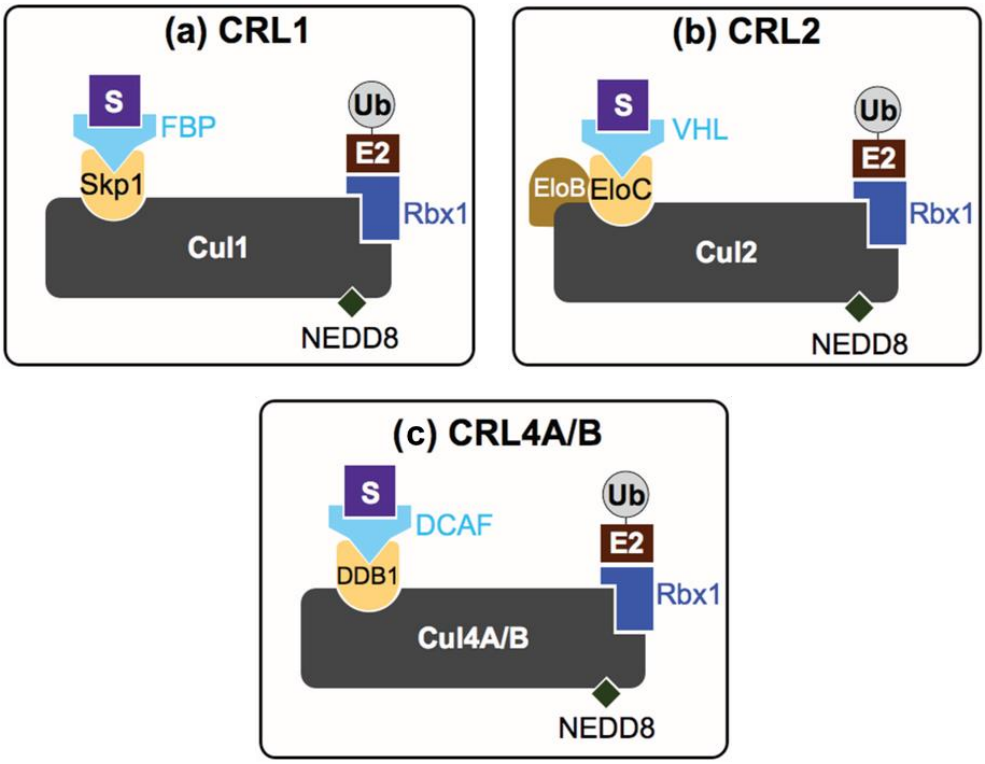

Figure 1.5: Schematic representation of cullin-RING ligase complexes. Cullin-RING ligase (CRL) complexes are composed of a cullin that serves as the complex scaffold, and a RING-finger protein (Rbx1) that recruits an E2 enzyme for substrate ubiquitylation. Moreover, CRLs have a variable adaptor protein that links the substrate receptor to the cullin placing the substrate and the E2 in close proximity. S, substrate; Skp1, S phase kinase associated protein 1; FBP, F-box protein; EloB, Elongin B; EloC, Elongin C; VHL, von-Hippel-Landau; DDB1, DNA damage binding protein 1; DCAF, DDB1 and Cul4-associated factors; Ub, ubiquitin (modified from Mahon et al, 2014).

CUL1, CUL2 and CUL4 are all implicated in the regulation of eukaryotic replication and/or S phase progression (Cukras et al, 2014; Feng et al, 1999; Craney & Rape, 2013).

CRLs which are based on cullin 1 as the scaffold are also named CRL1 or SCF ligases (Fig. 1.5). They contain a RING-box protein 1 (Rbx1), which recruits the E2 enzyme, and the S phase kinase associated protein 1 (Skp1) as the cullin-specific adaptor protein that binds the substrate-binding F-box protein (Zheng et al, 2002). In humans, 69 different F-box proteins target diverse sets of substrates, thereby contributing to the broad functional range of the SCF ligase (Skaar et al, 2009; Silverman et al, 2012). One of the F-box proteins that have been linked to the regulation of cell cycle progression is βTrCP. There are two orthologs, βTrCP1 and βTrCP2 (also known as Fbxw11), which are biochemically indistinguishable and referred to as βTrCP1/2 or simply βTrCP. It binds to substrate phosphodegrons via WD40 repeats in its C-terminus. Among others, βTrCP is implicated in the DDR, where it mediates degradation of the CDC25A phosphatase (Kanemori et al, 2005).

In contrast, CUL2-Rbx1 interacts with VHL and Elongin B and C to mediate the degradation of the hypoxia-inducible transcription factor HIF1α (Pause et al, 1997; Kamura, 1999; Ohh et al, 2000; Hwang et al, 2015).

CUL4 was shown to be involved in nucleotide excision repair (NER). The CUL4-Rbx1 complex associates with the global genome NER-associated factor DNA damage binding protein 2 (DDB2) or the transcription-coupled NER-associated factor Cockayne syndrome complementary group A (CSA) to form similar E3 ubiquitin ligase complexes (Shiyanov et al, 1999; Groisman et al, 2003). Following exposure to ultraviolet (UV) light, DDB2 recognizes UV lesions and binds tightly to the DNA damage binding protein 1 (DDB1), thereby recruiting the ubiquitin ligase CUL4-DDB1 to photolesion sites. At lesion sites, CUL4-DDB1 ubiquitylates DDB2, the UV damage sensor xeroderma pigmentosum group C (XPC), and histones H2A, H3 and H4 around the site of damage (Sugasawa et al, 2005; El-Mahdy et al, 2006; Kapetanaki et al, 2006; Wang et al, 2006). Ubiquitylation of histones H3 and H4 was shown to loosen nucleosome binding *in vitro* (Wang et al, 2006), providing space for NER proteins in the otherwise inaccessible chromatin environment.

When the RNA polymerase II encounters UV lesions during transcription, it stalls and is proteolytically released from chromatin with the help of the Cockayne syndrome complementary group A and B (CSA and CSB; Bregman et al, 1996; Svejstrup, 2002; Anindya et al, 2007). CSA binds RNA polymerase II in a UV-dependent manner (Kamiuchi et al, 2002; Groisman et al, 2003). Moreover, CSA associates with CUL4-

DDB1 to form an E3 ubiquitin ligase (Groisman et al, 2003) and ubiquitylates CSB, resulting in its proteasomal degradation (Groisman, 2006).

Furthermore, CUL4-DDB1 together with the substrate receptor CDT2 is responsible for ubiquitylation of the replication licensing factor CDT1 and its subsequent turnover by the proteasome (Hu et al, 2004; Jin et al, 2006; Higa et al, 2006). CDT2 is recruited to replication forks by PCNA-bound CDT1 (Jin et al, 2006) and associates with CUL4-DDB1 to form a ubiquitin ligase that mediates CDT1 ubiquitylation.

Another prominent E3 ubiquitin ligase involved in cell cycle regulation is the anaphase promoting complex/cyclosome (APC/C). APC/C activity is restricted to the period between metaphase and the end of G1. It associates with one of its two substrate-specific adaptors Cdc20 and Cdh1 dependent on the stage of mitosis. APC/C^{Cdc20} is responsible for anaphase onset and mitotic exit, whereas APC/C^{Cdh1} participates in the final stages of mitosis and establishes a stable G1 state (Acquaviva, 2006; Li & Zhang, 2009).

1.2.2 The proteasome

The proteasome is one of the major cellular structures responsible for the degradation of dispensable or defective proteins by proteolysis, which is the hydrolysis of peptide bonds. In this process, proteases break down proteins into peptides of typically seven to nine amino acids that can be further degraded and recycled for the synthesis of new proteins (Voges et al, 1999). The proteasomal degradation pathway is substantial for diverse cellular processes, including the cell cycle and the cellular response to DNA damage. Proteasomes are present in all eukaryotes and archaea as well as in some bacteria. In eukaryotes, they are located in the nucleus and the cytoplasm (Peters et al, 1994). In mammals, the most common form is the 26S proteasome, which contains a 20S protein core subunit and two 19S regulatory subunits that cap each end of the core (Fig 1.6).

The 20S core subunit of the proteasome has a cylindrical structure consisting of four stacked hetero-heptameric rings forming a central pore (Lowe et al, 1995; Groll et al, 1997). The two inner rings are composed of seven β subunits which bear protease activity. The active sites of the proteases reside at the inward facing surface of the rings so that target proteins have to enter the central pore for degradation. In mammals, the subunits β1, β2, and β5 are catalytically active with three distinct substrate specifities which are considered to be chymotrypsin-like, trypsin-like and peptidylglutamyl-peptide hydrolyzing (Heinemeyer et al, 1997). The two outer rings are composed of seven α subunits forming a gate that inhibits uncontrolled entry of substrates to the interior cavity (Smith et al, 2007). Moreover, the α subunits associate

with the 19S regulatory subunits, which harbor multiple ATPase active sites and ubiquitin binding sites to recognize polyubiquitylated proteins with at least four ubiquitins and target them to the catalytic core (Thrower, 2000; Liu et al, 2006). ATP binding to the 19S subunit stimulates substrate binding, association of the 19S to the 20S subunit and gate opening (Köhler et al, 2001; Smith et al, 2005; Liu et al, 2006) by docking of the C-terminal HbYX motif of the 19S ATPases into pockets of the 20S alpha rings (Smith et al, 2007). The narrow entrance of the proteasome (13 Å) demands that substrate proteins have to be at least partially unfolded already prior to entry (Coux et al, 1996; Larsen & Finley, 1997; Verhoef et al, 2008). Upon ATP hydrolysis, polyubiquitylated substrate proteins are unfolded, deubiquitylated and subsequently translocated to the interior of the proteasome (Zhu et al, 2005; Liu et al, 2006). Proteasomal degradation can be supported by ubiquitin receptors that escort polyubiquitylated proteins to the proteasome (Elsasser & Finley, 2005). These receptors have ubiquitin-associated (UBA) domains to bind ubiquitylated substrate proteins and ubiquitin-like (UBL) domains that are recognized by the 19S proteasome.

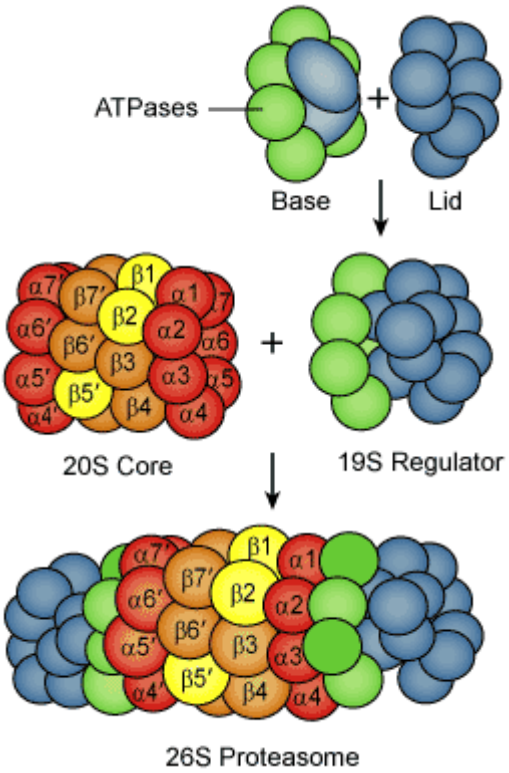

Figure 1.6: The structure of the 26S proteasome. The 26S proteasome contains a 20S core subunit and two 19S regulatory subunits attached to each end of the core. The 20S core consists of four hetero-heptameric rings. The two outer rings are composed of seven distinct α subunits (red), the two inner rings of seven distinct β subunits (orange and yellow). The subunits β1, β2, and β5 have protease activity (yellow). The 19S regulatory particle consists of a base and a lid (blue). The base harbors multiple ATPases (green; http://www.bostonbiochem.com/products/proteasome).

1.3 The AAA ATPase p97 is part of the ubiquitin-proteasome system

Downstream of ubiquitylation, ubiquitin receptors recognize the substrate proteins with K11- or K48-polyubiquitin chains and facilitate their degradation by the proteasome (Verma et al, 2004). One key regulator in facilitation of proteasomal degradation is the AAA protein family member valosin-containing protein (VCP)/p97 (also called Cdc48 in yeast and plants, CDC-48 in worms, and Ter94 in flies). p97 is an essential and highly abundant protein sharing 69% sequence identity from yeast to human (Fröhlich et al, 1991).

Mechanistically, p97 acts as a ubiquitin-selective chaperone as it catalyzes the segregation of ubiquitylated substrates from protein complexes, aggregates, or membranes and thereby facilitates their degradation (Fig. 1.7; Rape et al, 2001; Meyer, 2002; Shcherbik & Haines, 2007). The energy required for this segregase activity derives from ATP hydrolysis, which is coupled with conformational changes of p97 itself (Rouiller et al, 2002). These changes result in conformational remodeling or unfolding of substrate proteins, thereby assisting proteasomal degradation (Yamanaka et al, 2012).

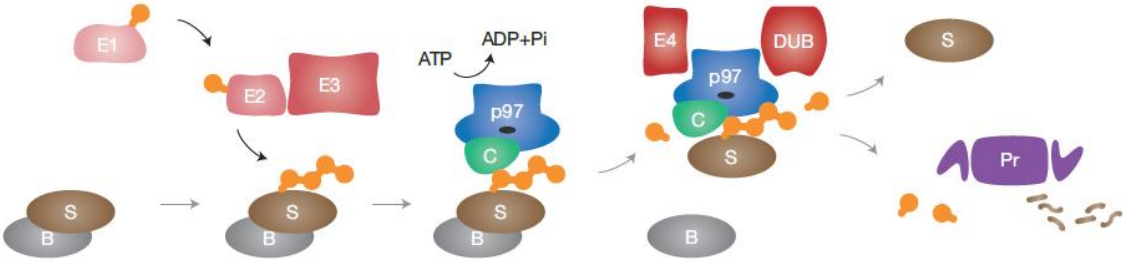

Figure 1.7: General model for p97 in substrate segregation and ubiquitin chain editing. Ubiquitin (orange) is post-translationally attached to substrate proteins (S) by a cascade of a ubiquitin-activating enzyme E1, a ubiquitin-conjugating enzyme E2, and an E3 ubiquitin ligase. p97 binds to ubiquitylated substrates via ubiquitin-binding cofactors (C). Then, p97 uses the energy of ATP hydrolysis to segregate the substrate from binding partners (B) or cellular surfaces. Interactions with ubiquitin-editing factors, like E4 chain extension factors or deubiquitylating enzymes (DUBs), are able to modify ubiquitin chains to either recycle the substrate or target it to the proteasome (Pr) for degradation (adopted from Meyer et al, 2012).

1.3.1 Structure and activity of p97

p97 is a homo-hexameric protein. Each protomer consists of a globular N-terminal domain, the two ATPase domains D1 and D2, and a disordered C-terminal tail (DeLaBarre & Brunger, 2003). Two linker regions connect the N and D1 as well as the D1 and D2 domains, respectively. Both ATPase domains contain a Walker A and Walker B motif, which are important for ATP binding and hydrolysis, respectively.

Hexamerization is essential for p97 activity and is promoted by ATP binding to the D1 domain (Wang et al, 2003).

The three-dimensional structure of hexameric p97 has been investigated by X-ray crystallography, small angle X-ray scattering (SAXS) and electron microscopy (EM; Fig. 1.8). These studies revealed that p97 has two stacked rings consisting of the D1 and D2 ATPase domains, respectively, whereas the N domains protrude from the periphery of the D1 ring (DeLaBarre & Brunger, 2003; Dreveny et al, 2004).

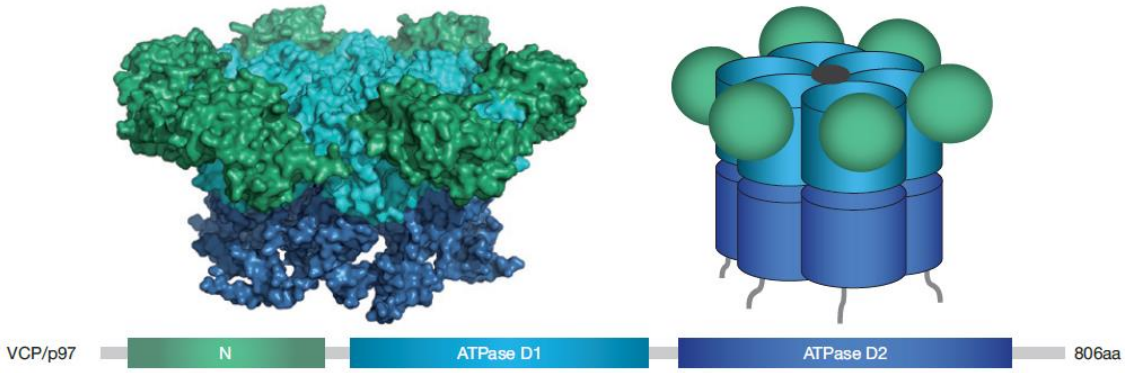

Figure 1.8: The structure of the hexameric AAA protein p97. Each subunit consists of a globular N-terminal domain (green), the two AAA ATPase domains D1 (cyan) and D2 (blue), and a C-terminal tail (gray). D1 and D2 form two stacked hexameric rings, while the N domain resides at the periphery of the D1 ring. The crystal structure was generated by PyMOL using the PDB id: 1R7R (adopted from Meyer et al, 2012).

The latest Cryo-EM study on p97 structure discriminates three distinct conformations of p97, depending on the binding of nucleotides (Banerjee et al, 2016). In conformation I, ADP is bound to D1 and D2 domains. Concomitantly, the N domains are coplanar with the D1 ring (also called down conformation or locked conformation in other studies; Niwa et al, 2012; Yeung et al, 2014). Upon ATP binding to the D2 domain, the N-D1 and D2 hexameric rings rotate relatively to each other, resulting in conformation II (Noi et al, 2013; Yeung et al, 2014; Banerjee et al, 2016). Additional binding of ATP to D1 finally induces a conformational switch to conformation III (Banerjee et al, 2016). In conformation III, the N domain is released from the D1 plane and adopts a state above the D1 ring (also called up conformation or flexible conformation; Niwa et al, 2012; Yeung et al, 2014). Cryo-EM studies of different p97 complexes demonstrated that in this conformation, cofactors of p97 can bind to the N domain (Beuron et al, 2006; Bebeacua et al, 2012; Ewens et al, 2014). Moreover, the D2 pore is contracted in comparison to the other conformations (Yeung et al, 2014; Banerjee et al, 2016).

Notably, the D1 ring hydrolyzes ATP at a lower rate than the D2 ring (Fang et al, 2015). This discrepancy might be based on very tight binding of ADP to the D1 ring (DeLaBarre & Brunger, 2003; Huyton et al, 2003; Briggs et al, 2008). Still, ATP

hydrolysis of the D1 domain is important for p97 function since a point mutation in the D1 Walker B motif, which abrogates ATP hydrolysis, is lethal (Ye et al, 2003; Esaki & Ogura, 2010).

While it seems clear that ATP hydrolysis implies conformational changes of p97 that create mechanical force allowing substrate unfolding, dissociation or remodeling, the underlying mechanism is still controversial. There are studies speculating that p97 unfolds ubiquitylated proteins by threading them completely through its central pore (Ye et al, 2003; Rothballer et al, 2007; Barthelme & Sauer, 2013; Tonddast-Navaei & Stan, 2013). Yet, the crystal structure of p97 revealed that the axial pore of the D1 ring is severely constrained by a zinc-ion coordinated to multiple H317 side chains (DeLaBarre & Brunger, 2003). Thus, it was proposed that substrate unfolding occurs by interaction with an external surface region of p97 rather than by translocation through the central pore. However, it is unclear if the pore block also exists in solution. An alternative model suggests that substrates are only threaded through the axial pore of the D2 ring to avoid the D1 pore block (DeLaBarre et al, 2006). Though, an unfoldase activity of p97 was so far only observed upon simultaneous deletion of the N domain and mutation of the D1 ring pore residues to tyrosines (Rothballer et al, 2007; Barthelme & Sauer, 2013). Moreover, some chromatin-associated p97 targets remain active after segregation suggesting that p97 activity does not necessarily involve substrate unfolding. Yet, it was shown that the degradation of a substrate with an unstructured C-terminus is no longer dependent on p97 activity (Beskow et al, 2009). A recent study claims that p97 can indeed unfold polyubiquitylated proteins and that this process is ATP-independent (Song et al, 2015).

In addition to the mechanism of substrate unfolding and dissociation, the interaction of p97 and the proteasome remains elusive. The C-terminus of archaeal p97 terminates with an HbYX motif that might mediate the direct association with the 20S proteasome (Barthelme & Sauer, 2012; Barthelme & Sauer, 2013). Thus, p97 could identify and thread substrates into the proteolytic chamber of the proteasome for hydrolysis. In yeast, however, p97 hands substrates over to other shuttling factors, Rad23 and Dsk2, which then target the substrates to the proteasome (Richly et al, 2005). In contrast, studies with human p97 suggest direct binding of p97 to the proteasome (Alexandru et al, 2008; Verma et al, 2011).

1.3.2 Biological functions of p97

p97 accounts for more than 1% of cytosolic proteins (Ye, 2006) and accordingly plays a role in a large variety of independent cellular processes (Meyer et al, 2012). The main role of p97 is to ensure protein homeostasis. The best studied function of p97 is in

endoplasmic reticulum-associated degradation (ERAD; Kothe et al, 2005). p97 is important for coordinating retrotranslocation of misfolded proteins from the ER to the cytosol, their ubiquitylation and subsequent degradation by the proteasome. In addition to its well established role in ERAD, which results in proteasomal degradation, p97 has been linked to the other major cellular degradative system, the lysosome. p97 is implicated in endolysosomal and autophagolysosomal pathways, where it mediates the sorting of cargo proteins (Ju & Weihl, 2010; Ritz et al, 2011; Meyer et al, 2012; Kirchner et al, 2013). Furthermore, p97 is responsible for the maturation of autophagosomes and inclusion body formation (Tresse et al, 2010). Moreover, p97 is involved in chromatin-associated degradation, where it governs cell cycle progression and the DDR (Dantuma & Hoppe, 2012). Besides, p97 regulates apoptosis through degradation of key apoptotic factors, such as Mcl1 or DIAP1 (Rumpf et al, 2011; Xu et al, 2011). Furthermore, p97 was implicated in mitochondria-associated degradation. It is critical for protein quality control at the outer mitochondrial membrane and regulates mitochondrial membrane fusion and destruction of mitochondria through mitophagy (Heo et al, 2010; Tanaka et al, 2010; Wild & Dikic, 2010; Livnat-Levanon & Glickman, 2011; Xu et al, 2011). Recently, p97 was found to play a role in ribosome-associated degradation, where it co-translationally eliminates misfolded nascent peptides, which may comprise up to about 30% of newly synthesized proteins (Brandman et al, 2012; Fujii et al, 2012; Verma et al, 2013). Thus, it is directly involved in ribosome-associated protein quality control and the translational stress response. In addition, p97 is critical for lysosomal destruction of the ribosomal component Rpl25 upon starvation in a process called ribophagy (Ossareh-Nazari et al, 2010). Additionally, p97 participates in the regulation of signaling processes. For instance, p97 is required to selectively separate the transcription factor NF-κB from its polyubiquitylated inhibitor IκBα. As a result, NF-κB is released to enter the nucleus and activate transcription, while IκBα is degraded (Dai, 1998). Another p97 substrate in signaling processes is the hypoxia-inducible factor 1α (HIF1α), of which degradation is induced by $CUL2^{VHL}$-mediated ubiquitylation and results in down-regulation of the hypoxic response (Alexandru et al, 2008). However, the removal of a ubiquitylated substrate from a protein complex or a subcellular structure is not necessarily linked to subsequent (proteasomal) degradation. p97 is also implicated in proteasome-independent membrane trafficking events, including Golgi reassembly after mitosis, where p97 promotes membrane-protein segregation (Kondo et al, 1997; Meyer, 2005). Moreover, p97 has been shown to control lipid droplet biogenesis (Olzmann et al, 2013).

1.3.3 p97 cofactors

Alternative cofactors have been described that define the pathway-specific functions of p97 (Yeung et al, 2008). So far, about 40 p97 cofactors have been identified that link p97 to specific pathways and substrates. Although p97 is able to bind ubiquitin directly *in vitro*, *in vivo* p97 requires the binding of substrate-recruiting cofactors to obtain optimal activity (Meyer, 2002; Ye et al, 2003). These substrate-recruiting factors link p97 to its ubiquitylated substrates via ubiquitin-binding domains and thus, mediate a more stable enzyme-substrate complex (Meyer, 2002). For some cofactors, it was shown that the substrate-recruiting factor binds to the substrate before p97 recruitment (Madsen et al, 2009), while other adaptor proteins first assemble with p97 to create a complex that is able to bind ubiquitylated substrates.

Apart from interacting with diverse substrate-recruiting cofactors, p97 also associates with a large variety of substrate-processing cofactors, including DUBs. p97-associated DUBs are either able to prevent p97 substrates from degradation or they can promote substrate degradation by modulating ubiquitin chains to those types that are recognized by the proteasome (Rumpf & Jentsch, 2006). Several DUBs have been found to interact with p97, for example VCIP135, which regulates the p97-mediated Golgi and ER membrane fusion (Uchiyama, 2002; Wang et al, 2004; Zhang et al, 2013), YOD1 (and its yeast ortholog Otu1), USP13, ataxin3 and USP25, which are linked to the regulation of ERAD (Rumpf & Jentsch, 2006; Ernst et al, 2009; Sowa et al, 2009; Blount et al, 2012; Liu et al, 2014), and USP50, which has been implicated in the regulation of the DNA damage checkpoint (Sowa et al, 2009; Aressy et al, 2014).

Cofactor binding to the N-terminus of p97 can be promoted by different domains (Fig. 1.9), including the ubiquitin regulatory X (UBX) domain, the UBX-like (UBX-L) domain, or short binding motifs like the SHP box (also called binding site 1, BS1), the VCP-binding motif (VBM) or the VCP-interacting motif (VIM; Meyer, 2002; Buchberger, 2010; Kloppsteck et al, 2012; Meyer et al, 2012). Other cofactors bind to the C-terminal tail of p97 via their PUB (peptide N-glycosidase/UBA or UBX containing proteins; also known as PUG) or PUL (PLAA, Ufd3, and Lub1) domains (Madsen et al, 2009).

In mammals, the largest group of p97 cofactors is constituted by the 13 UBX proteins (p37, p47, UBXD1-8, FAF1, SAKS1, and ASPL). Apart from UBXD1, they bind p97 via a highly conserved FPR motif of their UBX domain, which features a ubiquitin-like fold (Buchberger et al, 2001; Dreveny et al, 2004; Schuberth & Buchberger, 2008). UBXD1 instead lacks the conserved FPR motif and interacts via its VIM and its PUB domain with the N domain and the C-terminus of p97, respectively (Kern et al, 2009). Recently, a further p97-binding site at the N-terminus of UBXD1 was identified (Trusch et al, 2015). While eight of the UBX proteins (p37, ASPL, UBXD1 to UBXD6) are referred to

as UBX-only proteins, the other five (p47, UBXD7, UBXD8, FAF1, and SAKS1) also have an N-terminal ubiquitin-associated UBA domain, classifying them as UBA-UBX proteins (Alexandru et al, 2008; Schuberth & Buchberger, 2008). The UBA domain is involved in binding of ubiquitylated substrates. In addition to p97-binding, the UBA-UBX proteins also interact with E3 ubiquitin ligases, including cullins 1 through 4, nine RING ligases, and three HECT domain enzymes (Alexandru et al, 2008).

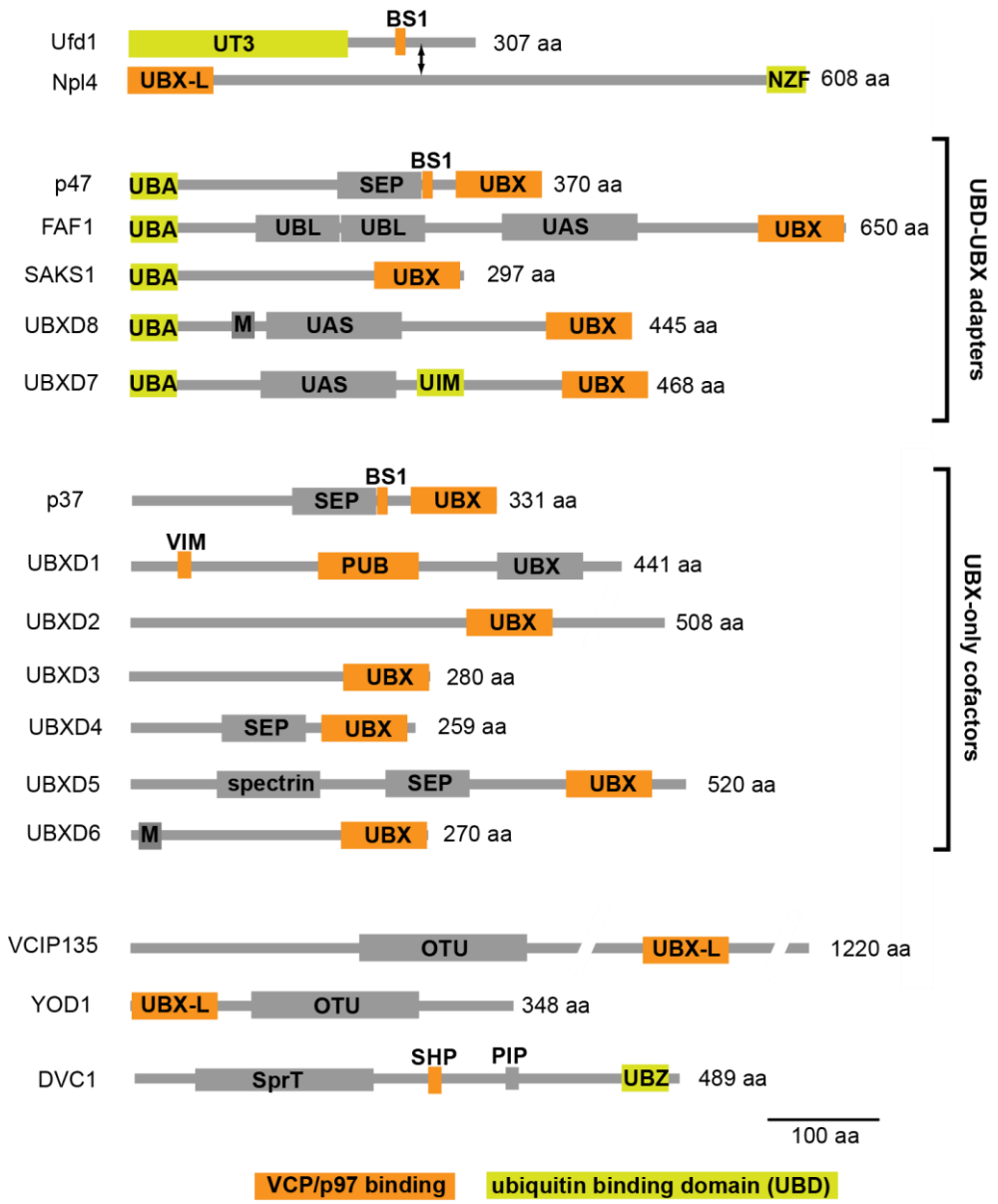

Figure 1.9: Domain structure of selected p97 adaptor proteins. UBX or UBX-L domains or short motifs such as the binding site 1 motif (BS1, also called SHP), the VCP-interacting motif (VIM) or the VCP-binding motif (VBM) interact with the N domain of p97. PUB (peptide N-glycosidase/UBA or UBX containing proteins) or PUL (PLAA, Ufd3 and Lub1) domains bind the C-terminus of p97. The ubiquitin-associated (UBA) domain, the Npl4 zinc finger (NZF), the ubiquitin-interacting motif (UIM), the Ufd1 truncation 3 (UT3) and the UBZ are able to bind ubiquitin. The ovarian tumor (OTU) domain has deubiquitylating activity. SEP, Shp1-eyc-p47 domain; UAS, ubiquitin-associating domain; SprT, potential zinc binding domain; PIP, PCNA-interacting protein motif; aa, amino acids.

Some adaptor proteins, like p47, UBXD1 and the heterodimer Ufd1-Npl4, target identical or overlapping sites on p97. Thus, they bind to p97 in a mutually exclusive manner (Meyer et al, 2000; Bruderer et al, 2004). However, simple competition for p97-binding sites is not the only determinant in cofactor selectivity since these protein complexes can combine with additional cofactors to form higher-order protein complexes (Alexandru et al, 2008; Schuberth & Buchberger, 2008). These additional cofactors can alter p97 localization and provide additional enzymatic activity and thereby further specify p97 functions. Three p97 cofactors have been linked to chromatin-associated p97 functions, namely the Ufd1-Npl4 heterodimer, UBXD7, and DVC1.

Ufd1-Npl4

The best studied p97 cofactor is the heterodimeric Ufd1-Npl4 ubiquitin adaptor. In yeast, this is the only essential cofactor (Johnson et al, 1995; DeHoratius & Silver, 1996). The nuclear protein localization 4 (Npl4) binds to the ubiquitin fusion degradation 1 protein (Ufd1) in a 1:1 stoichiometry (Meyer et al, 2000; Bruderer et al, 2004). In the absence of Npl4, Ufd1 is unstable (Bruderer et al, 2004; Dobrynin et al, 2011). Studies revealed that ATP binding to the D1 domain regulates the recruitment of p97 adaptor proteins to the N domain including Ufd1-Npl4 (Chia et al, 2012). Ufd1-Npl4 binds to p97 in a 1:6 stoichiometry (Pye et al, 2007). The N domain of Ufd1 shows structural similarity to the N domain of p97 and contains binding sites for both mono- and polyubiquitin (Park et al, 2005). In contrast, Npl4 comprises an N-terminal UBX-L domain and a C-terminal zinc-finger (NZF), which binds to K48 and K63 polyubiquitin chains (Meyer, 2002; Ye et al, 2003; Bruderer et al, 2004; Isaacson et al, 2007). Like UBXD1, Ufd1-Npl4 binds to p97 in a bipartite manner, involving the p97-interacting UBX-L domain of Npl4 and the BS1 motif of Ufd1 (Bruderer et al, 2004). A 3D electron cryomicroscopy reconstruction of the $p97^{Ufd1\text{-}Npl4}$ complex showed that this complex is highly dynamic and that Ufd1-Npl4 assumes distinct positions relative to the p97 ring upon addition of a nucleotide (Bebeacua et al, 2012). In complex with Ufd1-Npl4, p97 acts in cellular pathways as diverse as ERAD, activation of transcription factors and chromatin-associated degradation of proteins. Among others, it is involved in the regulation of cell cycle progression and the regulation of the DDR.

UBXD7

In 2011, it was shown for the first time that UBXD7 (also called UBXN7) binds to the $p97^{Ufd1\text{-}Npl4}$ complex, but not to free p97 (Hänzelmann et al, 2011). This demonstrates a hierarchy in cofactor binding to p97. It might be that binding of Ufd1-Npl4 induces

conformational changes in p97, resulting in an asymmetry of p97, which allows for tight interaction of UBXD7 with only one of the vacant p97 subunits (Hänzelmann et al, 2011).

UBXD7 is the only p97 adapter with an ubiquitin-interacting motif (UIM), with which it directly binds to neddylated CRLs (Bandau et al, 2012; den Besten et al, 2012). UBXD7 comprises a ubiquitin-binding UBA domain, a ubiquitin-associating domain (UAS) of unknown function, the UIM and a p97-interacting UBX domain. A current model proposes that the UBA and UBX domains interact with each other intra- or intermolecularly, thereby maintaining UBXD7 in an inactive state. Only upon binding of a ubiquitylated substrate via the UBA domain, the UBX domain would become available to recruit the $p97^{Ufd1\text{-}Npl4}$ complex. Thus, substrate binding to UBXD7 precedes the formation of UBXD7 complexes with $p97^{Ufd1\text{-}Npl4}$ and may be a prerequisite for complex formation (Alexandru et al, 2008). In addition, the UIM domain recognizes the ubiquitin-like small protein modifier NEDD8, which is dynamically conjugated to the cullin subunit of the CRL, thereby activating its ligase activity (Petroski & Deshaies, 2005; Saifee & Zheng, 2008). NEDD8 conjugation induces conformational changes in the CRL, which allow the RING domain of Rbx1 to spring free from the cullin and to position the ubiquitin-conjugating enzyme E2 in the vicinity of the substrate and thus promote ubiquitin transfer (Duda et al, 2008; Saha & Deshaies, 2008; Saifee & Zheng, 2008). There is evidence that UBXD7 binds CUL2- and CUL4-based CRLs preferentially over CUL1 and CUL3 (den Besten et al, 2012).

In budding yeast, it was demonstrated that $Cdc48^{Ufd1\text{-}Npl4}$ and the UBXD7 homologue Ubx5 are required for CUL3-dependent degradation of the largest subunit of RNA polymerase II, Rpb1, after UV treatment (Verma et al, 2011). In this case, Ubx5 links substrate ubiquitylation to p97-mediated extraction, which is important for subsequent degradation of this substrate by the proteasome. In human cells, UBXD7 together with p97 was shown to participate in turnover of HIF1α, a $CUL2^{VHL}$ substrate that is constitutively degraded under normoxic conditions (Alexandru et al, 2008). Intriguingly, while Ubx5 is required for efficient turnover of Rpb1 in yeast, depletion of UBXD7 in human cells accelerates HIF1α degradation. Consistently, overexpression of UBXD7 inhibits HIF1α ubiquitylation dependent on the presence of the UIM. Here, UBXD7 antagonizes substrate ubiquitylation and degradation. An explanation for this observation could be that UBXD7 attachment to neddylated CRLs might sterically hinder the transition of the CRL complex to an open conformation and thereby weaken the positive effect NEDD8 has on CRL E3 activity (Bandau et al, 2012). Indeed, UBXD7 binding interferes with recruitment of the E2 Cdc34 to the $SCF^{\beta TrCP}$ ligase and decreases substrate ubiquitylation (den Besten et al, 2012).

Thus, one study proposes that the function of UBXD7 is to inhibit the CRL, so that shorter ubiquitin chains are attached to substrate proteins which target them for p97-dependent proteasomal degradation (Bandau et al, 2012). In contrast, the other study suggests that UBXD7 binding to CRLs only occurs if the ligase stalls, when it encounters a substrate which is difficult to extract from a binding partner or a subcellular structure (den Besten et al, 2012). In this case, UBXD7 would bind to NEDD8 and recruit p97 for substrate extraction. This provides an explanation as to why only certain substrates of CRLs require $p97^{UBXD7}$. However, it does not explain why a subset of CRL substrates require p97 but not UBXD7 for degradation, as in the case of chromatin-bound CDT1, a replication licensing factor targeted by CUL4A (den Besten et al, 2012).

Finally, an analysis of the functional implications of the chromosome 3q amplicon in lung squamous cell carcinoma (SCC) revealed that UBXD7 regulates cellular proliferation in lung SCC that harbor the amplicon (Wang et al, 2013).

DVC1

The p97 adaptor protein DVC1 (for DNA damage-targeting VCP/p97 adaptor C1orf124, also known as C1orf124 or Spartan) plays a role in translesion synthesis (Centore et al, 2012; Davis et al, 2012; Ghosal et al, 2012; Juhasz et al, 2012; Machida et al, 2012; Mosbech et al, 2012; Kim et al, 2013). Moreover, it was shown that DVC1 is not recruited to DNA double-strand breaks (DSBs) and therefore not involved in DSB repair (Centore et al, 2012; Davis et al, 2012; Ghosal et al, 2012; Juhasz et al, 2012; Mosbech et al, 2012). DVC1 expression is restricted to S and G2 phase (Mosbech et al, 2012). Impairment of DVC1 was reported to increase UV light-induced mutagenesis (Machida et al, 2012) and leads to hypersensitivity towards replication stress-inducing agents in human cells and *Caenorhabditis elegans* (Juhasz et al, 2012; Mosbech et al, 2012). Importantly, DVC1 deficiency was linked to genome instability, premature ageing and cancer predisposition both in humans (Lessel et al, 2014) and in mice (Maskey et al, 2014).

DVC1 binds p97 via a SHP motif. Moreover, DVC1 contains an UBZ4-type ubiquitin-binding domain and a PIP box with which it interacts with monoubiquitylated PCNA (Centore et al, 2012; Davis et al, 2012; Ghosal et al, 2012; Juhasz et al, 2012; Machida et al, 2012; Mosbech et al, 2012). In addition, DVC1 comprises a SprT-like domain bearing a HEXXH motif which is typical of metallopeptidases. Due to structural and functional similarities, some studies argue on DVC1 being the mammalian representative of the yeast weak suppressor of smt3-331 (Wss1), hence acting as a protease (Davis et al, 2012; Mosbech et al, 2012; Stingele et al, 2015). Wss1 is a DNA-

dependent metalloprotease involved in the repair of DNA-protein crosslinks by cleaving them and thereby enabling helicase progression and translesion synthesis (Stingele et al, 2014). Wss1 is recruited to DNA lesion sites, where it binds to targets modified with the small ubiquitin-like modifier (SUMO). There, it catalyzes SUMO chain extension (Balakirev et al, 2015). Upon SUMO polymerization, more Wss1 is accumulated and its protease activity is activated (Balakirev et al, 2015). Wss1 cleaves itself and associated proteins in the repair complex, leading to extraction of the sumoylated proteins and subsequent proteasomal degradation (Balakirev et al, 2015). It forms a complex with Cdc48 and the Cdc48-adaptor protein Doa1 (Balakirev et al, 2015). However, so far no protease or metallopeptidase activity associated with the SprT domain of DVC1 has been detected. Yet, the SprT domain is essential for DVC1 function (Kim et al, 2013).

1.4 The role of p97 and its cofactors in the cell cycle and the DNA damage response

p97 has emerged as a central player in various chromatin-associated processes including cell cycle progression, DNA replication, transcription, and the DDR. The *Cdc48* gene was identified in the first genetic screen for cell division cycle mutants in yeast (Moir et al, 1982). Several studies in yeast and other organisms have clearly demonstrated that Cdc48 is essential for cell cycle progression (Mouysset et al, 2008; Deichsel et al, 2009). In yeast, mutations in the Cdc48 gene result in delayed G1/S transition and G2/M arrest (Fu et al, 2003). In the nematode *Caenorhabditis elegans*, knockdown of CDC-48, or one of its cofactors UFD-1 or NPL-4, delays S phase progression due to activation of replication checkpoints (Mouysset et al, 2008). In human cell lines and *Xenopus laevis* egg extracts, inactivation of $p97^{Ufd1\text{-}Npl4}$ causes delayed progression through anaphase and exit from mitosis (Ramadan et al, 2007; Dobrynin et al, 2011). All these observations highlight the pivotal role of p97 in protein degradation which is necessary for cell cycle progression.

1.4.1 p97 in mitosis

The first p97 substrate discovered in chromatin was Aurora B kinase that functions in the bipolar attachment of the mitotic spindle to the centromeres of chromosomes (Ramadan et al, 2007). In *Xenopus laevis* egg extracts and *Caenorhabditis elegans*, the $p97^{Ufd1\text{-}Npl4}$ complex extracts Aurora B from chromatin at the end of mitosis, allowing chromatin decondensation and nuclear envelope formation. Importantly, although Aurora B extraction from chromatin is mediated by K48-linked polyubiquitin chains, chromatin dissociation is not coupled to degradation. Since Aurora B activity is stimulated by chromatin, it is possible that chromatin removal is sufficient to suppress

Aurora B (Kelly et al, 2007). In contrast, in human somatic cells, Aurora B is proteolysed after ubiquitylation by the ubiquitin ligase APC/C^{Cdh1} (Stewart, 2005) at the exit of mitosis with the help of p97$^{Ufd1-Npl4}$ (Dobrynin et al, 2011). Knockdown of Ufd1 or Npl4 increases Aurora B activity, which causes defects in chromosomal alignment in anaphase and subsequently missegregated chromosomes and multi-lobed nuclei. Thus, p97$^{Ufd1-Npl4}$ antagonizes Aurora B activity. Interestingly, extraction of Aurora B from mitotic chromosomes during anaphase is regulated by the CRL3$^{KLHL9-KLHL13}$ ubiquitin ligase complex (Sumara et al, 2007) and its subsequent relocalization together with survivin to the midbody is governed by CRL3^{KLHL21} (Maerki et al, 2009). Recruitment of survivin at the centromere depends on K63 ubiquitin chains and the p97 cofactor Ufd1, which indicates a role for p97$^{Ufd1-Npl4}$ in survivin relocalization (Vong, 2005). Similar to its role in mitosis, CDC-48 in *Caenorhabditis elegans* is essential for proper condensation and segregation of meiotic chromosomes by controlling AIR-2/Aurora B (Sasagawa et al, 2012). Another p97 complex, Cdc48^{Shp1} (p97^{p47} in metazoans), counteracts Aurora B activity by facilitating localization of the Aurora B antagonist Glc7, the yeast ortholog of protein phosphatase-1 (PP1; Cheng & Chen, 2010). Inactivation of Cdc48^{Shp1} results in a metaphase arrest due to erroneous kinetochore-spindle attachment and thus, activation of the spindle assembly checkpoint. In addition to Aurora B regulation, p97 together with its cofactors Ufd1 an Npl4 is crucial for proper spindle disassembly at the end of mitosis (Cao et al, 2003). Targets of p97$^{Ufd1-Npl4}$ are spindle assembly factors XMAP215, TPX2, and Plx1, or in yeast, ase1 and Cdc5. Moreover, Cdc48^{UBXN2} and p97$^{p37/p47}$ limit the association of Aurora A with centrosomes in nematodes and human cells, respectively (Kress et al, 2013).

1.4.2 p97 in G1/S transition

In yeast, G1/S transition is governed by Cdc28/Cln, analogous to CDK-cyclin-dependent cell cycle transition in mammals. Cdc28/Cln is antagonized by Far1p, which has to be degraded for G1/S progression and this degradation depends on Cdc48 (Fu et al, 2003). For eukaryotes, no similar p97-dependent process has been identified so far. However, in yeast, Cdc48$^{Ufd1-Npl4}$ additionally regulates G1/S transition via cell wall integrity pathway mechanisms (Hsieh et al, 2011). The underlying mechanism remains unclear, although Cdc48 appears to regulate the activity of Mpk1, a MAP kinase family member essential for cell wall integrity, in response to stress conditions including heat shock (Hsieh et al, 2011).

1.4.3 p97 in DNA replication

In addition to its role in mitosis and G1/S transition, CDC-48/p97 has been linked to DNA replication in several studies. The first hint for a role of CDC-48 in S phase progression of mitotic cells was found by Mouysset and colleagues (Mouysset et al, 2008). In *Caenorhabditis elegans*, inactivation of the CDC-48$^{UFD-1/NPL-4}$ complex caused hypersensitivity toward replication blocking agents, a reduced DNA synthesis, and a replication checkpoint-dependent delay in S phase progression.

In 2011, two independent studies revealed that p97 regulates DNA replication by degradation of the replication licensing factor CDT1 (Franz et al, 2011; Raman et al, 2011). The recruitment of CDT1 to origins of replication during G1 phase by the multi-subunit origin recognition complex is a critical step in the initiation of DNA replication. CDT1 licenses origins by recruiting the Mcm2-7 helicase which unwinds double-stranded DNA at the beginning of S phase (Arias & Walter, 2007).

Upon initiation of replication in S phase, CDT1 is degraded to prevent re-firing of licensed origins (Arias & Walter, 2007). The E3 ubiquitin ligase CUL4-DDB1^{CDT2} is thought to be the primary E3 ligase that ubiquitylates PCNA-bound CDT1 before it is targeted to the proteasome for degradation (Zhong et al, 2003; Hu et al, 2004; Havens & Walter, 2009). In *Caenorhabditis elegans*, CDC-48 was found to be responsible for CDT-1 degradation after initiation of DNA replication, as well as for the release of the essential replication factors CDC-45 and the GINS complex (Franz et al, 2011). As part of the active replisome, CDC-45 and GINS move with the replication fork during the elongation step of DNA synthesis (Gambus et al, 2006; Moyer et al, 2006; Pacek et al, 2006; Aparicio et al, 2009). A lack of CDC-48 or its cofactors UFD-1/NPL-4 leads to accumulation of CDT-1 on mitotic chromatin and subsequently to persistent chromatin association of CDC-45/GINS in *Caenorhabditis elegans* embryos. Furthermore, p97 together with its cofactor UFD1 was identified as a key player of DNA damage-dependent CDT1 destruction in HeLa cells in a genome-wide siRNA screen (Raman et al, 2011). After UV irradiation, the E3 ubiquitin ligase CUL4-DDB1^{CDT2} ubiquitinates PCNA-bound CDT1, before p97^{UFD1} unfolds and removes it from chromatin in an ATP-dependent manner and targets it to the proteasome for degradation. Other studies link the role of Cdc48 in the release of CDC45 and GINS from replication forks to the termination of DNA replication (Maric et al, 2014; Moreno et al, 2014). When replication is completed, a subunit of the Mcm2-7 helicase, Mcm7, is polyubiquitylated with K48-linked ubiquitin chains. It was shown that Mcm7 ubiquitylation is mediated by a SCF ubiquitin ligase, with Dia2 as the F-box protein in budding yeast (Maric et al, 2014; Maculins et al, 2015). SCF^{Dia2} consists of the cullin scaffold protein Cdc53, the RING protein Hrt1, the adaptor protein Skp1 and the substrate recognition F-box protein

Dia2. In higher eukaryotes, the ubiquitin ligase targeting Mcm7 has not been identified so far, since Dia2 does not have a sequence homolog in higher eukaryotes. However, Mcm7 polyubiquitylation with K48-linked chains is followed by disassembly and release of the CMG complex from DNA dependent on Cdc48 (Maric et al, 2014; Moreno et al, 2014). Intriguingly, proteasome inhibition did not stall CMG disassembly despite the well-known role of K48-linked ubiquitin chains as a marker for degradation of the modified substrate by the proteasome system. It has been proposed that Cdc48 associates with polyubiquitylated Mcm7 and removes it from the CMG complex without targeting it for proteasomal degradation. By removal of Mcm7, the hexameric Mcm2-7 ring is opened, providing an exit for DNA. Although Mcm7 does not interact with CDC45 or GINS, Maric and colleagues show that associations between multiple Mcm2-7 subunits are disrupted during CMG release, presumably resulting in the release of CDC45 and GINS. It remains unclear how elongating replisomes are distinguished from terminated replisomes, since an inactive replisome is not sufficient for Mcm7 ubiquitylation.

Recently, it was reported that replication fork progression is coordinated by the p97 cofactor UBXN-3 in *Caenorhabditis elegans* and FAS-associated factor 1 (FAF1) in humans, respectively (Franz et al, 2016). It was shown that UBXN-3/FAF1 binds to CDT-1 and additional ubiquitylated proteins, thereby recruiting CDC-48/p97 for turnover and disassembly of DNA replication factor complexes. Consequently, inactivation of UBXN-3/FAF1 stabilized CDT-1 and CDC-45/GINS on chromatin, which led to replication stress. This replication stress provoked a pronounced decrease in replication fork velocity, an increased number of stalled forks, and newly fired origins, finally resulting in genotoxic DNA breaks and thus, genome instability. The replication checkpoint was activated and DNA repair foci were formed.

In addition to its role in replication initiation and termination, p97 probably regulates further steps during DNA synthesis, since it directly interacts with several replicative helicases including the Werner protein and HIM-6 (Bloom helicase homolog; Partridge et al, 2003; Indig et al, 2004; Caruso et al, 2008).

1.4.4 p97 in transcription

Like mitosis, G1/S transition, and DNA replication, DNA transcription requires p97 activity. In the budding yeast *Saccharomyces cerevisiae*, the transcriptional repressor MATα2 is crucial for the regulation of mating type-specific gene expression. While ubiquitin-dependent turnover of MATα2 is responsible for the switch to the α-mating type (Laney, 2003), instant derepression of target genes also requires acute removal of the MATα2 repressor from promoters. MATα2 is ubiquitylated by Doa3 and Slx8 (Xie et

al, 2010), before it is turned over with the help of $Cdc48^{Ufd1-Npl4}$ (Wilcox & Laney, 2009). Although free MATα2 is rapidly degraded by the proteasome, the ubiquitin-dependent extraction of MATα2 was independent of protein stability. This indicates that chromatin eviction and degradation of MATα2 are independent processes (Wilcox & Laney, 2009).

Moreover, in yeast Cdc48 mediates the dissociation of Spt23p into two forms, p90 and p120, and allows the ubiquitylated p90 to translocate into the nucleus and act as a transcription factor inducing gene expression (Rape et al, 2001).

In *Caenorhabditis elegans*, CDC-48 cooperates with the ubiquitin ligase CUL-2 to regulate levels of the transcription factor TRA-1 and thereby controls sex determination (Sasagawa et al, 2009).

1.4.5 p97 and its cofactors in the DNA damage response

Cells are constantly exposed to a multitude of genotoxic insults, including environmental factors like UV light or ionizing radiation (IR) and endogenous metabolic products such as formaldehyde which can cause DNA damage. DNA damage, if unrepaired, can lead to mutagenesis and genome instability, and thus contribute to tumorigenesis and aging. To encounter this problem, cells have evolved diverse DNA repair and DNA damage tolerance pathways that are activated in the DDR (Nyberg et al, 2002; Jackson & Bartek, 2009). The choice between these pathways depends on the type of lesion and the cell cycle stage. Over the last decade, p97 has been linked to many of these pathways. Notably, upon DNA damage, p97 is phosphorylated at S784 by DNA-PK and accumulates at sites of DNA lesion (Livingstone et al, 2005).

1.4.5.1 DNA damage during DNA replication – translesion synthesis and template switch

Since cells are constantly exposed to genomic stress, they also must attempt to replicate damaged DNA. During S phase, secondary DNA structures, DNA-protein complexes or damaged bases can impede DNA replication. To ensure faithful replication in the presence of DNA damage, cells activate an intra S phase checkpoint to slow down replication (Branzei & Foiani, 2010). When replication forks encounter DNA lesions, they stall because the high-fidelity polymerases cannot accommodate damaged bases in their active sites. This can potentially lead to fork collapse, giving rise to highly cytotoxic DSBs. To cope with this issue, cells have evolved strategies to bypass replication-blocking lesions. Either, the lesions can be bypassed by specialized DNA polymerases in a process called translesion synthesis (TLS; Sale et al, 2012), or the cell uses the complementary strand and makes a template switch. The decision

between these two pathways is triggered by ubiquitylation of PCNA. Monoubiquitylation at K164 by the ubiquitin ligase RAD6/RAD18 leads to TLS (Friedberg et al, 2005), while polyubiquitylation with K63-linked ubiquitin chains results in a template switch. When PCNA is monoubiquitylated, it recruits TLS polymerases via interactions with their ubiquitin-binding domains, followed by a polymerase switch at the lesion. Many TLS polymerases belong to the Y family, characterized by large active sites that accommodate distorted bases or bulky DNA lesions (Prakash et al, 2005). These polymerases are Polη, Polι, Polκ and Rev1. TLS across moderate lesions like UV-induced cyclobutane pyrimidine dimers (CPDs) is established by Polη. Bulkier adducts such as UV-induced 6-4photoproducts (6-4PPs) require the activity of at least two TLS polymerases. While a member of the Y family polymerases inserts nucleotides opposite of the lesion, the B family member Polζ carries out an extension step (Prakash, 2002; Livneh et al, 2010; Sale et al, 2012). Due to the low fidelity of TLS polymerases, TLS is a potentially error-prone process and bears an intrinsic mutagenic nature (Kunz et al, 2000). Thus, ideally, TLS polymerase activity has to be restricted to sites of DNA damage. After lesion bypass, PCNA is deubiquitylated by the ubiquitin specific peptidase USP1 (Huang et al, 2006). This induces the switch from translesion back to replicative polymerases and continuation of DNA replication (Fox et al, 2011).

Recently, the p97 adaptor protein DVC1 has been identified as a central factor in TLS (Centore et al, 2012; Davis et al, 2012; Ghosal et al, 2012; Juhasz et al, 2012; Machida et al, 2012; Mosbech et al, 2012; Kim et al, 2013). DVC1 can bind ubiquitin via an UBZ4-type domain and it can interact with PCNA via a PIP box (Centore et al, 2012; Davis et al, 2012; Ghosal et al, 2012; Juhasz et al, 2012; Machida et al, 2012; Mosbech et al, 2012). While some studies suggest that DVC1 recruitment to stalled replication forks requires RAD18-mediated monoubiquitylation of PCNA (Centore et al, 2012; Ghosal et al, 2012; Juhasz et al, 2012; Machida et al, 2012), two other studies report that DVC1 recruitment is independent of RAD18 (Davis et al, 2012; Mosbech et al, 2012). Moreover, one group claims that DVC1 promotes a feed-forward loop to enhance PCNA ubiquitylation and TLS (Centore et al, 2012), whereas according to another group, DVC1 protects ubiquitylated PCNA from deubiquitylation by USP1 and hence supports TLS (Juhasz et al, 2012). Yet another study suggests that DVC1 negatively influences TLS dependent on POLD3, which is the accessory subunit of the replicative Polδ. By interaction of its SprT domain with POLD3, DVC1 inhibits the extension step of Rev1/Polζ-dependent error-prone TLS (Kim et al, 2013). Apart from its UBZ domain and its PIP box, DVC1 contains a SHP box, with which it recruits p97 to stalled replication forks (Davis et al, 2012; Ghosal et al, 2012; Mosbech et al, 2012). Ghosal and colleagues propose that DVC1 prevents removal of RAD18 and

monoubiquitylated PCNA from chromatin by p97 (Ghosal et al, 2012). Furthermore, they and another independent group suggest that DVC1 removes the replicative Polδ at UV lesions to allow recruitment of Polη (Ghosal et al, 2012; Juhasz et al, 2012). Conversely, two studies claim that DVC1 recruits p97 to stalled replication forks to extract Polη and allow the switch to replicative polymerases after bypassing the UV lesion (Davis et al, 2012; Mosbech et al, 2012). Moreover, it is under debate whether the p97 cofactors Ufd1 and Npl4 are involved in TLS (Davis et al, 2012) or not (Mosbech et al, 2012). In summary, there is controversy, if DVC1 positively regulates TLS (Centore et al, 2012; Ghosal et al, 2012; Juhasz et al, 2012; Machida et al, 2012) or if it prevents excessive TLS and limits the incidence of mutations induced by DNA damage (Davis et al, 2012; Mosbech et al, 2012; Kim et al, 2013).

1.4.5.2 p97 in nucleotide excision repair

UV-induced DNA lesions like CPDs and 6-4PPs are removed by NER to preserve genome integrity. NER is subdivided in transcription-coupled NER (TC-NER), which selectively removes UV lesions from actively transcribed genes, and global genome NER (GG-NER). When RNA polymerase II complexes stall at photolesions during transcription, they are displaced to make the lesion accessible to NER proteins. Following its displacement, the largest subunit of RNA polymerase II, Rpb1, is degraded by the proteasome in a ubiquitin-dependent manner (Wilson et al, 2013). In yeast, Rpb1 ubiquitylation is mediated by the HECT ubiquitin ligase Rsp5 and the CUL3-based $CRL3^{ELC1}$ complex. After K63-linked polyubiquitylation of Rpb1 catalyzed by Rsp5 (Huibregtse et al, 1997; Kim & Huibregtse, 2009), the DUB Ubp2 trims these chains to single ubiquitin moieties, before $CRL3^{ELC1}$ extends these single ubiquitin moieties to K48-linked ubiquitin chains required for Rpb1 degradation (Harreman et al, 2009). In contrast, in human cells the Rsp5-related NEDD4 governs UV-induced turnover of Rpb1 (Anindya et al, 2007; Harreman et al, 2009). A study in budding yeast demonstrated that $Cdc48^{Ufd1\text{-}Npl4}$ is required for degradation of Rpb1 after UV treatment (Verma et al, 2011). In addition to the ubiquitin adapter Ufd1-Npl4, this process requires the less well-characterized Cdc48 adapters Ubx4 (UBXD9 in humans) and Ubx5 (UBXD7 in humans).

In addition to Rpb1 degradation, p97 mediates the degradation of CSB, which is required for the proteolytic release of RNA polymerase II (Bregman et al, 1996; Svejstrup, 2002; Anindya et al, 2007). CSB has a translocase (DNA-dependent ATPase) activity which is able to remodel the interface between RNA polymerase II and damaged DNA to allow repair to take place (Citterio, 1998; Citterio et al, 2000; Svejstrup, 2002; Cho et al, 2013). CSB undergoes proteasomal degradation after

ubiquitylation by the CUL4A-DDB1^{CSA} E3 ligase (Groisman, 2006). It has been shown that p97, Ufd1, and UBXD7 are involved in CSB turnover (He et al, 2016). The degradation of CSB is suggested as a prerequisite for post-TC-NER recovery of RNA synthesis. It is conceivable that the timely removal of lesion-arrested RNA polymerase II or CSB from lesion sites promotes the productive sequential assembly of the pre-incision complex.

Independently of transcription, the DNA damage sensor proteins DDB2 and XPC recognize UV lesions and induce the GG-NER pathway (de Laat et al, 1999). While XPC detects various helix-distorting photoproducts and DNA adducts, DDB2 is specialized on the recognition of UV-induced CPDs and 6-4PPs (Hwang et al, 1999; Wakasugi et al, 2002; Wittschieben, 2005; Fischer et al, 2011; Yeh et al, 2012). Interestingly, DDB2 is part of a CUL4A-DDB1 ubiquitin ligase complex which is recruited to DNA lesions by DDB2 (Scrima et al, 2008). This ubiquitin ligase complex catalyzes ubiquitylation of DDB2 itself, leading to its proteasomal degradation, and of the second DNA lesion sensor XPC, which has been proposed to enhance its binding to DNA (Sugasawa et al, 2005). Then, p97 is recruited to UV lesions in a ubiquitin- and DDB2-dependent manner and helps to remove chromatin extraction of DDB2 and XPC (Puumalainen et al, 2014). For DDB2 removal, it was shown that p97 acts together with Ufd1-Npl4 and UBXD7. Prolonged chromatin retention of DDB2 and XPC results in impaired DNA repair of UV lesions and compromised genome integrity.

Following damage recognition, about 25-30 nucleotides around the lesion site of the damaged strand are excised by structure-specific endonucleases. The resulting gap is filled by DNA polymerization dependent on PCNA and CUL4A^{DDB2}. Like in normal DNA replication, CDT1 binds to PCNA to initiate gap-filling DNA synthesis. Upon initiation, CDT1 is polyubiquitylated by CUL4-DDB1$^{DDB2-CDT2}$, segregated from chromatin by p97$^{Ufd1-Npl4}$ and degraded by the proteasome (Nishitani et al, 2006; Raman et al, 2011; Ramanathan & Ye, 2011).

1.4.5.3 p97 in the Fanconi anemia DNA repair pathway

DNA interstrand crosslinks are an obstacle to ongoing DNA replication and transcription machineries (Kim & D'Andrea, 2012; Kottemann & Smogorzewska, 2013). In order to repair interstrand crosslinks, cells activate the Fanconi anemia (FA) DNA repair pathway. The key player of this repair pathway, which relies on the programmed formation of a DSB, is the FANCI/FANCD2 complex (ID complex). ATM/ATR kinases phosphorylate FANCI, which is suggested to stabilize the interaction between FANCD2 and FANCI (Ishiai et al, 2008; Joo et al, 2011). Subsequently, FANCD2 is monoubiquitylated at K561 and FANCI on K523 by the FA core complex, a large

multisubunit ubiquitin ligase (Kim & D'Andrea, 2012). Upon ubiquitylation, nucleases like XPF/ERCC1 are recruited to the ID complex, which then incise the DNA in proximity to the interstrand crosslink to cut out the crosslink with the concomitant formation of a DSB (Knipscheer et al, 2009; Hodskinson et al, 2014; Klein Douwel et al, 2014). Monoubiquitylation of the ID complex is antagonized by the DUB complex USP1-UAF1 (Cohn et al, 2007). In addition to phosphorylation and monoubiquitylation, the tumor suppressors FANCI and FANCD2 are sumoylated by the SUMO E3 ligases PIAS1/PIAS4 upon replication fork stalling (Gibbs-Seymour et al, 2015). This sumoylation is antagonized by the SUMO protease SENP6. Sumoylation of the ID complex, in turn, triggers its polyubiquitylation by the SUMO-targeted ubiquitin ligase RNF4, thereby promoting its dissociation from sites of DNA damage through the $p97^{DVC1}$ ubiquitin segregase complex (Gibbs-Seymour et al, 2015). The FA pathway uses translesion synthesis, homologous recombination, and nucleotide excision repair to complete the repair process (Knipscheer et al, 2009; Zhang & Walter, 2014).

1.4.5.4 p97 in DSB repair

The most deleterious type of DNA lesion is the DSB. If not repaired, it can lead to chromosomal rearrangements, deletions and genome instability or even cell death. It is estimated that approximately 1% of single-strand breaks are converted to DSBs in human cells per cell cycle, which yields about 50 endogenous DSBs (Vilenchik & Knudson, 2011). This number resembles the number of DSBs induced by 1.5-2.0 Gy of IR.

After DNA damage, the histones H2A and H2AX are ubiquitylated at sites of DSBs (Bekker-Jensen & Mailand, 2011). The two ubiquitin ligases RNF8 and RNF168 have emerged to catalyze ubiquitin chain formation at sites of DNA damage. Together, they assemble K63 ubiquitin chains, while RNF8 alone forms K48 ubiquitin chains. RNF8 recruits proteasomes to DNA lesions (Galanty et al, 2012) and targets chromatin-associated proteins for proteasomal degradation. The histones H2A and H2AX are modified by K63 ubiquitin chains at K13-15 (Mattiroli et al, 2012). Subsequently, p97 is recruited to RNF8/K48 ubiquitin conjugates via its ubiquitin adapter Ufd1-Npl4 and removes them to orchestrate proper association of the DDR proteins BRCA1, Rad51, and 53BP1 (Meerang et al, 2011). Thus, p97-dependent degradation of K48 ubiquitylated proteins is critical for activation of the DDR (Ramadan, 2012). Impairment of p97 activity reduces the main branches of DSB repair, homologous recombination (HR) and non-homologous end-joining (NHEJ), and decreases cell survival after IR (Meerang et al, 2011). However, the specific p97 substrates at DSB sites as well as the mechanisms by which p97 influences DSB repair remain unknown.

In contrast to RAD18 and the BRCA1/RAP80 complex, 53BP1 directly interacts with a dimethyl mark at K20 of the core histone H4 (H4K20me$_2$) at sites of DNA damage via its tandem Tudor domain (Botuyan et al, 2006). In undamaged chromatin, the same mark is bound by the second malignant brain tumor (MBT) domain of the tumor suppressor L3MBTL1 (Min et al, 2007). Upon DNA damage in form of DSBs, L3MBTL1 is removed from chromatin by the ubiquitin ligases RNF8/RNF168 and the segregase p97$^{Ufd1-Npl4}$ (Acs et al, 2011). Release of L3MBTL1 from H4K20me$_2$ at DSBs then allows binding of 53BP1 to the newly exposed histone methyl marks. Recently, it was shown that 53BP1 additionally binds to the ubiquitylated lysine residue 15 of histone H2A (H2AK15ub; Fradet-Turcotte et al, 2013), of which ubiquitylation is catalyzed in response to DNA damage by RNF168 (Mattiroli et al, 2012). Thus, 53BP1 recognizes two DNA damage-induced histone modifications by which it is recruited to DSBs.

Another protein which associates with H4K20me$_2$ is the histone demethylase JMJD2A/B, which is ubiquitylated by RNF8 before it is degraded by the proteasome (Mallette et al, 2012). Regarding JMJD2A/B degradation, it remains to be clarified if p97 is implicated.

Repair of DSBs by HR implicates the formation of a nucleoprotein filament formed by the recombinase RAD51 between the sister chromatids. In *Saccharomyces cerevisiae*, loading of RAD51, which replaces RPA on single-stranded DNA, depends on DNA damage-induced sumoylation of its binding partner RAD52. Modification of RAD52 with the small ubiquitin-related modifier SUMO promotes the interaction of RAD52 with RAD51, which contains a SUMO-interacting motif (SIM; Bergink et al, 2013). Intriguingly, Cdc48 and Ufd1 in yeast also bear a SIM (Hannich et al, 2005; Nie et al, 2012) that binds to sumoylated RAD52 resulting in destabilization of RAD51-RAD52 interaction *in vitro* (Bergink et al, 2013). However, the significance of this pathway in mammals remains elusive. Notably, it was shown that impaired p97 function entails compromised RAD51 accumulation after IR concomitant with decreased HR (Meerang et al, 2011). Thus, p97 possibly restricts spontaneous HR by removing RAD52 from chromatin, while it promotes IR-induced HR through another unknown mechanism.

1.5 p97-associated diseases

The participation of p97 in a wide variety of cellular processes suggests a diverse involvement in disease. Indeed, p97 has been implicated in the pathogenesis of many human diseases, including Paget's disease of bone, several types of neurodegenerative disorders, and different kinds of cancer (Vij, 2008; Haines, 2010).

Inclusion body myopathy associated with Paget's disease of bone and frontotemporal dementia (IBMPFD) has been directly associated with p97 dysfunction (Kimonis et al,

2008). IBMPFD is an autosomal dominant negative inherited degenerative disorder caused by a missense mutation in p97 (Watts et al, 2004). Patients suffering from IBMPFD have different p97 mutations that are all primarily located at the interface of the N and the D1 domain (Weihl et al, 2009). The most frequent mutation is the exchange of arginine at position 155 for histidine (R155H; Hubbers et al, 2007). IBMPFD is characterized by disabling weakness, osteolytic lesions consistent with Paget's disease of bone and frontotemporal dementia. In tissues of patients with IBMPFD, cytoplasmic and nuclear ubiquitin-positive aggregates are accumulated. There is evidence that defective p97 functioning in lysosomal degradation is the primary cause of IBMPFD (Ju et al, 2009; Ju & Weihl, 2010; Tresse et al, 2010; Bug & Meyer, 2012).

Additionally, p97 mutations have been linked to 2% of isolated familial amyotrophic lateral sclerosis (ALS; Johnson et al, 2010).

Furthermore, dysfunctional p97 was found in cells expressing numerous polyglutamine proteins which give rise to neurodegenerative diseases like Huntington's disease, spinal and bulbar muscular atrophy and several inheritable spinocerebellar ataxias (La Spada & Taylor, 2010). Recently, a study connected DNA repair defects to polyglutamine diseases. This study revealed that the p97-mediated extraction of L3MBTL1 at DNA lesions was impaired in cellular as well as fly models of multiple polyglutamine diseases (Fujita et al, 2013).

Despite the crucial role of p97 for genomic maintenance (Cheng & Chen, 2010; Dobrynin et al, 2011; Riemer et al, 2014) and for modulation of various oncogenes and tumor suppressors (e.g. HIF1α, p53, IκBα, NF-κB, BRCA1), so far, there is no direct proof that mutations in p97 are related to cancer. Yet, p97 expression levels were found to be altered in cancer patients. Thereby, increased levels of p97 correlated with the progression, prognosis, and metastatic potential of many cancers (Chapman et al, 2015). Patients with tumors that express high levels of p97 display a higher recurrence rate, poorer disease-free periods and overall survival. Tumors, where elevated p97 levels have been observed, include colorectal carcinoma, pancreatic cancer, thyroid cancer, breast cancer, squamous cell carcinoma, gastric carcinoma, osteosarcoma, liver, ovary, and lung cancer. In contrast, low p97 expression levels have been found in adenomas. It remains unclear, if higher p97 levels are responsible for the turnover of growth inhibitory proteins or if elevated p97 expression is the result of protein-induced stress in cancer (Haines, 2010).

Not only p97 itself, but also a few of its cofactors have been linked to cancer. For example, haploinsufficiency of the FAF1 gene, which belongs to the UBX family of p97 adaptor proteins, was found in 30% of cervical carcinomas and 12.5% of mantle-cell

lymphomas (Hidalgo et al, 2005; Bea et al, 2009). Moreover, FAF1 protein levels are decreased in gastric carcinomas and a large percentage of mesotheliomas (Bjørling-Poulsen et al, 2003; Altomare et al, 2009). Recently, a homozygotic mutation in the p97 adaptor DVC1 has been associated with genome instability, premature ageing and cancer predisposition both in humans (Lessel et al, 2014) and in mice (Maskey et al, 2014).

While the neurodegenerative diseases associated with dysfunctional p97 would require restoration of p97 function for cure, cancers with increased p97 levels could be treated with p97 inhibition. Indeed, tumor growth of non-small cell lung carcinoma was significantly reduced *in vitro* and *in vivo* by inhibition of p97 with the small molecule Eeyarestatin I (Valle et al, 2011). Additionally, there is a direct link between p97 and the levels of p53 and NF-κB, two transcription factors involved in cancer cell survival (Valle et al, 2011). This suggests that elevated p97 levels may be directly responsible for tumorigenesis. There is growing evidence that tumor cells are susceptible to p97 inhibition (Valle et al, 2011; Chou et al, 2011; Chou et al, 2013; Magnaghi et al, 2013; Cervi et al, 2014; Anderson et al, 2015; Zhou et al, 2015; Parzych et al, 2015; Nadeau et al, 2015).

1.6 p97 inhibitors

Currently, the only established drugs targeting protein quality control used in the clinics are proteasome inhibitors like bortezomib or carfilzomib that are applied to treat multiple myeloma and lymphoma (Jain et al, 2011; Goldberg, 2012). It has been proposed that these drugs mainly affect the secretory pathway and thus, are effective against blood cancers that derive from cells producing large numbers of secretory proteins. The success of bortezomib and carfilzomib proves that targeting protein quality control is a viable treatment option. However, the search for other targets in the protein quality control pathway was expanded to achieve enhanced cancer cell specificity, increased clinical utility, a lower resistance rate, decreased toxicity, and mitigated site effects. Over the last decade, p97 has evolved as a promising target since it is involved in ERAD, activates pro-survival transcription factors, is implicated in autophagy and regulates the cell cycle, all of which are proven to be critical in cancer therapy (Braun & Zischka, 2008; Haines, 2010; Chapman et al, 2011; Choi et al, 2013).

In 2004, the first p97 inhibitor eeyarestatin I (EerI) was identified (Fiebiger, 2004). EerI was shown to inhibit ERAD (Wang et al, 2008; Wang et al, 2010) and to work in concert with bortezomib in inducing ER-stress-mediated apoptosis in cancer cells (Wang et al, 2009; Auner et al, 2013). Recently, it was demonstrated that EerI induces DNA damage rather than ER stress and that it selectively kills canine lymphoma cells

(Nadeau et al, 2015). However, EerI suffers from irreversibility, and low potency (Wang et al, 2008; Wang et al, 2010).

The first reversible, selective small molecule p97 inhibitor was discovered in 2011 (Chou et al, 2011). N^2, N^4-dibenzylquinazoline-2,4-diamine (DBeQ) efficiently blocks p97-dependent processes, including autophagy and proteasome-mediated degradation of ubiquitin fusion degradation and ERAD substrates (Chou et al, 2011). Moreover, DBeQ rapidly activates apoptotic cell death and inhibits cancer cell growth (Chou et al, 2011; Chou & Deshaies, 2011). Further studies revealed that DBeQ binds to the D1 and the D2 domain of p97 (Chou et al, 2014).

In 2013, alkylsulfanyl-1,2,4-triazoles were identified as a new class of p97 inhibitors with sub-micromolar IC50 values (Polucci et al, 2013). Among these alkylsulfanyl-1,2,4-triazoles that affect p97 were the covalent inhibitor NMS-859 and the allosteric inhibitor NMS-873 (Magnaghi et al, 2013). NMS-859 binds to C522 in the D2 ATP binding pocket (Magnaghi et al, 2013). In contrast, the allosteric inhibitor NMS-873 targets the D2 Walker B motif and prevents ADP-release from the D1 and the D2 domain (Magnaghi et al, 2013; Burrell et al, 2013; Chou et al, 2014). Both molecules caused an accumulation of ubiquitylated proteins, induced the unfolded protein response due to ER stress, compromised autophagy, and induced apoptosis in HCT116 cells (Magnaghi et al, 2013). In addition, they led to a cell cycle arrest in G2 in HCT116 cells (Magnaghi et al, 2013). The effect of NMS-873 was compared to the effect of bortezomib in 37 cancer cell lines (Magnaghi et al, 2013). It was observed that specific cell lines were differentially sensitive to the two inhibitors, arguing for a therapeutic use of p97 inhibitors in the treatment of diverse cancers, not only of blood cancers as in the case of bortezomib. Furthermore, it was demonstrated that the presence of the p97 cofactor p47, which inhibits p97 ATPase activity, increased the IC50 of NMS-873 (Chou et al, 2014). Altogether, these studies confirmed NMS-873 as a potent, highly specific p97 inhibitor.

Recently, the potent, ATP-competitive, D2-selective, and orally bioavailable p97 inhibitor CB-5083, which is a derivative of DBeQ, has been taken into phase 1 clinical trials in patients with multiple myeloma and solid tumors (Anderson et al, 2015; Zhou et al, 2015).

1.7 Aims of the thesis

At the start of this thesis, accumulating evidence from different organisms suggested that p97 was not only involved in mitosis, but also in the DNA damage response and replication stress responses in interphase. The aim of this thesis was therefore to

explore possible mechanisms and the relevance of these roles in human cells. To do so, this study concentrated on three major aspects.

The first aim was to clarify a possible implication of p97 in DNA damage checkpoints. Thereby, this study contributes to understanding the function of the $p97^{Ufd1\text{-}Npl4}$ complex in the G2/M checkpoint, facilitating the degradation of CDC25A (published in Riemer et al., 2014).

Second, we analyzed the significance of p97 and its cofactors for survival of human cancer cells after replication stress. This included an investigation of possible synergistic effects of novel p97 inhibitors with genotoxic chemotherapeutic agents and their influence on the DNA damage response.

Third, we explored the role of the novel p97 cofactor UBXD7 that was recently linked to DNA repair. For this purpose, we examined the relevance of UBXD7 for diverse p97 substrate proteins including CDC25A and a detailed structure-function analysis of UBXD7 to investigate its functional relationship to p97.

2 Results

2.1 The role of p97 for the G1/S and intra S checkpoints

Recently, our laboratory has shown that $p97^{Ufd1-Npl4}$ is required for the activation of the G2/M checkpoint by facilitating the degradation of the phosphatase CDC25A (Riemer et al, 2014). CDC25A is responsible for removing inhibitory phosphates from CDKs, leading to their activation and thus cell cycle progression. Hence, inactivation of CDC25A by degradation leads to a cell cycle arrest. As part of the study published in Riemer et al, 2014, we raised the question if $p97^{Ufd1-Npl4}$ helps to degrade CDC25A only in the G2/M checkpoint, or additionally in the G1/S checkpoint and the intra S checkpoint, since CDC25A is involved in G1/S transition, S phase progression and G2/M transition.

2.1.1 No effect of Ufd1-Npl4 depletion on the G1/S checkpoint

To explore the importance of p97 and its cofactors for the G1/S checkpoint, a dual-color flow cytometric analysis with 5-bromo-2'-deoxyuridine (BrdU) and the DNA-binding dye propidium iodide (PI) was performed (Xu & Kastan, 2004). BrdU is a synthetic nucleoside which is incorporated into newly synthesized DNA of replicating cells in place of its analog thymidine. BrdU incorporation can then be detected with specific antibodies, highlighting cells that were undergoing DNA replication. Counterstaining with PI shows the cell cycle.

In our setting, HeLa cells were depleted of p97, Ufd1, or Npl4 with small interfering RNAs (siRNAs) for 48 h and irradiated with 6 Gy to activate DNA damage checkpoints. An siRNA targeting luciferase (siluc) served as a negative control, whereas downregulation of the checkpoint kinase Chk1 was supposed to inhibit the checkpoint. The cells were pulse-labeled with 10 µM BrdU for 30 min 24 h post irradiation and then harvested and fixed with 80% ethanol. To allow antibody binding, DNA was denatured by acid treatment with hydrochloric acid. Finally, staining of anti-BrdU antibody and PI were detected by flow cytometry.

Data analysis revealed that mock-depleted cells showed a marked decrease in DNA synthesis after irradiation, indicated by reduced BrdU incorporation (Fig. 2.1 and 2.2). In contrast, knockdown of Chk1 resulted in an override of the checkpoint, since irradiation did not affect the percentage of BrdU-positive cells. Depletion of Ufd1 or Npl4 displayed a decrease in DNA synthesis after irradiation, indicating a functional G1/S checkpoint. Intriguingly, knockdown of p97 significantly reduced the percentage of BrdU-incorporating cells in non-irradiated cells. Moreover, this drop in replicating

cells was not further reduced upon irradiation. Notably, none of the depletions led to a major change in cell cycle distribution (Fig. 2.1).

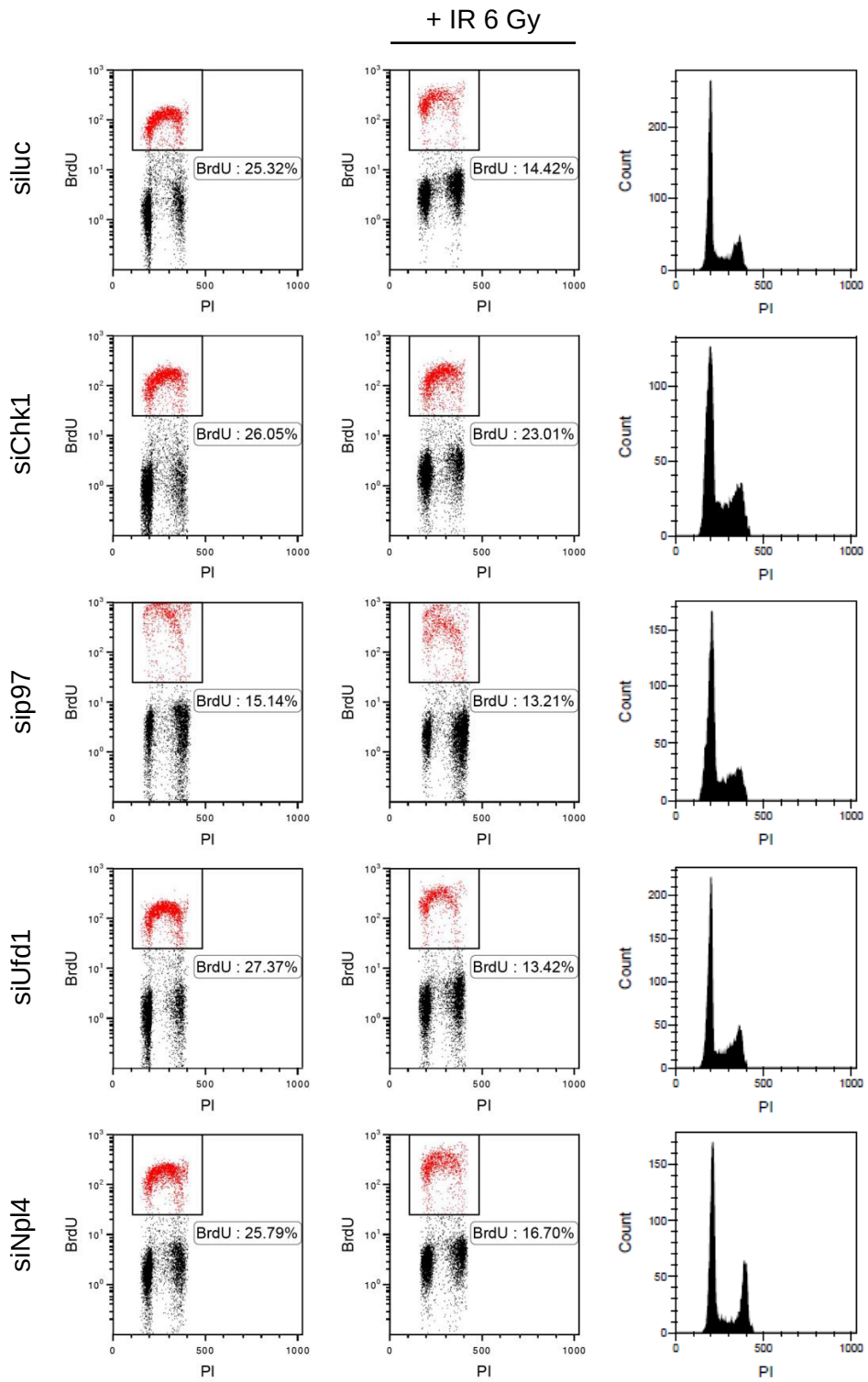

Figure 2.1: Representative dot plots and histograms of siRNA-treated cells for analysis of the G1/S checkpoint. HeLa cells were mock-transfected with siluc or with siRNAs targeting Chk1, p97, Ufd1, or Npl4 for 48 h. The cells were irradiated with 6 Gy and fixed 24 h later. Prior to fixation, the cells were pulse-labeled with BrdU for 30 min. Samples were co-stained with an anti-BrdU antibody and the DNA-binding dye propidium iodide (PI), before they were analyzed by flow cytometry. The BrdU-positive cells are highlighted in red. Histograms show no major impact on the cell cycle upon depletion of the indicated proteins.

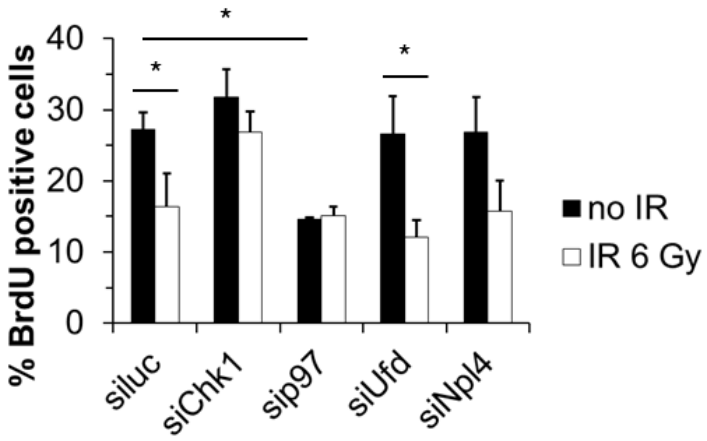

Figure 2.2: Ufd1-Npl4 depletion does not affect the G1/S checkpoint. Quantification of BrdU-positive cells in an analysis of the G1/S checkpoint. HeLa cells were depleted of the indicated proteins for 48 h. The cells were irradiated with 6 Gy and fixed 24 h later. Prior to fixation, the cells were pulse-labeled with BrdU for 30 min. The staining with an anti-BrdU antibody was detected by flow cytometry. Shown are means of three to four independent experiments and error bars represent s.d. * $p < 0.05$.

Taken together, these data show that Ufd1-Npl4 depletion has no effect on the G1/S checkpoint. However, p97 seems to be important for DNA replication.

2.1.2 βTrCP and DVC1 are important for the intra S checkpoint

To investigate if p97 participates in the intra S checkpoint, a replication assay (radioresistant DNA synthesis, shortly RDS) was applied (Xu & Kastan, 2004). Similar to the BrdU assay, the RDS assay is based on the incorporation of radioactively labeled thymidine into newly synthesized DNA. Since DVC1 was shown to be involved in TLS, we included this p97 adaptor in our setting.

HeLa cells were mock-transfected with siluc or transfected with siβTrCP, sip97, siNpl4, siUfd1, or siDVC1 for 48 h. Knockdown of βTrCP served as a positive control, as its downregulation by RNA interference (RNAi) was already demonstrated to result in a defective intra S checkpoint and RDS due to stabilization of CDC25A phosphatase (Busino et al, 2003). The cells were irradiated with 10 Gy and fixed with ethanol after 15 min, 1 h, and 4 h, respectively. Before fixation, the cells were pulse-labeled for 15 min with ^{3}H-thymidine. Incorporation of ^{3}H-thymidine was quantified by a scintillation counter.

In general, 1 h after irradiation, the cells showed a decrease in DNA synthesis, from which they recovered 4 h after irradiation (Fig. 2.3A to D). Cells depleted of βTrCP or DVC1 showed a significant increase in RDS 1 h after irradiation compared to control-depleted cells (Fig. 2.3E). In contrast, knockdown of p97, or its cofactors Npl4 or Ufd1 only displayed a minor increase in RDS. However, DVC1 and again p97 depletion led

to a significant decrease in DNA synthesis in non-irradiated cells, respectively (Fig. 2.4).

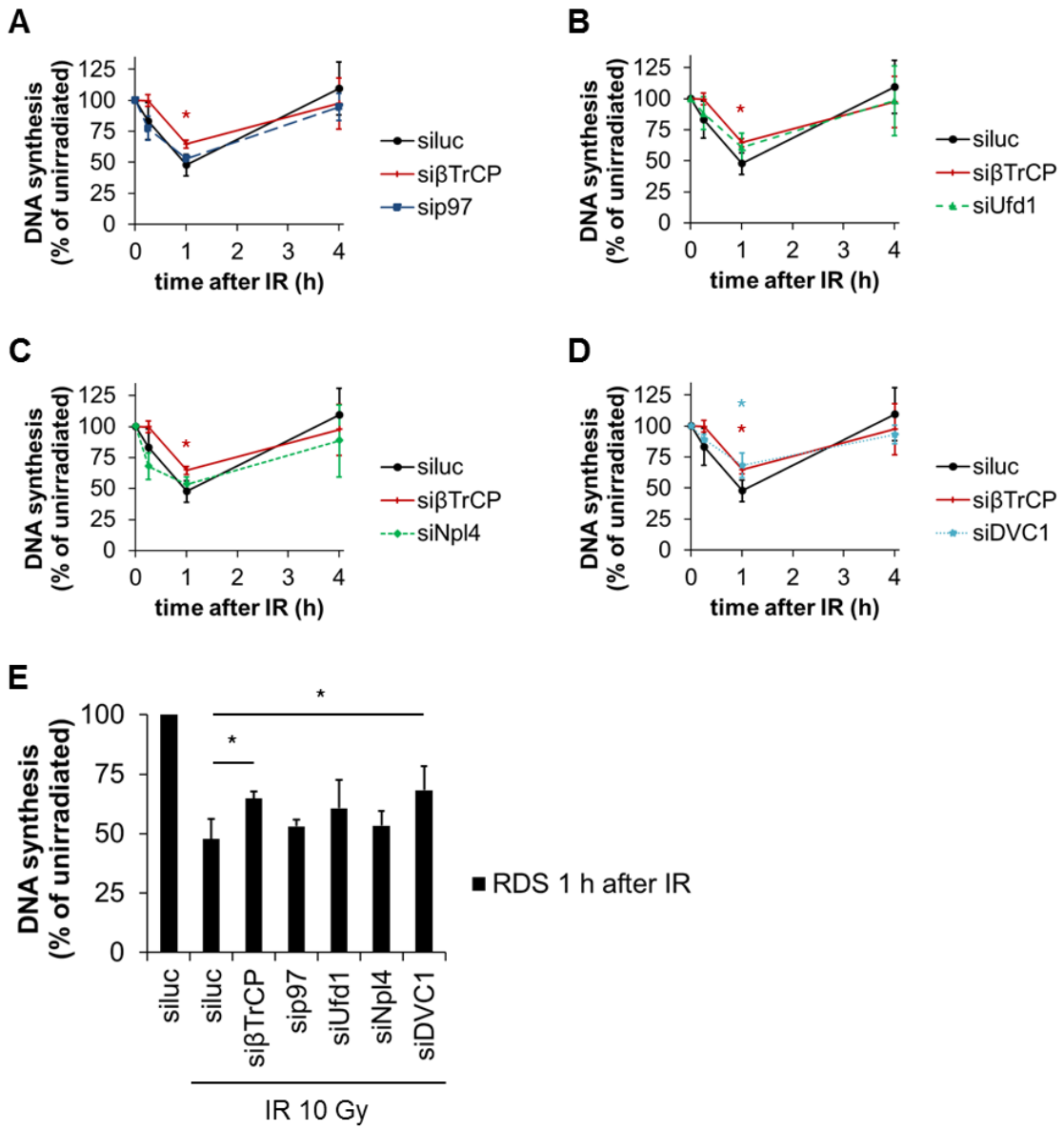

Figure 2.3: Knockdown of βTrCP and DVC1 leads to radioresistant DNA synthesis. (**A, B, C, D**) The kinetics of radioresistant DNA synthesis in depleted cells. HeLa cells were mock-transfected with siluc or with siRNAs targeting βTrCP, p97, Ufd1, Npl4, or DVC1 for 48 h. The cells were irradiated with 10 Gy and fixed after 15 min, 1 h, and 4 h, respectively. Prior to fixation, the cells were pulse-labeled for 15 min with ^{3}H-thymidine. ^{3}H-thymidine was then detected by a scintillation counter. Shown are means of three to five independent experiments and error bars represent s.d. * $p < 0.05$. DNA synthesis levels without IR were set to 100% for each depletion. (**E**) Remaining DNA synthesis 1 h after 10 Gy IR. Data are taken from subfigure **A** to **D**.

Together, these data show that p97 and DVC1 are essential for efficient DNA replication and that DVC1 has a role in the intra S checkpoint.

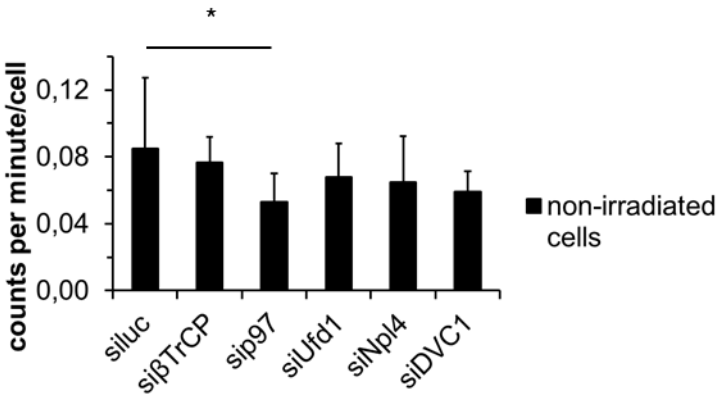

Figure 2.4: Knockdown of p97 leads to a significant reduction in DNA synthesis in non-irradiated cells. HeLa cells were transfected with the indicated siRNAs for 48 h and pulse-labeled for 15 min with ^{3}H-thymidine. ^{3}H-thymidine was then detected by a scintillation counter. Shown are means of three to five independent experiments and error bars represent s.d. * $p < 0.05$.

2.2 p97 ensures robustness of the G2/M checkpoint by facilitating CDC25A degradation

Our laboratory confirmed CDC25A as the p97 target in the G2/M checkpoint by monitoring checkpoint signaling via immunoblot analysis (Riemer et al, 2014). Upon knockdown of Ufd1 or Npl4, the checkpoint kinase Chk1 was phosphorylated at S317 and S345 after treatment with IR suggesting that it was fully activated in the response to DNA damage. Moreover, phosphorylation of CDC25C, which leads to its inactivation by sequestration in the cytoplasm, was unaffected. However, CDC25A was stabilized in Ufd1- as well as Npl4-depleted cells after DNA damage induction. A cycloheximide (CHX) chase revealed that CDC25A degradation after IR is delayed in cells lacking Ufd1 or Npl4, resulting in a compromised G2/M checkpoint.

2.2.1 Generation and characterization of a cell line inducibly expressing GFP-CDC25A

As part of the study published in Riemer et al, 2014, we aimed to further analyze the role of p97 and its cofactors in CDC25A degradation by fluorescence microscopy. For this purpose, a U2OS reporter cell line expressing GFP-CDC25A under control of a doxycycline-inducible promoter was generated and characterized. In the first step, N-terminally tagged GFP-CDC25A was cloned from the vector pOPINE (a gift from Dr. Christian Ottmann, Chemical Genomics Centre, Dortmund, Germany) into the vector pcDNA 5.0/FRT/TO (Invitrogen). To generate a stable cell line inducibly expressing GFP-CDC25A, pcDNA 5.0/FRT/TO-GFP-CDC25A was transfected together with pOG44 Flp-recombinase (Invitrogen) into U2OS-FRT-TO cells for integration into the

genome at the FRT recombination site. The Tet repressor can be removed upon induction with a tetracycline such as doxycycline. Expression of GFP-CDC25A was confirmed by fluorescence microscopy and immunoblot analysis. Fluorescence images show that GFP-CDC25A is expressed in the nuclei after doxycycline treatment (Fig. 2.5A). Moreover, the GFP-CDC25A levels differ from cell to cell. Western blot analysis revealed that doxycycline-induced expression levels of GFP-CDC25A clearly exceed levels of endogenous CDC25A (Fig. 2.5B). Furthermore, induced cells show several GFP-CDC25A degradation products.

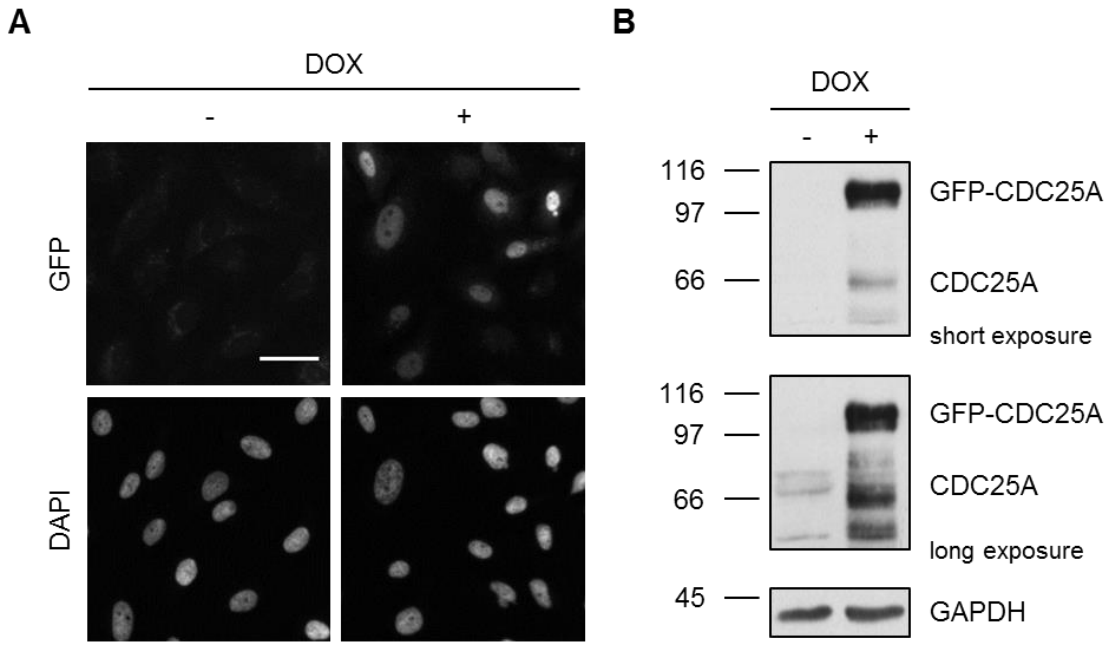

Figure 2.5: A reporter cell line inducibly expressing GFP-CDC25A was generated. (**A**) Microscopy images of doxycycline (DOX)-induced GFP-CDC25A expression. GFP-CDC25A expression of the stably transfected U2OS cells was induced by doxycycline treatment for 24 h. The cells were fixed with paraformaldehyde and nuclei were stained with DAPI. GFP-CDC25A expression was examined by fluorescence microscopy. Scale bar: 50 µm. (**B**) Immunoblot of doxycycline-induced GFP-CDC25A expression. GFP-CDC25A expression of the U2OS reporter cell line was induced by doxycycline for 6 h. The cells were lysed and cell lysates were subjected to SDS-PAGE and Western blotting. GFP-CDC25A and endogenous CDC25A were detected by an anti-CDC25A antibody. GAPDH served as loading control.

2.2.2 GFP-CDC25A is degraded upon IR

Since CDC25A is degraded in the DDR, it was examined if the generated reporter cell line responds to IR. In order to characterize this cell line, the kinetics of GFP-CDC25A degradation was evaluated using fluorescence microscopy and immunoblotting (Fig. 2.6). For fluorescence microscopy, the cells were induced with doxycycline for 24 h. Then, the cells were mock-irradiated or irradiated with 10 Gy and CHX was added to inhibit protein biosynthesis. Thus, protein turnover can be monitored after addition of CHX since no proteins are re-synthesized. At different time points (0, 30, or 60 min) the

cells were fixed with paraformaldehyde and mounted with Mowiol containing the DNA dye DAPI. Fluorescence microscopy showed a significant decrease in GFP intensity already 30 min after irradiation and CHX treatment (Fig. 2.6A and B). GFP-CDC25A degradation can also be followed by immunoblotting. In this approach, again GFP-CDC25A expression was induced by doxycycline treatment for 6 h. Then, the cells were mock-irradiated or irradiated with 10 Gy and CHX was added. At different time points (0, 30, or 60 min) the cells were lysed and cell lysates were subjected to SDS-PAGE and analyzed by Western blotting (Fig. 2.6C). In non-irradiated cells, GFP-CDC25A was degraded within 60 min. After irradiation with 10 Gy, the rate of GFP-CDC25A degradation was accelerated (Fig. 2.6D). This confirms that the reporter cell line inducibly expressing GFP-CDC25A has a functional checkpoint responding to IR-induced DNA damage with CDC25A degradation.

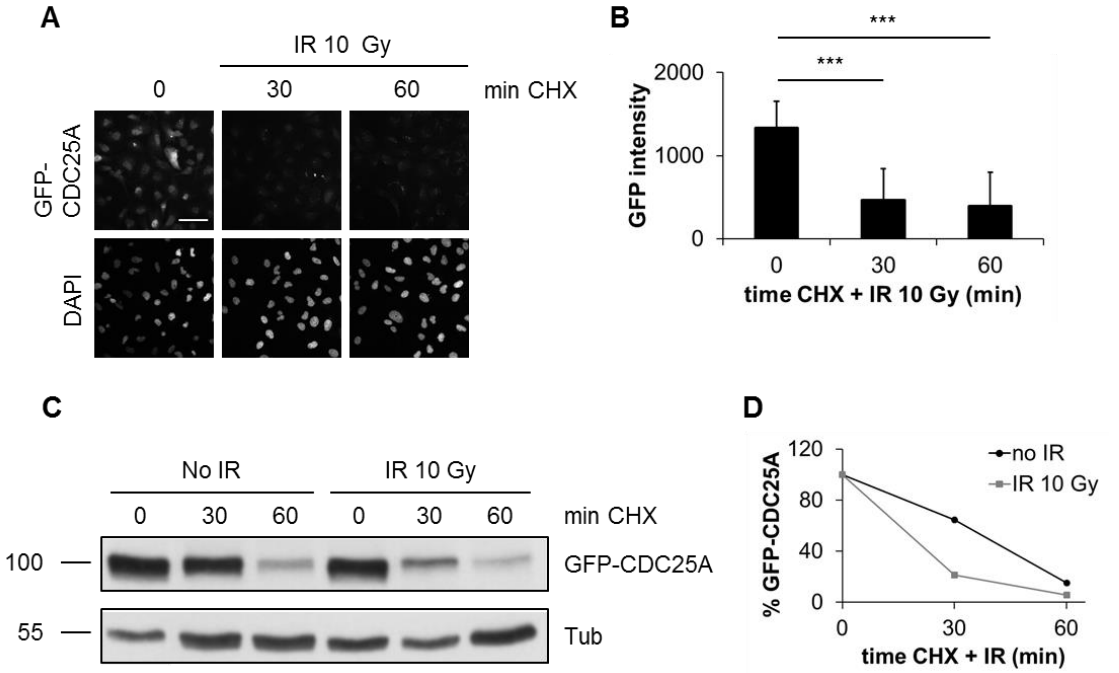

Figure 2.6: The reporter cell line inducibly expressing GFP-CDC25A responds to IR by accelerated GFP-CDC25A degradation. (**A**) Microscopy images of IR-induced GFP-CDC25A degradation. GFP-CDC25A expression of the stably transfected U2OS cells was induced by doxycycline treatment for 24 h. Then, the cells were mock-irradiated or irradiated with 10 Gy and treated with 50 µg/mL CHX to inhibit protein re-synthesis. After 0, 30, or 60 min, the cells were fixed with paraformaldehyde and stained with DAPI. GFP-CDC25A expression was examined by fluorescence microscopy. Scale bar: 100 µm. (**B**) Quantification of **A**. Shown are means of three independent experiments and error bars represent s.d. *** $p < 0.001$. GFP intensity was quantified by ImageJ. (**C**) Immunoblot of IR-induced GFP-CDC25A degradation. GFP-CDC25A expression was induced by doxycycline for 6 h. The cells were mock-irradiated or irradiated with 10 Gy and treated with 50 µg/mL CHX. After 0, 30, or 60 min, the cells were lysed and cell lysates were subjected to SDS-PAGE and Western blotting. GFP-CDC25A was detected by an anti-CDC25A antibody. α-tubulin (Tub) served as loading control. (**D**) Quantification of **C**. Signal density on X-ray films was quantified using BIO1D. GFP-CDC25A levels without CHX were set to 100% for each condition.

2.2.3 GFP-CDC25A degradation is dependent on p97, Npl4, and UBXD7

Next, it was explored if the dependency on $p97^{Ufd1-Npl4}$ for the degradation of endogenous CDC25A is also seen with GFP-CDC25A degradation. For this purpose, irradiation was combined with siRNA-mediated depletions of the p97 cofactors Ufd1 or Npl4 in a CHX chase. First, the U2OS Flp-In cells were mock-transfected with a non-targeting siRNA (siCtrl) or transfected with siRNAs targeting Ufd1, Npl4, or the F-box protein βTrCP for 48 h. $SCF^{\beta TrCP}$ was shown to be the E3 ubiquitin ligase responsible for CDC25A ubiquitylation and therefore served as a positive control (Busino et al, 2003; Kanemori et al, 2005). During the last 6 h of depletion, GFP-CDC25A expression was induced by addition of doxycycline. Then, the cells were mock-irradiated or irradiated with 10 Gy and CHX was added. At different time points (0, 30, or 60 min) the cells were lysed and cell lysates were examined by Western blotting (Fig. 2.7).

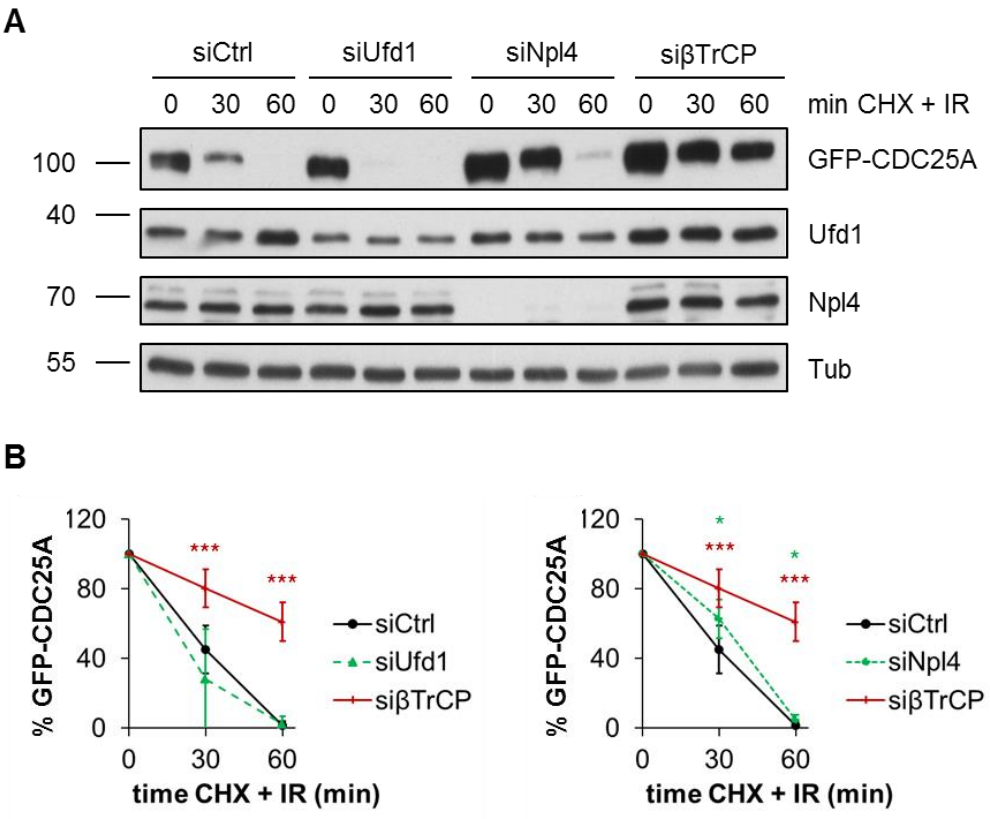

Figure 2.7: Knockdown of Npl4 leads to delayed GFP-CDC25A degradation after IR-induced DNA damage. (**A**) CHX chase of IR-induced GFP-CDC25A degradation in depleted cells. U2OS cells inducibly expressing GFP-CDC25A were mock-depleted or depleted of Ufd1, Npl4, or βTrCP for 48 h. GFP-CDC25A expression was induced during the last 6 h of depletion. Subsequently, the cells were mock-treated or treated with 10 Gy of IR and 50 µg/mL CHX to inhibit protein re-synthesis. After 0, 30, or 60 min, the cells were lysed and cell lysates were subjected to SDS-PAGE and Western blotting. GFP-CDC25A was detected by an anti-CDC25A antibody. α-tubulin (Tub) served as loading control. (**B**) Quantification of **A**. Shown are means of three independent experiments and error bars represent s.d. * $p < 0.05$, *** $p < 0.001$. Signal density on X-ray films was quantified using BIO1D. GFP-CDC25A levels without IR were set to 100% for each depletion.

In control-depleted cells, GFP-CDC25A was degraded rapidly upon IR. Since βTrCP is the ligase that ubiquitylates CDC25A, thereby labeling it for degradation, βTrCP knockdown led to a marked increase in GFP-CDC25A levels and a significantly delayed degradation (Fig. 2.7A and B). GFP-CDC25A degradation was also significantly delayed upon Npl4 depletion, though to a lesser extent than upon βTrCP depletion. Interestingly, GFP-CDC25A levels in Npl4-depleted cells were increased in non-irradiated cells as well, indicating that Npl4, like βTrCP, mediates GFP-CDC25A destruction even in the absence of DNA damage. However, in contrast to knockdown of βTrCP and to our results for endogenous CDC25A, 60 min after irradiation GFP-CDC25A levels were hardly detectable in Npl4-depleted cells. Furthermore, in contrast to Npl4 depletion and unlike in experiments following endogenous CDC25A degradation, knockdown of Ufd1 did not affect GFP-CDC25A turnover compared to control-depleted cells.

Since the observation for Ufd1-depleted cells was contradictory to our results for endogenous CDC25A degradation, several siRNAs targeting Ufd1 were tested for their ability to stabilize GFP-CDC25A levels after DNA damage. To this end, the experiment was repeated with five different oligonucleotides able to downregulate Ufd1, named S1 to S5 (Fig. 2.8). In this experiment, samples were taken 0 and 60 min after IR. Intriguingly, knockdown of Ufd1 with any tested oligonucleotide led to a decrease in GFP-CDC25A levels compared to control-depleted cells, albeit to a different extent. However, all tested oligonucleotides depleted cells of Ufd1 to the same level. Moreover, none of the siRNAs targeting Ufd1 stabilized GFP-CDC25A after IR. In the previous experiment, the S2 oligo was used (Fig. 2.7).

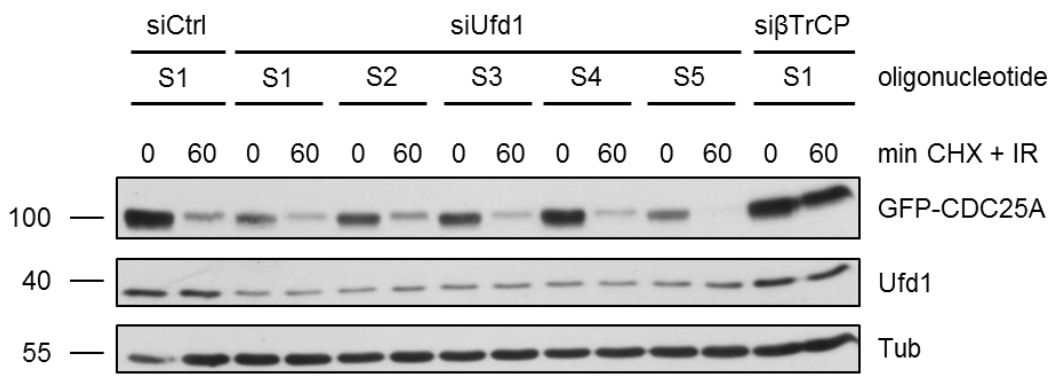

Figure 2.8: Knockdown of Ufd1 does not stabilize GFP-CDC25A after IR-induced DNA damage. U2OS cells inducibly expressing GFP-CDC25A were mock-depleted or depleted of Ufd1 or βTrCP for 48 h. For Ufd1 depletion, five different siRNAs named S1 to S5 were tested. GFP-CDC25A expression was induced during the last 6 h of depletion. Subsequently, the cells were mock-treated or treated with 10 Gy of IR and 50 µg/mL CHX to inhibit protein re-synthesis. After 0 or 60 min, the cells were lysed and cell lysates were subjected to SDS-PAGE and Western blotting. GFP-CDC25A was detected by an anti-CDC25A antibody. α-tubulin (Tub) served as loading control.

As the reporter cell line inducibly expressing GFP-CDC25A responded to Npl4 and βTrCP knockdown similar to our observations for endogenous CDC25A, we investigated if UBXD7 participates in GFP-CDC25A turnover. For this purpose, the CHX chase was performed with siRNAs targeting UBXD7 or the negative control UBXD8, a p97 cofactor involved in ERAD. Interestingly, depletion of UBXD7 caused GFP-CDC25A stabilization and delayed degradation to the same extent as Npl4 depletion, whereas knockdown of UBXD8 did not affect GFP-CDC25A turnover (Fig. 2.9).

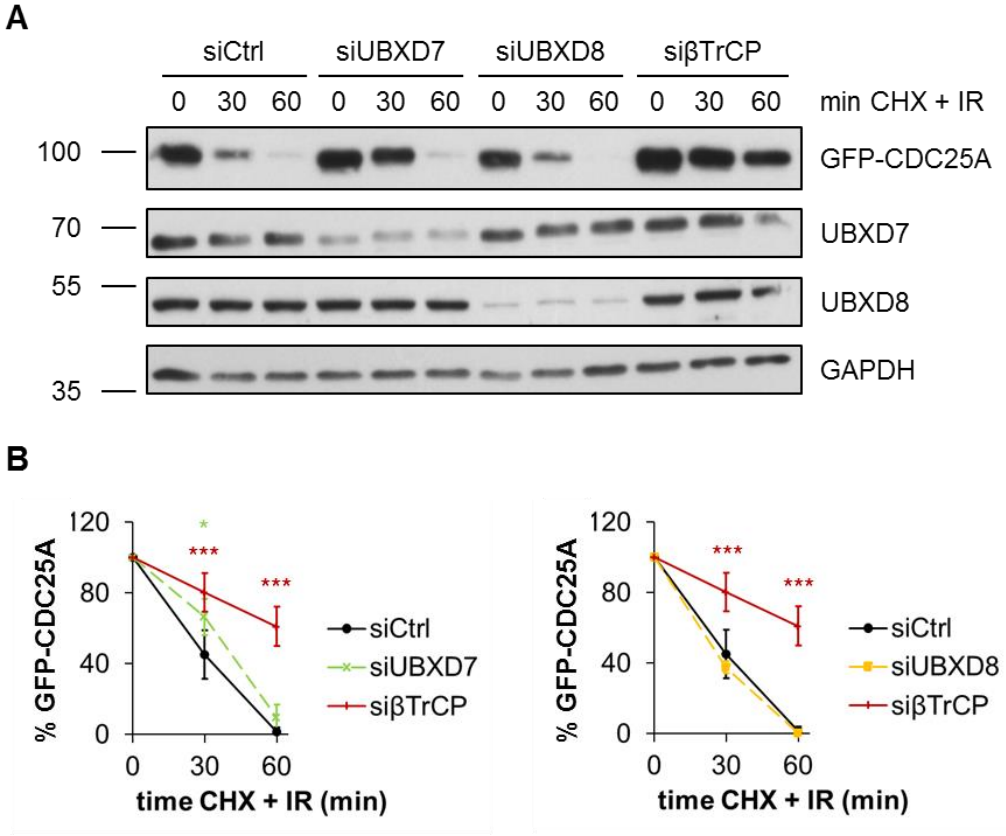

Figure 2.9: Knockdown of UBXD7 leads to delayed GFP-CDC25A degradation after IR-induced DNA damage. (**A**) CHX chase of IR-induced GFP-CDC25A degradation in depleted cells. U2OS cells inducibly expressing GFP-CDC25A were mock-depleted or depleted of UBXD7, UBXD8, or βTrCP for 48 h. GFP-CDC25A expression was induced during the last 6 h of depletion. Subsequently, the cells were mock-treated or treated with 10 Gy IR and 50 µg/mL CHX to inhibit protein re-synthesis. After 0, 30, or 60 min, the cells were lysed and cell lysates were subjected to SDS-PAGE and Western blotting. GFP-CDC25A was detected by an anti-CDC25A antibody. GAPDH served as loading control. (**B**) Quantification of **A**. Shown are means of three independent experiments and error bars represent s.d. * $p < 0.05$, *** $p < 0.001$. Signal density on X-ray films was quantified using BIO1D. GFP-CDC25A levels without IR were set to 100% for each depletion.

Taken together, these results show that Npl4 and UBXD7 participate in GFP-CDC25A degradation. However, Ufd1 knockdown caused a marked decrease in GFP-CDC25A levels. In contrast, we showed that depletion of Ufd1 stabilized endogenous CDC25A.

2.3 Unrepaired DNA damage from interphase leads to segregation errors in mitosis in cells depleted of p97$^{Ufd1-Npl4}$

In 2011, our laboratory showed that knockdown of the p97 cofactor Ufd1-Npl4 by siRNA caused defects in chromosome segregation during mitosis due to upregulated Aurora B kinase activity (Dobrynin et al, 2011). This demonstrated that p97$^{Ufd1-Npl4}$ antagonizes Aurora B which functions in the bipolar attachment of the mitotic spindle to the centromeres of the chromosomes. Moreover, we found that depletion of p97$^{Ufd1-Npl4}$ impaired the G2/M checkpoint by stabilizing CDC25A (Riemer et al, 2014). Since p97 is also implicated in diverse interphase functions, we were interested if the severe segregation defects observed in Ufd1-Npl4-depleted cells only originate from impaired mitotic functions of p97$^{Ufd1-Npl4}$ or if they additionally arise from replication-associated damage carried over into mitosis due to the G2/M checkpoint override.

To explore to what extent pre-mitotic functions of p97$^{Ufd1-Npl4}$ affect chromosome stability in human cells, mitotic segregation errors of HeLa cells depleted of p97, Ufd1, Npl4, or DVC1 were analyzed by light microscopy. Errors of mitotic or pre-mitotic origin were distinguished by staining of the centromere with CREST (Burrell et al, 2013). Lagging chromosomes in anaphase comprising a centromere were considered to result from defects in mitotic functions, whereas chromosome fragments without centromere and anaphase bridges were considered to be of pre-mitotic origin (Fig. 2.10A).

HeLa cells were mock-transfected with siluc or transfected with siRNAs targeting p97, Ufd1, Npl4, DVC1, or Chk1 for 48 h. Knockdown of Chk1 served as a positive control. All depletions led to an increase of acentric chromosomal fragments or chromosome bridges over control cells, when the cells were additionally challenged with 0.2 µM aphidicolin (APH), an inhibitor of DNA polymerases α and δ, for 24 h (Fig. 2.10B and C). This increase in mitotic defects of pre-mitotic origin suggests unrepaired or incompletely replicated DNA. Notably, cells depleted of Chk1 were apoptotic upon additional APH treatment indicating high levels of DNA damage. Therefore, the number of mitotic cells was too low to determine the percentage of cells with errors of mitotic or pre-mitotic origin. Taken together, there is evidence that p97$^{Ufd1-Npl4}$ suppresses chromosomal instability that stems from defects in interphase.

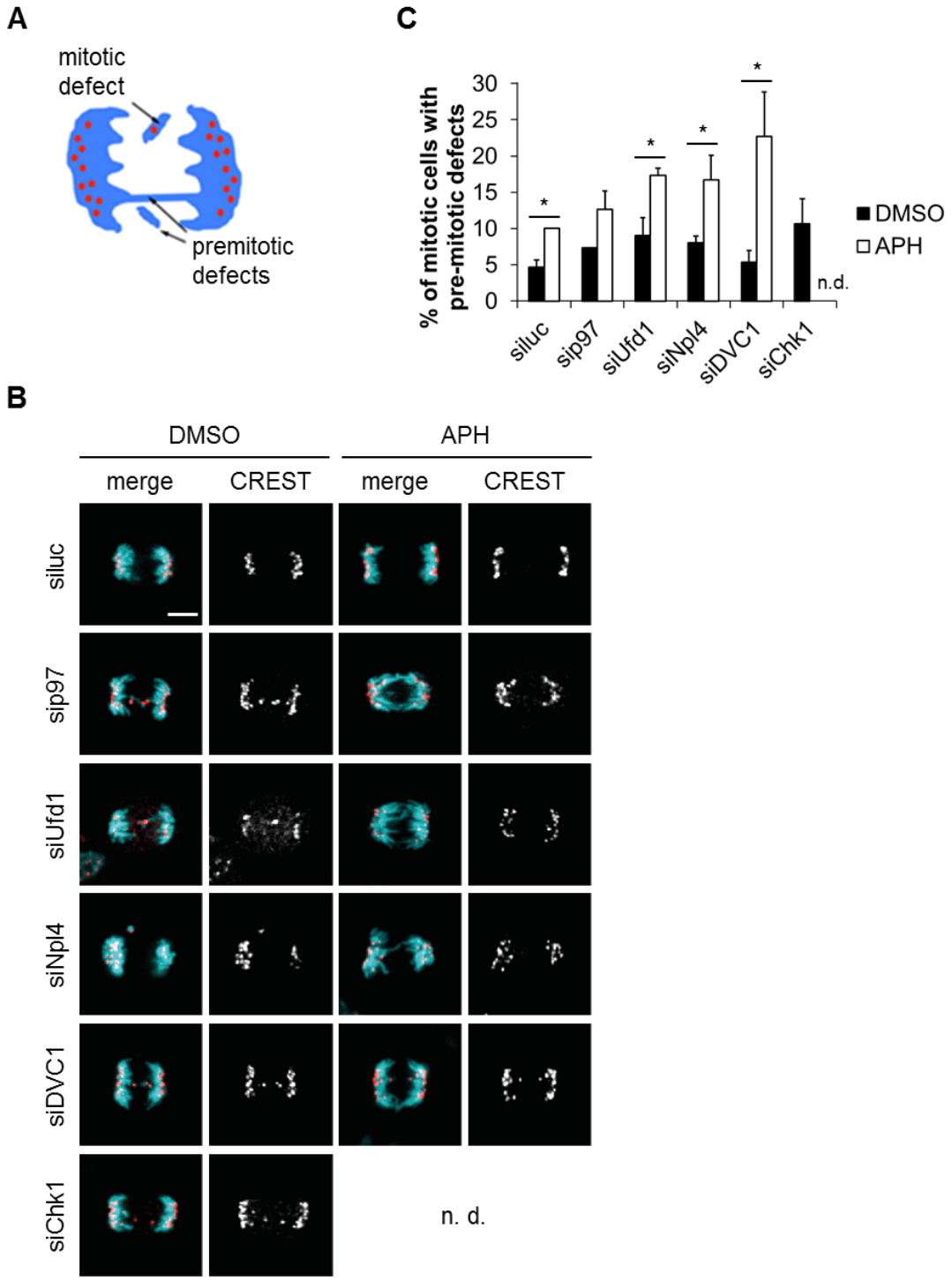

Figure 2.10: Unrepaired DNA damage after replication stress results in severe chromosome segregation defects in mitotic cells depleted of p97, Ufd1, Npl4, or DVC1. (**A**) Schematic illustration of mitotic and pre-mitotic defects in anaphase. Blue depicts chromatin, red dots depict centromeres. (**B**) Confocal micrographs of mitotic HeLa cells in anaphase depleted with the indicated siRNAs for 48 h and treated with DMSO or aphidicolin (APH) as depicted. Cells were fixed 24 h after DMSO or APH treatment and stained with DAPI and CREST antibodies to visualize chromatin and centromeres, respectively. RNAi against luciferase served as negative control, RNAi against Chk1 as positive control. n.d.: not determined due to low number of mitotic cells. Merge: DAPI – cyan, CREST – red. Scale bar: 10 µm. (**C**) Quantification of **B** according to classification in **A**. Shown are means of three independent experiments with at least 25 cells per condition and error bars represent s.d. * $p < 0.05$.

2.4 Knockdown of p97 sensitizes HeLa cells to replication stress-inducing drugs

Given that replication stress contributes to chromosomal instability in cells depleted of p97 and its cofactors Ufd1-Npl4 and DVC1, respectively, we asked if these proteins are important for survival of human tumor cells after replication stress. In addition, we included UBXD7 in this study due to the finding that it is crucial for NER. In this setting, we applied replication stress in form of increasing concentrations of cisplatin or doxorubicin. Cisplatin is a DNA crosslinker binding to two adjacent DNA bases either within the same DNA strand (intrastrand-crosslinks) or from opposing DNA strands (interstrand-crosslinks). In contrast, doxorubicin intercalates into DNA, thereby inhibiting topoisomerase II, which resolves DNA daughter molecules after replication. To examine if p97 and its cofactors are crucial for survival of human tumor cells after replication stress, a cell viability assay was performed. For this purpose, the MTS assay was chosen. MTS (3-(4,5-dimethylthiazol-2-yl)-5-(3-carboxymethoxyphenyl)-2-(4-sulfophenyl)-2H-tetrazolium) is a tetrazolium salt, which is reduced to a formazan product by NAD(P)H in the presence of phenanzine methosulfate (PMS) that acts as an intermediate electron acceptor. Thus, the amount of produced formazan corresponds proportionally to glycolysis rate. This reaction can be followed spectrophotometrically at 490 nm.

First, HeLa cells were mock-transfected with siluc or transfected with siRNAs targeting p97, Ufd1, Npl4, UBXD7 or DVC1 for 48 h. Then, cells were treated with increasing concentrations of the DNA crosslinker cisplatin (5-25 µM) or the topoisomerase II inhibitor doxorubicin (1-3 µM) for further 24 h to induce replication stress. Finally, MTS was added for 1 h and cell viability was determined spectrophotometrically.

p97-depleted cells were significantly more sensitive to increasing concentrations of cisplatin and doxorubicin than mock-depleted cells (Fig. 2.11A and B), while cells depleted of UBXD7 or DVC1 were not (Fig. 2.11G and H). Knockdown of Ufd1 or Npl4 only showed a slightly elevated sensitivity to cisplatin at high concentrations (Fig. 2.11C and E). In contrast, sensitivity to doxorubicin was significantly increased in Ufd1- or Npl4-depleted cells (Fig. 2.11D and F), albeit to a lesser extent than upon p97 depletion. This indicates that $p97^{Ufd1\text{-}Npl4}$ is involved in the response to replication stress and plays an important role in cell survival after DNA damage in S phase.

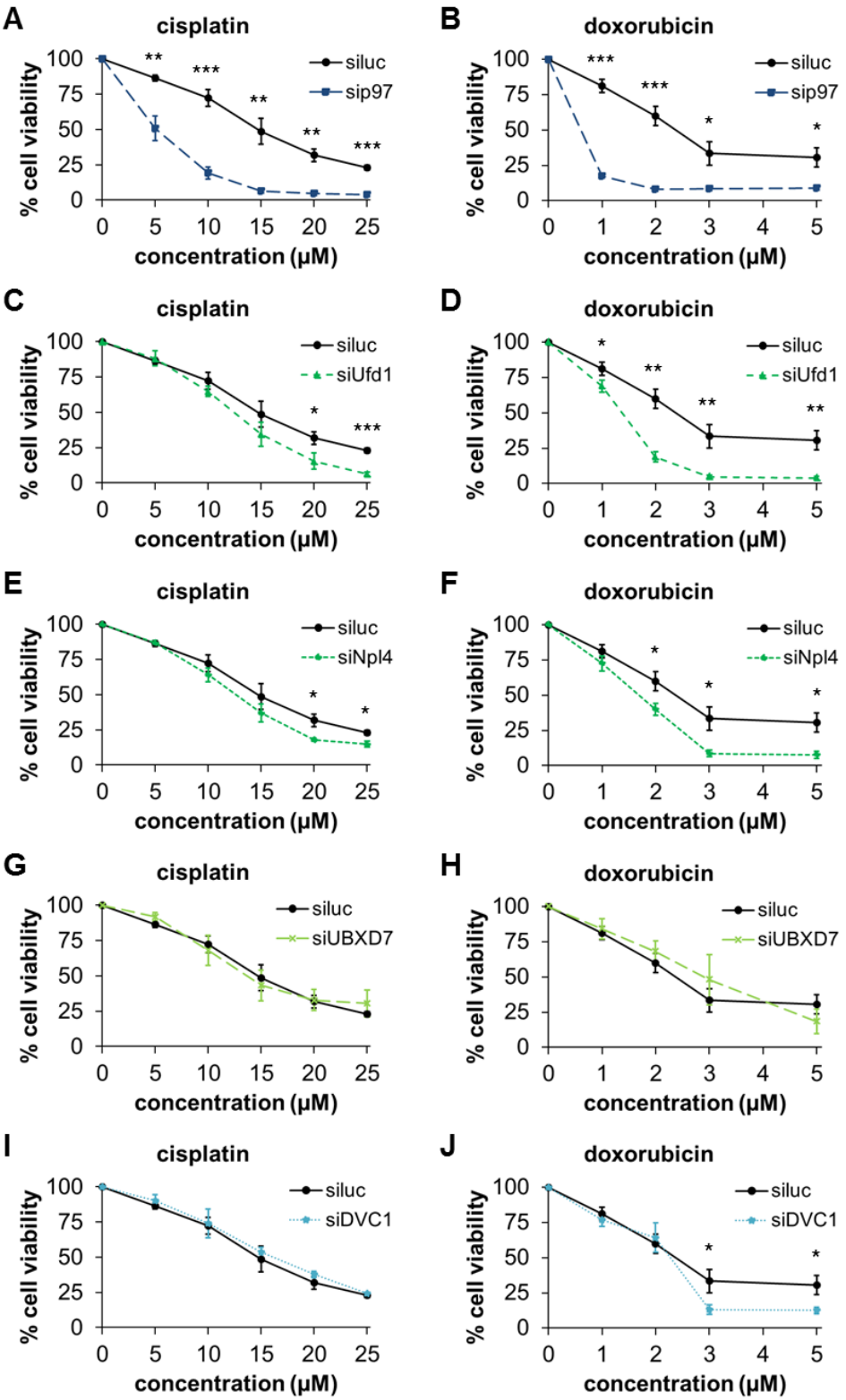

Figure 2.11: Cell survival of HeLa cells after knockdown of p97 or its cofactors and additional replication stress. HeLa cells were depleted of p97 (**A**, **B**), Ufd1 (**C**, **D**), Npl4 (**E**, **F**), UBXD7 (**G**, **H**) or DVC1 (**I**, **J**) for 48 h and challenged with increasing concentrations of the replication stress-inducers cisplatin (**A**, **C**, **E**, **G**, **I**) or doxorubicin (**B**, **D**, **F**, **H**, **J**) for further 24 h. Cell viability was determined by an MTS assay. RNAi against luciferase served as control. Data were collected in technical triplicates. Shown are means of three independent experiments and error bars represent s.d. * $p < 0.05$, ** $p < 0.01$, *** $p < 0.001$. Cell viability without replication stress was set to 100% for each depletion (for starting values see Fig. 2.12).

Notably, without additional challenge by cisplatin or doxorubicin, knockdown of p97 or Npl4 caused a significant reduction in cell proliferation over control cells in contrast to knockdown of the other analyzed proteins (Fig. 2.12).

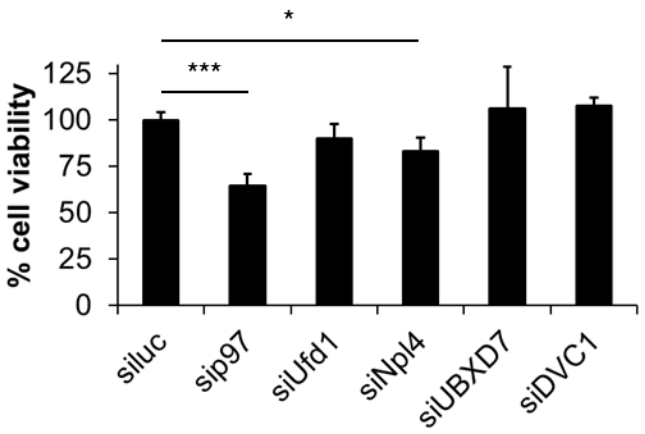

Figure 2.12: Cell survival of HeLa cells after knockdown of p97 or its cofactors. Cell viability was measured with an MTS assay after siRNA-mediated depletion of p97, Ufd1, Npl4, UBXD7 or DVC1 for 72 h. RNAi against luciferase served as control. Data were collected in technical triplicates. Shown are means of three independent experiments and error bars represent s.d. * $p < 0.05$, *** $p < 0.001$.

2.5 UBXD7 is not required for the degradation of all CRL substrates

Recently, the p97 adaptor UBXD7 was shown to be involved in the cellular response to DNA damage (Verma et al, 2011; Puumalainen et al, 2014; He et al, 2016). A unique feature of UBXD7 is its UIM domain which allows direct binding to neddylated CRLs (Alexandru et al, 2008; Bandau et al, 2012; den Besten et al, 2012). To date, only nuclear targets were confirmed for UBXD7, including CDC25A (own data), HIF1α, Rpb1, DDB2, and CSB (Alexandru et al, 2008; Verma et al, 2011; Puumalainen et al, 2014; He et al, 2016). However, the direct link of UBXD7 to p97 and to CRLs posed the question if UBXD7 is generally involved in CRL- and p97-dependent degradation both in the nucleus and in the cytoplasm. To address this issue, we examined degradation of the cytoplasmic inhibitor of NF-κB, IκBα. Cytokine-induced proteolysis of IκBα was shown to depend on the cullin RING ligase $SCF^{\beta TrCP}$ and $p97^{Ufd1\text{-}Npl4}$ (Li et al, 2014). To determine if UBXD7 also participates in IκBα turnover, the degradation was monitored by immunoblot analysis.

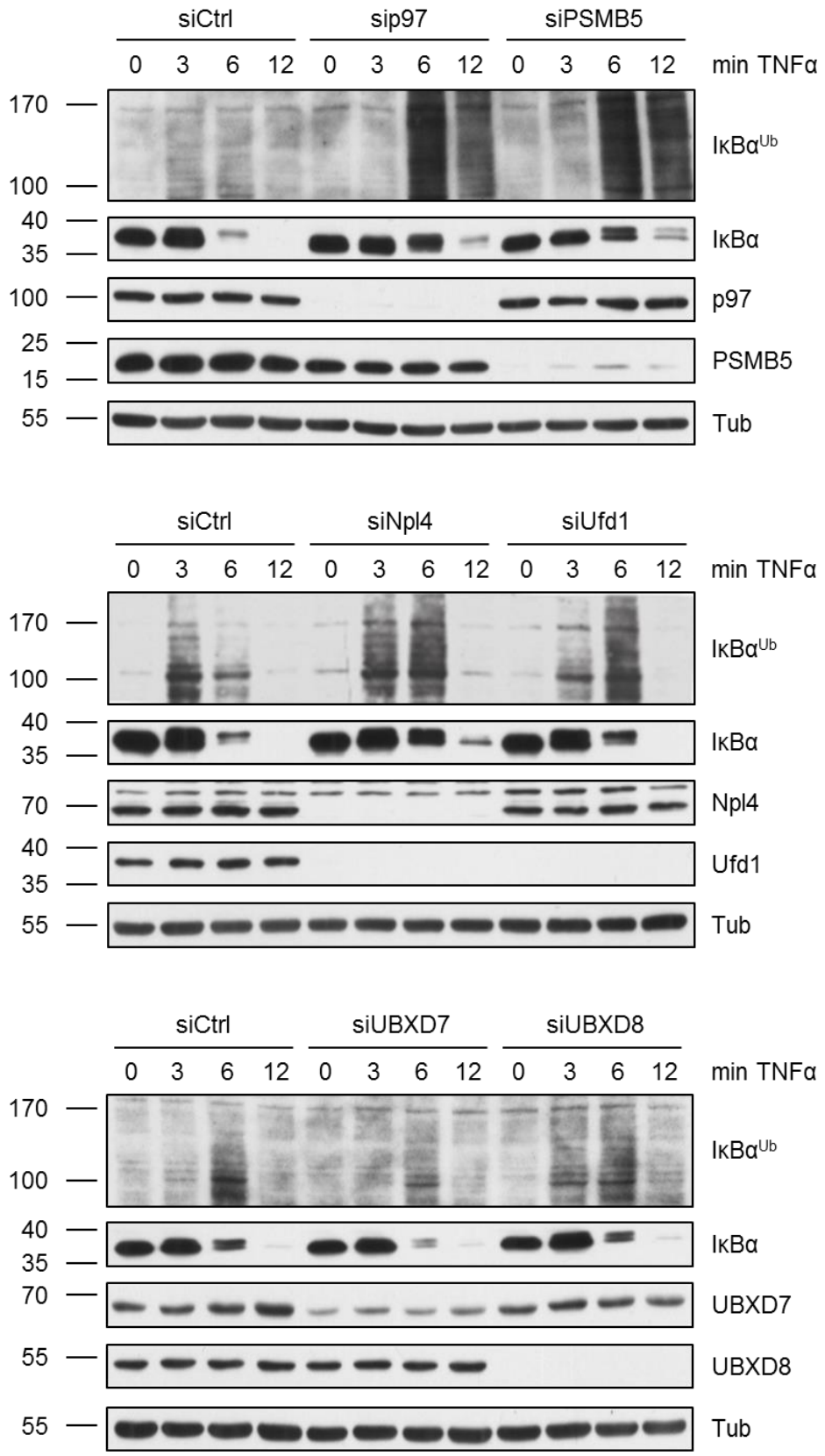

Figure 2.13: In contrast to p97$^{Ufd1\text{-}Npl4}$, UBXD7 is not required for TNFα-induced IκBα degradation. HeLa cells were mock-transfected or depleted of p97, Ufd1, Npl4, UBXD7, the ERAD factor UBXD8, or the proteasomal subunit PSMB5 for 48 h. IκBα ubiquitylation and degradation was induced by treatment with the cytokine TNFα. After 0, 3, 6, or 12 min, the cells were lysed and cell lysates were analyzed by Western blotting to detect unmodified and ubiquitylated IκBα. α-tubulin (Tub) served as loading control.

HeLa cells were either mock-transfected or transfected with siRNA targeting p97, its cofactors Ufd1, Npl4, UBXD7, or UBXD8, or PSMB5, which is a subunit of the 26S proteasome. Turnover of IκBα was induced by addition of TNFα for 0, 3, 6, or 12 min. Then, the cells were lysed and cell lysates were subjected to SDS-PAGE and Western blotting. To prevent deubiquitination, the DUB inhibitor PR619 and N-ethylmaleimide (NEM) were added to the lysis buffer.

In control cells, IκBα was rapidly degraded within 12 min after TNFα addition (Fig. 2.13). Consistent with other findings, knockdown of the proteasomal subunit PSMB5 had no impact on the abundance of IκBα, indicating that IκBα is stable in HeLa cells under unstimulated conditions. Moreover, depletion of PSMB5, p97, Ufd1, or Npl4 clearly delayed IκBα degradation, confirming that turnover of IκBα is mediated by the proteasome with the help of $p97^{Ufd1\text{-}Npl4}$. In addition to unmodified IκBα, the anti-IκBα antibody recognized proteins with high molecular weight which are supposed to be ubiquitylated forms of IκBα. Ubiquitylated IκBα ($IκBα^{Ub}$) was strongly increased upon knockdown of p97, Ufd1, Npl4 or PSMB5 and the accumulation of $IκBα^{Ub}$ was shifted to later time points after TNFα induction compared to control cells. This further confirms that $p97^{Ufd1\text{-}Npl4}$ and the 26S proteasome are essential for IκBα degradation downstream of ubiquitylation. In contrast, depletion of UBXD7 or the p97 cofactor UBXD8 that is involved in ERAD had no effect on IκBα turnover. Hence, this indicates that UBXD7 is not essential for all CRL substrates.

2.6 Binding to p97 and CRLs is essential for UBXD7 function

To shed light on the relevance of the various UBXD7 domains for its function, a structure-function analysis of UBXD7-mediated degradation was performed. For this purpose, the well-established UBXD7 substrate DDB2 was used (Puumalainen et al, 2014). DDB2 is rapidly recruited to DNA lesion sites after UV irradiation and is then ubiquitylated by CUL4A and degraded by the proteasome. It was shown that DDB2 degradation after UV irradiation is dependent on $p97^{Ufd1\text{-}Npl4}$ and UBXD7 in HEK293 cells. To confirm this finding for U2OS cells, which we used for the structure-function analysis of UBXD7, an immunoblot analysis of UV light-treated U2OS cells was performed.

Therefore, U2OS cells were mock-transfected or transfected with siRNAs targeting p97, Npl4, Ufd1, UBXD7, or UBXD1, a p97 cofactor implicated in endolysosomal sorting. The depleted cells were either mock-treated or exposed to UV light (10 J/m^2), before they were lysed 60 min later and subjected to SDS-PAGE and Western blotting. In control cells, DDB2 was degraded 60 min after UV radiation (Fig. 2.14). Consistent with the finding in HEK293 cells, knockdown of p97, Npl4, Ufd1, or UBXD7 reduced

UV light-triggered breakdown of DDB2 in U2OS cells, indicating that p97$^{Ufd1-Npl4}$ and UBXD7 are required for DDB2 degradation. As expected, depletion of UBXD1 did not affect DDB2 turnover.

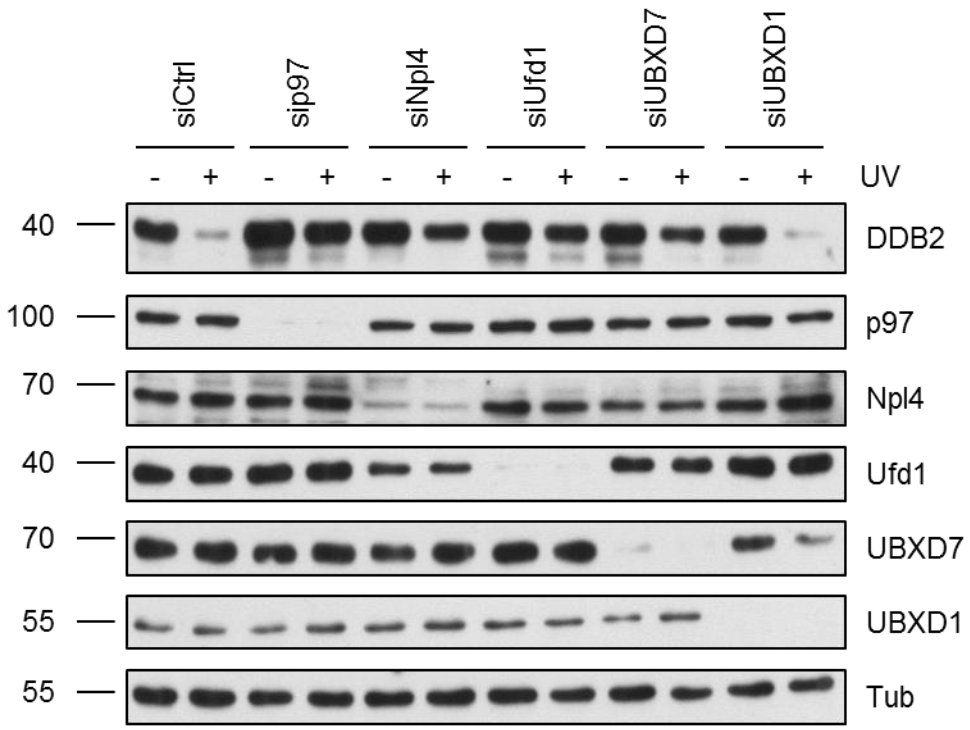

Figure 2.14: UV light-triggered degradation of DDB2 is inhibited in cells treated with siRNAs targeting p97, Npl4, Ufd1, or UBXD7. U2OS cells were treated with siRNAs against p97, Npl4, Ufd1, UBXD7, UBXD1, or non-targeting control (siCtrl) for 48 h. DDB2 degradation was induced by UV irradiation (10 J/m^2). After 60 min, the cells were lysed and cell lysates were analyzed by Western blotting to detect DDB2 levels. α-tubulin (Tub) served as loading control.

Next, it was investigated if the inhibition of UV light-induced DDB2 breakdown can be rescued by additional overexpression of RNAi-resistant wild-type UBXD7 (UBXD7 wt). Therefore, U2OS cells were treated with siRNAs against UBXD7 or non-targeting control. After 24 h, the cells were additionally transfected with UBXD7 wt-strep-HA or empty vector. Another 24 h later, the cells were either mock-treated or exposed to UV radiation (10 J/m^2), before they were lysed 15 or 60 min later and subjected to SDS-PAGE and Western blotting.

In control-depleted cells, DDB2 was degraded within 60 min after UV light exposure irrespective of additional transfection with UBXD7 wt-strep-HA (Fig. 2.15). Overexpression of UBXD7 wt-strep-HA was confirmed by staining with an anti-HA antibody. Consistent with the previous experiment, depletion of UBXD7 led to persistent DDB2 after UV irradiation. However, additional overexpression of UBXD7 wt-strep-HA was able to rescue inhibited UV light-triggered DDB2 degradation in cells depleted of endogenous UBXD7. Residual staining of UBXD7 at about 70 kDa in cells

depleted of endogenous UBXD7 and transfected with RNAi-resistant UBXD7 wt-strep-HA is likely to result from overexpressed UBXD7 wt-strep-HA lacking the C-terminal strep-HA tag instead of from incomplete depletion of endogenous UBXD7.

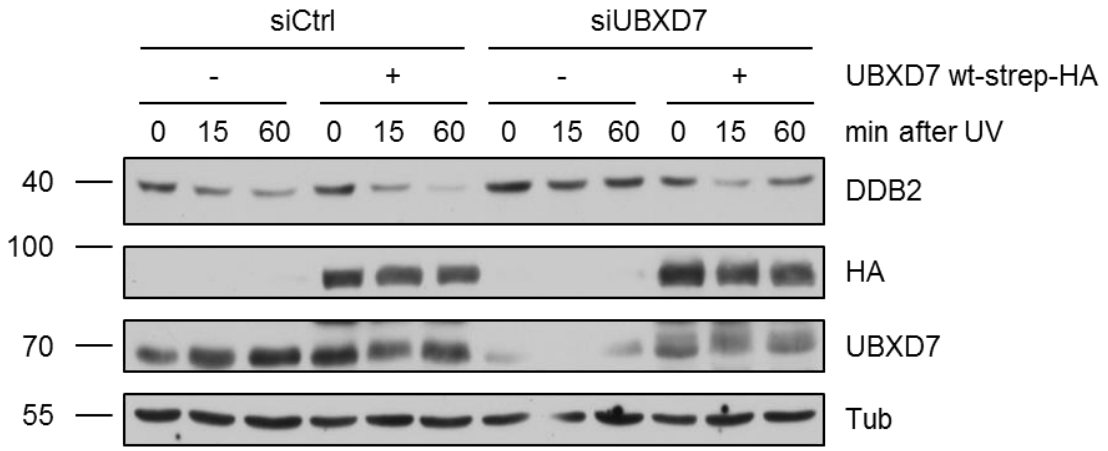

Figure 2.15: Overexpression of UBXD7 wt rescues inhibited UV light-induced DDB2 degradation in cells depleted of endogenous UBXD7. U2OS cells were treated with siRNAs against UBXD7 or non-targeting control (siCtrl) for 48 h. After 24 h of incubation, the cells were additionally transfected with UBXD7 wt-strep-HA or empty vector. DDB2 degradation was induced by UV irradiation (10 J/m^2). After 0, 15, and 60 min, the cells were lysed and cell lysates were analyzed by Western blotting to detect DDB2 levels. Overexpression of UBXD7 wt-strep-HA was confirmed by HA staining, depletion of endogenous UBXD7 by UBXD7 staining. α-tubulin (Tub) served as loading control.

Finally, the rescue experiment was applied to perform a structure-function analysis of UBXD7. UBXD7 contains an N-terminal UBA domain, followed by a UAS domain, a UIM and a C-terminal UBX domain (Fig. 2.16A). The UBA domain is able to bind ubiquitin, whereas the UAS domain is of unknown function. UBXD7 was shown to bind neddylated CRLs via its UIM which associates directly with NEDD8, but can also bind ubiquitin (Fisher et al, 2003; Bandau et al, 2012; den Besten et al, 2012). Interaction with p97 is mediated by the UBX domain. To investigate the requirement of the different domains for UBXD7 function in DDB2 degradation, the ability of UBXD7 mutants to rescue impaired DDB2 turnover in UBXD7-depleted cells was compared. Therefore, different mutants of UBXD7 were generated by Lena Weimann, including deletion mutants lacking the UBA, UAS or UIM domain as well as a UBXD7 variant with a point-mutation in the UBX domain which was shown to be deficient in p97-binding (P459G; Bandau et al, 2012).

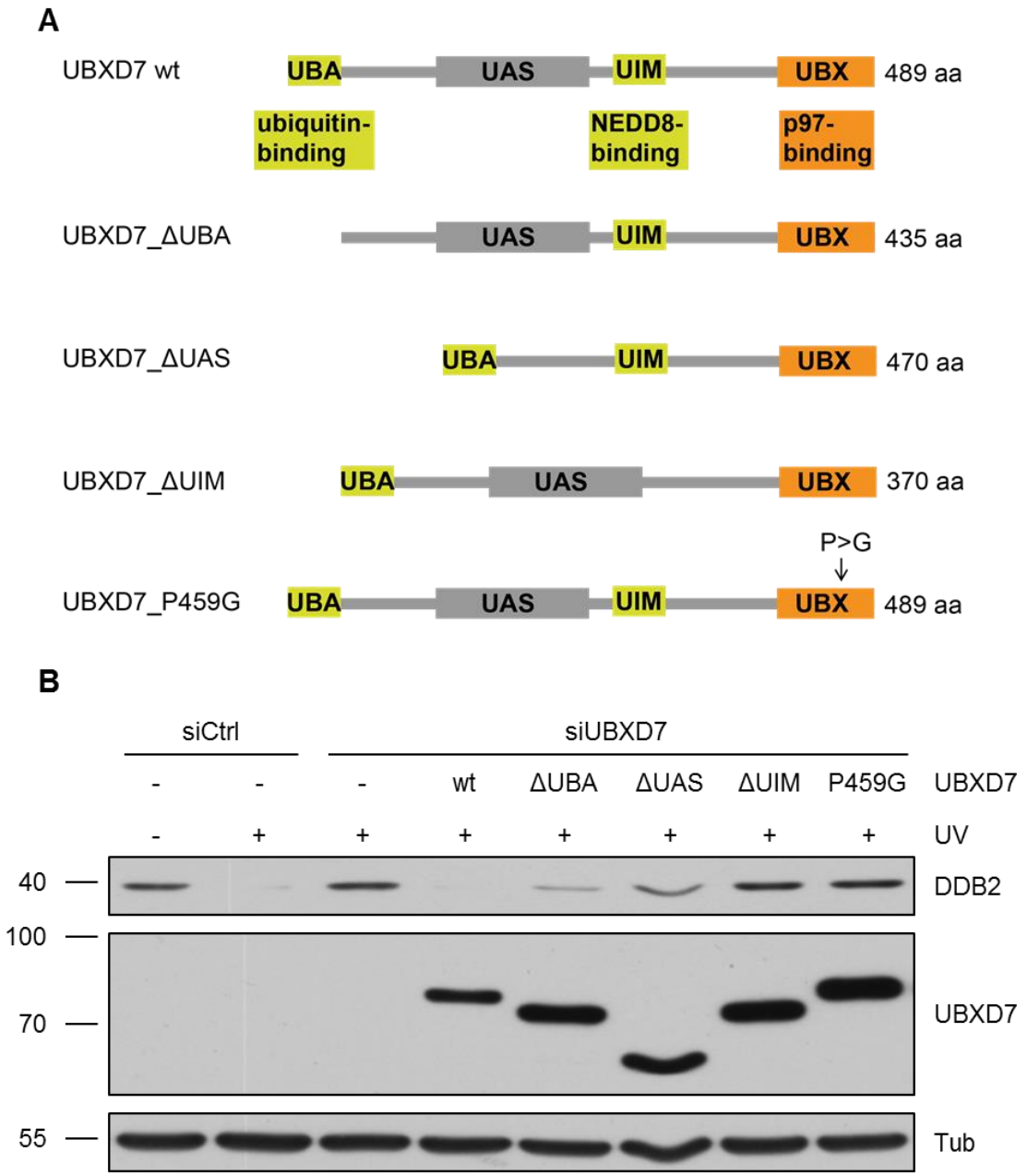

Figure 2.16: Structure-function analysis of UBXD7 in UV light-triggered DDB2 degradation. (**A**) Schematic representation of UBXD7 wt and UBXD7 mutants highlighting their various domains. UBA, ubiquitin-associated domain; UAS, ubiquitin-associating domain; UIM, ubiquitin-interacting motif; UBX, ubiquitin regulatory X domain; aa, amino acids. (**B**) U2OS cells were treated with siRNA targeting UBXD7 or non-targeting control (siCtrl) for 48 h. After 24 h of incubation, the cells were additionally transfected with empty vector, UBXD7 wt, or the indicated mutants. DDB2 degradation was induced by UV irradiation (10 J/m^2). After 60 min, the cells were lysed and cell lysates were analyzed by Western blotting to detect DDB2 levels. Overexpression of UBXD7 wt and the mutants was confirmed by UBXD7 staining. α-tubulin (Tub) served as loading control.

To evaluate the role of UBXD7's four domains for its function in DDB2 degradation, the generated constructs were expressed in U2OS cells depleted of endogenous UBXD7 and their ability to rescue DDB2 degradation was determined (Fig. 2.16B). Consistent with the previous experiments, DDB2 was destroyed 60 min after UV light exposure in

control-depleted cells. Knockdown of UBXD7 stabilized DDB2 after UV irradiation, whereas additional overexpression of RNAi-resistant UBXD7 wt rescues DDB2 turnover. Expression of UBXD7_ΔUBA was able to almost completely rescue DDB2 degradation in UBXD7-depleted cells. Furthermore, DDB2 destruction in cells lacking endogenous UBXD7 could be partially rescued by overexpression of UBXD7_ΔUAS. In contrast, UBXD7_ΔUIM and UBXD7_P459G did not affect DDB2 stabilization in UBXD7-depleted cells.

Taken together, the results of this experiment indicate that p97-binding and association with neddylated CRLs is essential for UBXD7 function in DDB2 degradation. In contrast, the ability of UBXD7 to bind ubiquitin does not seem to be required for proper UBXD7 function. The role of the UAS domain needs to be further investigated, since its function is still unknown.

2.7 Different p97 inhibitors elicit diverse effects

In addition to siRNA-mediated downregulation, chemical inhibition of p97 with small-molecule inhibitors provides an advantageous tool to explore p97 function in cells. Recently, our lab obtained the unpublished inhibitors I1, I5, and I8 to analyze their potential as p97 inhibitors for laboratory use.

2.7.1 Differential effects of p97 inhibitors on cell viability

In order to characterize these different first-generation p97 inhibitors, first the cytotoxicity of these inhibitors was investigated. To test this, HeLa cells were treated with increasing concentrations (1-35 µM) of five different p97 inhibitors (DBeQ, NMS-873, as well as the unpublished compounds I1, I5, and I8). After 5, 16, or 24 h of treatment, cell viability was measured with the MTS assay (Fig. 2.17).

Cell death was observed with increasing concentrations and incubation times. Data analysis revealed a cytotoxic effect of the p97 inhibitors after 24 h treatment in the following order of potency: NMS-873 > I8 > I5 > I1 ≥ DBeQ > NMS-859 (Fig. 2.17C). However, this order was not observed for the shorter time points. After 5 h or 16 h of p97 inhibition, NMS-873 just had a minor effect on cell survival, even at high concentrations (Fig. 2.17A and B). Still, at low concentrations up to 10 µM, NMS-873 was the most potent p97 inhibitor tested. At higher concentrations, I8 emerged as the most potent p97 inhibitor. Since I8 was more potent than the other unpublished p97 inhibitors, we decided to continue experiments on p97 inhibition with DBeQ, I8, and NMS-873.

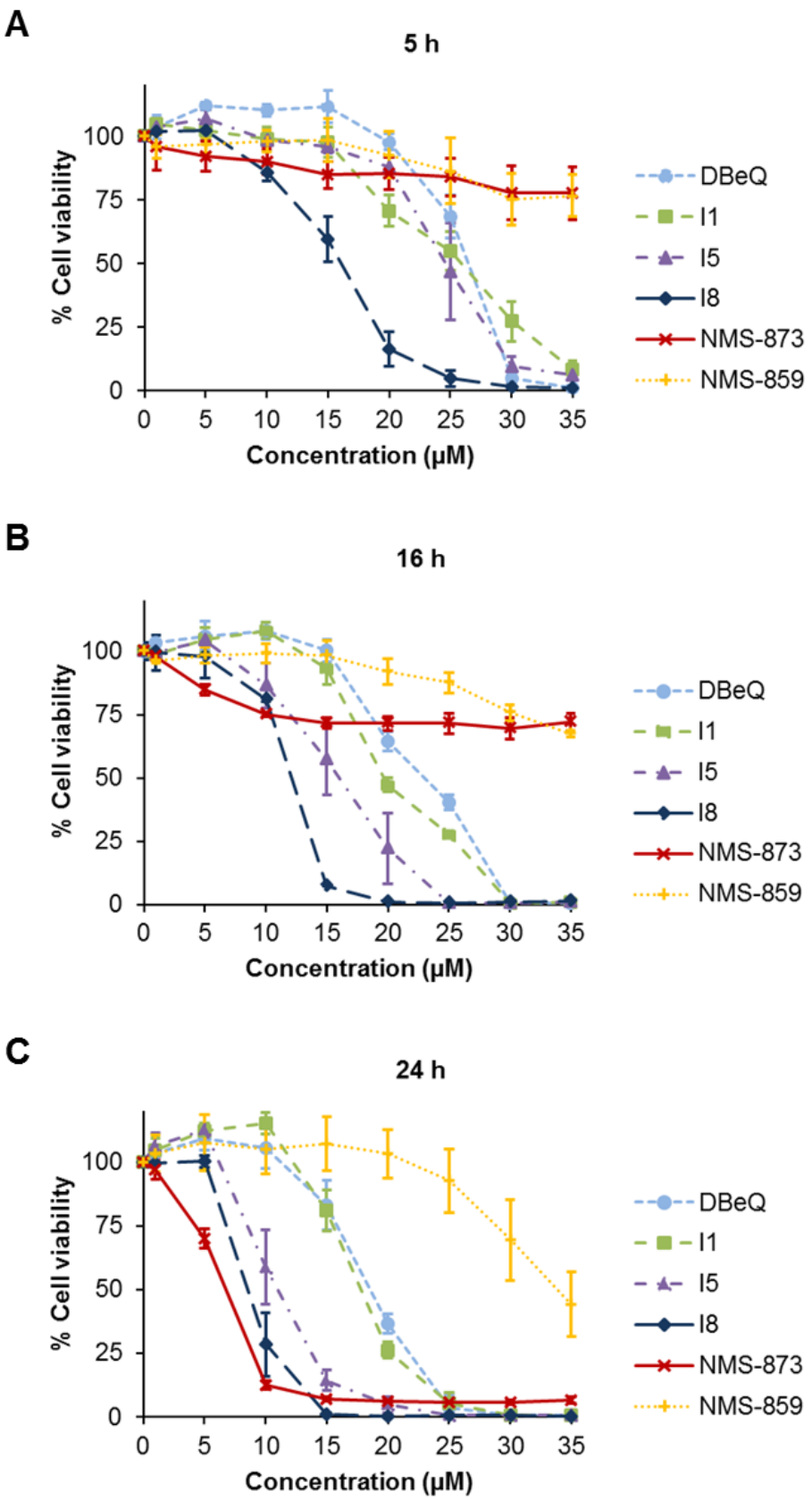

Figure 2.17: Cell survival of HeLa cells after p97 inhibiton. HeLa cells were treated with increasing concentrations of different p97 inhibitors for 5 h (**A**), 16 h (**B**), or 24 h (**C**). Cell viability was determined by an MTS assay. Data were collected in technical triplicates. Shown are means of three independent experiments and error bars represent s.d.

2.7.2 p97 inhibition with NMS-873 showed synthetic lethality with doxorubicin

In the next step, it was examined if pharmacological inhibition of p97 sensitizes human cancer cells to replication stress-inducing drugs, as observed in the case of p97 RNAi knockdown. For this purpose, HeLa cells were treated with increasing concentrations of cisplatin (5-25 µM) or doxorubicin (1-5 µM) together with either solvent (DMSO) or 3 µM DBeQ, 3 µM I8, or 3 µM NMS-873 for 24 h, before cell viability was determined with an MTS assay. The concentrations of p97 inhibitors were chosen based on preserving cell viability after 24 h.

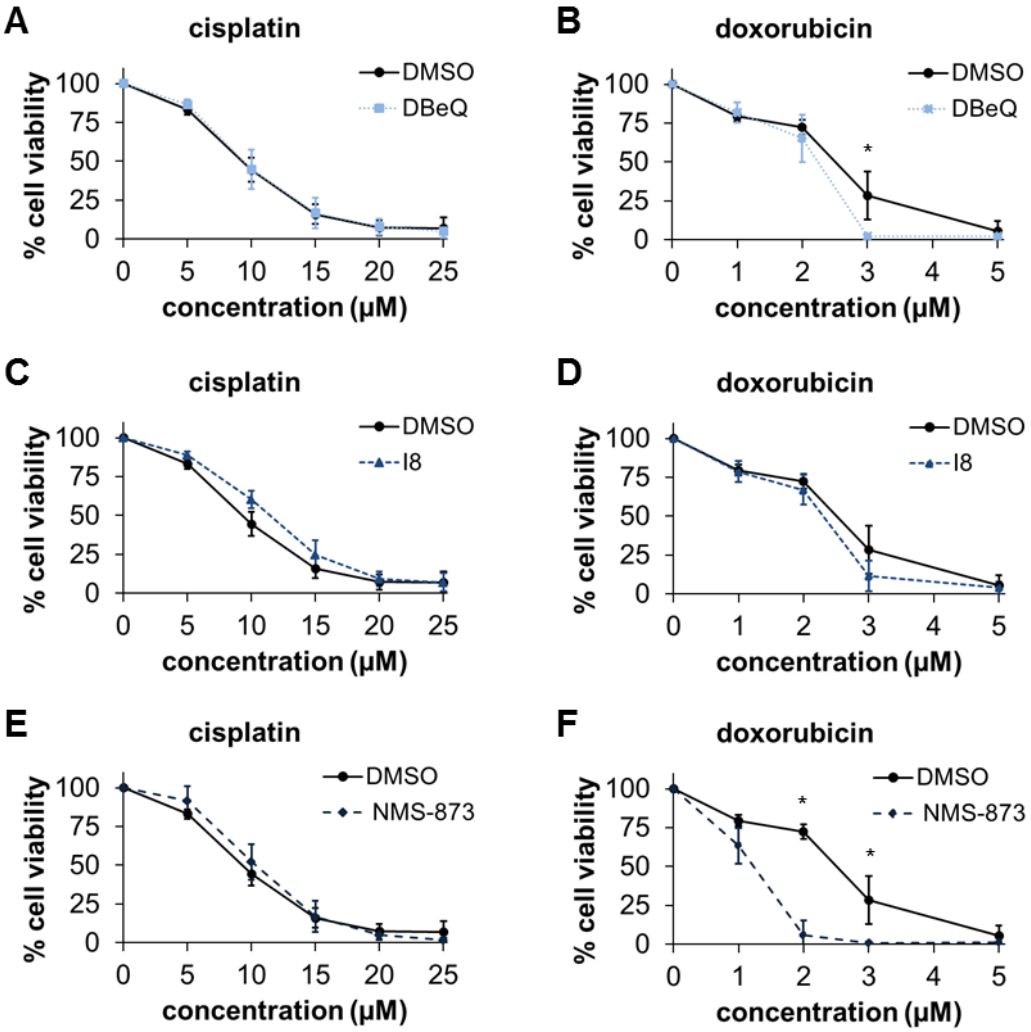

Figure 2.18: Cell survival of HeLa cells after p97 inhibition and additional replication stress. HeLa cells were simultaneously treated with 3 µM DBeQ (**A**, **B**), 3 µM I8 (**C**, **D**), or 3 µM NMS-873 (**E**, **F**) and increasing concentrations of the replication stress-inducers cisplatin (**A**, **C**, **E**) or doxorubicin (**B**, **D**, **F**) for 24 h. Cell viability was determined by an MTS assay. DMSO served as control. Data were collected in technical triplicates. Shown are means of three independent experiments and error bars represent s.d. * $p < 0.05$.

Inhibition of p97 showed no sensitization to cisplatin under the given conditions (Fig. 2.19A, C, and E). For doxorubicin treatment, only p97 inhibition with NMS-873 but not

with DBeQ or I8 showed significant synthetic lethality (Fig. 2.19B, D, and F). In summary, only p97 inhibition with NMS-873 potently sensitized human cancer cells to replication stress, albeit less efficiently than p97 depletion.

2.7.3 NMS-873 delayed GFP-CDC25A degradation after IR

To further analyze if the tested p97 inhibitors are useful tools for investigating p97 functions, their effect on the degradation of the p97 target CDC25A was explored. Therefore, the GFP-CDC25A reporter cell line was induced with doxycycline for 6 h. The cells were either treated with solvent (DMSO), or 10 µM DBeQ, 10 µM I8, 5 µM NMS-873, or 10 µM MG132 for 30 min. Treatment with the proteasome inhibitor MG132 served as a positive control. Then, the cells were irradiated with 10 Gy and CHX was added to block protein re-synthesis. Afterwards, the cells were lysed and cell lysates were analyzed by Western blotting.

In DMSO-treated cells, GFP-CDC25A was degraded within 60 min after IR with 10 Gy (Fig. 2.20). Moreover, proteasome inhibition with MG132 caused a significant delay in GFP-CDC25A degradation. Notably, inhibition of p97 with DBeQ or NMS-873 led to increased levels of GFP-CDC25A in general. However, while NMS-873 delayed degradation after IR compared to solvent-treated cells to a similar extent like MG132, DBeQ as well as I8 did not affect GFP-CDC25A degradation.

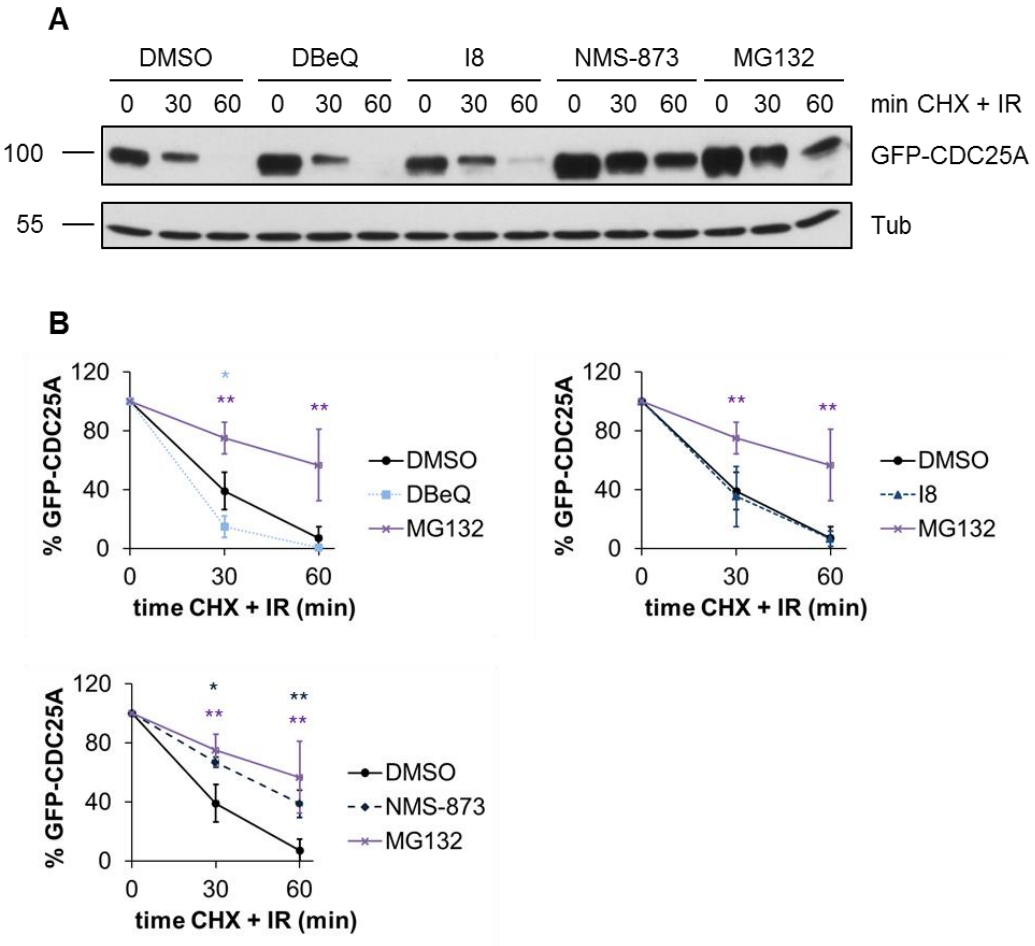

Figure 2.19: p97 inhibition with NMS-873 delayed GFP-CDC25A degradation after IR-induced DNA damage. (**A**) CHX chase of IR-induced CDC25A degradation after p97 inhibition. U2OS cells inducibly expressing GFP-CDC25A were mock-treated with solvent (DMSO) or inhibited of p97 with DBeQ, I8, or NMS-873 for 24 h. Treatment with the proteasome inhibitor MG-132 served as positive control. GFP-CDC25A expression was induced during the last 6 h of p97 inhibition. Subsequently, the cells were mock-treated or treated with 10 Gy IR and 50 µg/mL CHX to inhibit protein re-synthesis. After 0, 30, or 60 min, the cells were lysed and cell lysates were subjected to SDS-PAGE and Western blotting. GFP-CDC25A was detected by an anti-CDC25A antibody. α-tubulin (Tub) served as loading control. (**B**) Quantification of **A**. Shown are means of three independent experiments and error bars represent s.d. * $p < 0.05$, *** $p < 0.001$. Signal density on X-ray films was quantified using BIO1D. GFP-CDC25A levels without IR were set to 100% for each treatment.

3 Discussion

At the beginning of this thesis, little was known about the role of p97 in the cell cycle and the DNA damage response. While it was already clear that p97 is important for mitosis, there was increasing evidence from different organisms for p97 being involved in interphase functions. To investigate a possible implication of p97 in the response to replication stress and DNA damage in human cells and to evaluate the relevance of these functions, we focused on three major aspects. The first goal of this work was to clarify if p97 helps to maintain a DNA damage checkpoint. Next, we evaluated the significance of p97 and its cofactors for survival of human cancer cells after replication stress. This included the examination of possible synergistic effects of novel p97 inhibitors with genotoxic chemotherapeutic agents and their influence on the DNA damage response. However, several studies on the role of p97 in DNA replication and replication-associated repair pathways were published during the period of this work. For this reason, after publishing our study on the relevance of $p97^{Ufd1\text{-}Npl4}$ for the robustness of the G2/M checkpoint (Riemer et al, 2014), we refocused our studies on the p97 adaptor UBXD7 that has been recently linked to DNA repair (Verma et al, 2011; Puumalainen et al, 2014; He et al, 2016). This included an analysis of the role of UBXD7 for diverse p97 substrate proteins including CDC25A and a detailed structure-function analysis of UBXD7 to explore its functional relationship to p97.

3.1 p97 in cell cycle checkpoints

In the first part of this thesis, we wanted to clarify a possible involvement of p97 in the maintenance of a DNA damage checkpoint. Data from colleagues and from this study show that, while the $p97^{Ufd1\text{-}Npl4}$ complex may only play a minor role in the G1/S and intra S checkpoint, $p97^{Ufd1\text{-}Npl4}$ is required for activation of the G2/M checkpoint (published in Riemer et al, 2014). This work contributed to the finding that, in the G2/M checkpoint, p97 facilitates CDC25A degradation and thereby ensures robustness of the checkpoint.

After the confirmation of CDC25A being the p97 target in the G2/M checkpoint, we aimed to further analyze the role of p97 and its cofactors in CDC25A degradation by fluorescence microscopy. For this purpose, a U2OS reporter cell line expressing GFP-CDC25A under control of a doxycycline-inducible promoter was generated and characterized. The cell line was sensitive to IR, since GFP-CDC25A degradation was accelerated after IR compared to non-irradiated cells. Moreover, depletion of βTrCP and Npl4 led to increased levels of GFP-CDC25A and a delay in its degradation, consistent with our findings for the degradation of endogenous CDC25A in HeLa cells.

However, siRNA-mediated knockdown of Ufd1 with five different oligonucleotides caused a pronounced decrease in GFP-CDC25A levels in contrast to our findings for endogenous CDC25A, which was stabilized upon Ufd1 depletion to even higher levels than upon Npl4 depletion (Riemer et al, 2014). Thus, we assume that the observed reduction of GFP-CDC25A levels in Ufd1-depleted cells of the U2OS-FRT-TO reporter cell line is probably an off-target effect. It remains unclear why the reporter cell line responds differently to Ufd1 depletion than normal HeLa cells. Yet, the cell line does not only show delayed degradation of GFP-CDC25A after the depletion of βTrCP or Npl4, but also after the depletion of UBXD7 which was shown for the first time in this work and only later confirmed for endogenous CDC25A. Furthermore, we observed that p97 inhibition with NMS-873 stabilized GFP-CDC25A to a similar extent as proteasome inhibition with MG132 and significantly delayed IR-induced GFP-CDC25A degradation. In contrast, RNAi-mediated knockdown of p97 did not compromise the degradation of endogenous CDC25A as described in the PhD thesis by Dr. Grzegorz Dobrynin. This effect was explained by the impairment of a wide variety of p97-dependent pathways upon p97 knockdown and a subsequent checkpoint adaptation. Interestingly, the depletion of p97 resulted in reduced levels of WEE1 which is the counteracting kinase of the CDC25A phosphatase in the G2/M checkpoint. Why p97 inhibition leads to a different phenotype than p97 depletion remains elusive. Most likely, these observations are due to remaining p97 ATPase activity upon NMS-873 treatment, in contrast to depletion of p97 where p97 ATPase activity is almost absent. Nevertheless, the discrepancy in our observations for endogenous CDC25A in HeLa cells and overexpressed GFP-CDC25A in U2OS-FRT-TO cells upon Ufd1 depletion led us to the decision that the U2OS-FRT-TO reporter cell line is not suitable for further studies.

The evidence for $p97^{Ufd1\text{-}Npl4}$ being required to activate the G2/M checkpoint by facilitating CDC25A degradation led us to ask, whether p97 is also involved in CDC25A degradation in the G1/S and intra S checkpoint. Our results showed that depletion of Ufd1 or Npl4 did not affect the G1/S checkpoint, but $p97^{Ufd1\text{-}Npl4}$ may play a minor role in the intra S checkpoint. In contrast, DVC1 is important for the intra S checkpoint. It remains unclear, if DVC1 has a direct role in the checkpoint itself or if this is rather an indirect effect due to the role of DVC1 in DNA replication. Cells depleted of DVC1 continue replication after DNA damage, probably because DVC1 is crucial for TLS, a strategy of the cell to bypass replication-blocking lesions (Centore et al, 2012; Davis et al, 2012; Ghosal et al, 2012; Juhasz et al, 2012; Machida et al, 2012; Mosbech et al, 2012; Kim et al, 2013). An intact intra S checkpoint requires the activation of TLS to

allow DNA repair and this process is accompanied by retarded DNA synthesis. Replication forks encountering DNA lesions stall because replicative polymerases cannot accommodate bulky lesions in their active sites. Lesion bypass is achieved by a switch to translesion polymerases that are able to accommodate damaged bases.

It is under debate, if DVC1 removes the replicative Polδ at UV lesions to allow recruitment of the TLS polymerase Polη (Ghosal et al, 2012; Juhasz et al, 2012), or if DVC1 recruits p97 to stalled replication forks to extract Polη and allow the switch back to replicative polymerases after bypassing the UV lesion (Davis et al, 2012; Mosbech et al, 2012). Our data rather support the model that DVC1 is involved in the switch from normal replication to TLS, because cells with impaired DVC1 did not exhibit a slower DNA synthesis, which would be expected for an intact TLS activation. However, we applied DNA damage in the form of IR instead of UV damage. UV light mainly induces the formation of CPDs and 6-4PPs which can be bypassed by TLS, whereas IR rather provokes DSBs that are repaired by HR or NHEJ. If and how DVC1 is involved in the repair of DSBs occurring during S phase remains to be clarified.

3.2 p97 in replication

In addition to the checkpoints, we examined the function of p97 and its cofactors in DNA replication and the replication stress response. Intriguingly, while we observed only a minor role of p97 in the intra S checkpoint, BrdU as well as ^{3}H-thymidine incorporation into newly synthesized DNA revealed a significant reduction in DNA synthesis upon p97 depletion in non-irradiated cells. The same holds true for depletion of DVC1. This demonstrates that p97 and DVC1 are essential for efficient DNA replication.

Consistent with this, inactivation of the CDC-48$^{\text{UFD-1/NPL-4}}$ complex in *Caenorhabditis elegans* led to a reduction in DNA synthesis and a replication checkpoint-dependent delay in S phase progression (Mouysset et al, 2008). This reduction in DNA synthesis for cells with impaired p97 is most likely due to inhibited degradation of the replication licensing factor CDT1 at the beginning of DNA replication which was shown to be conserved in mammalian cells (Franz et al, 2011; Raman et al, 2011). Additionally, in yeast p97 mediates the disassembly of the CMG helicase in S phase (Maric et al, 2014; Moreno et al, 2014). However, this p97-dependent process is unlikely to contribute to the phenotype of reduced DNA synthesis, since this disassembly only occurs after replication termination.

In *Caenorhabditis elegans*, the cofactors shown to be involved in CDT-1 degradation are UFD-1, NPL-4, and the novel p97 cofactor UBXN-3 (FAF1 in humans; Franz et al, 2011; Franz et al, 2016). Inactivation of CDC-48/p97 or one of these cofactors

stabilized CDT-1 on chromatin, resulting in replication stress. This replication stress caused a marked decrease in replication fork velocity, an increased number of stalled forks, and newly fired origins (Franz et al, 2011; Franz et al, 2016). Furthermore, the involvement of Ufd1 and FAF1 in CDT1 degradation were shown to be conserved in human cells (Raman et al, 2011; Franz et al, 2016).
However, in our setting we only observed a decrease in DNA synthesis for p97 and, intriguingly, for DVC1 which can most likely be explained by its involvement in TLS. Cells are constantly exposed to genotoxic insults which can cause DNA damage in form of base damage or DNA-protein crosslinks leading to TLS, meaning that TLS is activated even under unchallenged conditions. What remains unclear is if the reduction in DNA synthesis upon knockdown of p97 or DVC1 is due to a decreased number of origins of replication firing or to a decreased replication fork velocity as observed in *Caenorhabditis elegans*.

A few years ago, our laboratory found that depletion of Ufd1 or Npl4 leads to chromosome segregation errors during mitosis (Dobrynin et al, 2011). So far, these defects in mitosis have been linked only to the mitotic function of $p97^{Ufd1\text{-}Npl4}$ in antagonizing Aurora B which mediates the bipolar attachment of the mitotic spindle to the centromeres of the chromosomes. However, over the last decade p97 has been associated with functions in S phase, including S phase progression, CDT1 destruction at the beginning of DNA replication, and release of the CMG helicase at the end of DNA replication (Mouysset et al, 2008; Franz et al, 2011; Raman et al, 2011; Maric et al, 2014; Maculins et al, 2015; Franz et al, 2016). Additionally, we could prove that a non-functional $p97^{Ufd1\text{-}Npl4}$ complex weakens the G2/M checkpoint (Riemer et al, 2014). All these findings led us to ask, if the severe segregation defects observed in Ufd1-Npl4-depleted cells exclusively arise from compromised mitotic functions of $p97^{Ufd1\text{-}Npl4}$ or if they additionally originate from replication-associated damage carried over into mitosis due to the G2/M checkpoint override.
By staining with the centromere marker CREST, we could distinguish errors of mitotic or pre-mitotic origin (Burrell et al, 2013). Lagging chromosomes in anaphase bearing a centromere were considered to originate from improper spindle attachment and therefore defects in mitotic functions, whereas acentric chromosomal fragments and chromosome bridges in anaphase were considered to result from pre-mitotic defects. Notably, anaphase bridges usually result from improper fusion of DNA strands with a DSB (Geigl et al, 2008). However, they can also arise from erroneous spindle attachment (Maia et al, 2012).

Our results revealed that replication stress in form of APH, an inhibitor of DNA polymerases α and δ, led to an increase in segregation errors in mitosis that arise from S phase defects after depletion of p97, Ufd1, Npl4, or DVC1. This increase in mitotic defects of pre-mitotic origin indicates unrepaired or incompletely replicated DNA, providing evidence that $p97^{Ufd1\text{-}Npl4}$ and DVC1 suppress chromosomal instability that stems from defects in interphase.

Further experiments in our group confirmed that cells depleted of Ufd1 or Npl4 enter mitosis despite DNA damage (Riemer et al, 2014). For instance, Ufd1- or Npl4-depleted cells display an increase in γH2AX foci on the mitotic chromatin after IR. Moreover, we observed a drastically elevated occasion of chromosomal aberrations in metaphase spreads following IR in cells depleted of Ufd1 or Npl4.

Consistent with our results, in *Caenorhabditis elegans*, it was shown that in embryos depleted of CDC-48, UFD-1 or NPL-4 separating chromatids often remained connected by chromosomal bridges, indicating replication defects (Mouysset et al, 2008). However, the underlying mechanism was not identified. Yet, this indicates a conserved role for $p97^{Ufd1\text{-}Npl4}$ in S phase.

Intriguingly, depletion of the p97 adaptor DVC1 also led to a prominent increase in mitotic segregation errors with pre-mitotic origin after replication stress. Since DVC1 is involved in TLS, it is not surprising that cells lacking DVC1 display more DNA damage (Centore et al, 2012; Davis et al, 2012; Ghosal et al, 2012; Juhasz et al, 2012; Machida et al, 2012; Mosbech et al, 2012; Kim et al, 2013). However, it remains unclear, how cells depleted of DVC1 override the G2/M checkpoint so that this damage manifests in mitosis.

The contribution of replication stress to chromosomal instability in cells with impaired p97 function raised the question, if p97 and its cofactors are crucial for the survival of human tumor cells after replication stress. To address this issue, we depleted HeLa cells of p97 or its cofactors Ufd1, Npl4, UBXD7, or DVC1 and examined cell viability with an MTS assay after additional application of replication stress. In our setting, we applied replication stress by treatment with the DNA crosslinker cisplatin or the topoisomerase II inhibitor doxorubicin that are genotoxic chemotherapeutics. Cytotoxicity of cisplatin and doxorubicin was significantly elevated in cells depleted of p97. Depletion of Ufd1 or Npl4 provoked a slightly increased sensitivity to cisplatin at high concentrations and a significantly increased sensitivity to doxorubicin, albeit not as pronounced as in the case of p97. In contrast, knockdown of UBXD7 or DVC1 did not affect cell viability after replication stress. Notably, depletion of p97 or Npl4 resulted in

a significant reduction in cell proliferation over control cells in unchallenged cells in contrast to depletion of the other analyzed proteins.

Additionally, we examined if p97 inhibition was able to sensitize human cancer cells to the genotoxic chemotherapeutic drugs cisplatin or doxorubicin. Only upon p97 inhibition with the potent inhibitor NMS-873, we observed significant synthetic lethality with doxorubicin treatment, although to a lesser extent than upon p97 depletion. It remains unclear if these observations are due to weak inhibition of the p97 ATPase activity or whether the absence of p97 itself causes sensitization in depleted cells.

Similar to our observations, Puumalainen and colleagues revealed a hypersensitivity to UV light of p97-depleted cells in a colony formation assay (Puumalainen et al, 2014). Consistently, p97 inhibition with DBeQ significantly decreased cell survival after UV irradiation in an MTT assay (He et al, 2016). UV light induces the formation of CPDs and 6-4PPs that are mainly repaired by NER, whereas cisplatin-induced base crosslinks activate three different repair or tolerance pathways, namely HR, NER, and TLS.

In cells with compromised p97 function, cell viability after UV damage is aggravated due to impaired DNA repair after UV irradiation because p97 is involved in the repair of UV lesions. In GG-NER, it targets the DNA damage sensors XPC and DDB2, and in TC-NER, it targets CSB (Puumalainen et al, 2014; He et al, 2016). Reduced survival of p97-depleted cells after cisplatin can be explained by the role of p97 in HR, NER, and TLS, even though the underlying mechanism for compromised HR and TLS in p97-deficient cells remains elusive. Surprisingly, knockdown of UBXD7 or DVC1 had no influence on cell viability after cisplatin treatment, although UBXD7 and DVC1 have been linked to NER and TLS, respectively. In contrast, depletion of the two p97 adaptor proteins Ufd1 or Npl4 caused an elevated sensitivity to cisplatin. This stronger effect of Ufd1 or Npl4 depletion compared to UBXD7 or DVC1 depletion might be due to the involvement of Ufd1-Npl4 in more than only one of the three repair/tolerance pathways required to cope with cisplatin-induced DNA crosslinks. So far, for the Ufd1-Npl4 adaptor only the participation in NER is clearly confirmed (Verma et al, 2011; Puumalainen et al, 2014; He et al, 2016). However, its involvement in TLS is controversial (Davis et al, 2012; Mosbech et al, 2012) and for HR there are no data yet.

In *Caenorhabditis elegans*, the synergistic effect of impeded CDC-48, UFD-1, or NPL-4 combined with sublethal doses of another replication stress, the replication blocking agent hydroxyurea, was analyzed. Hydroxyurea inhibits the ribonucleotide reductase and thus decreases the production of dNTPs. In worms, downregulation of CDC-48, UFD-1, or NPL-4 led to an increased sensitivity towards hydroxyurea, resulting in embryonic lethality and sterile worms (Mouysset et al, 2008). This phenotype was

accompanied by the activation of the DNA replication checkpoint kinases ATL-1/ATR and CHK-1/Chk1 (Mouysset et al, 2008). Additionally, co-depletion of CDC-48 and UBXN-3, the worm ortholog of FAF1, potently impaired embryonic viability in *Caenorhabditis elegans* and this was further aggravated upon hydroxyurea treatment (Franz et al, 2016). This shows that the importance of p97, Ufd1, and Npl4 for survival under stress conditions is conserved.

Furthermore, Meerang and colleagues investigated the survival of human tumor cells after IR by a colony formation assay (Meerang et al, 2011). IR mainly induces DSBs, similar to doxorubicin. Doxorubicin intercalates into DNA and is able to covalently link topoisomerase II to DNA, which results in a DSB when encountered by a replication fork in the following round of replication (Li & Baker, 2000). The results of the colony formation assay showed a decreased survival after IR and additional depletion of p97, Ufd1, or Npl4 or after p97 inactivation by the expression of p97EQ (Meerang et al, 2011). p97EQ is a dominant negative p97 variant, where the conserved glutamate in the Walker B motif of the D2 domain is changed to glutamine, resulting in an ATPase-deficient p97 mutant able to bind, but unable to release substrates (DeLaBarre & Brunger, 2003). Similar to the observations by Meerang and colleagues, we monitored decreased cell viability upon depletion of p97, Ufd1, or Npl4 and additional treatment with doxorubicin. Impeded survival after IR or doxorubicin can be explained by the relevance of $p97^{Ufd1\text{-}Npl4}$ for DSB repair, although the exact role of p97 in DSB repair is unclear. However, impairment of p97 activity reduced HR and NHEJ (Meerang et al, 2011). Moreover, there is evidence that p97 is involved in the removal of L3MBTL1 from $H4K20me_2$ at DSBs allowing for binding of 53BP1 to the newly exposed histone methyl marks (Acs et al, 2011).

In *Saccharomyces cerevisiae*, seven UBX-containing genes were identified. Deletion of any of these genes results in viable yeast cells. However, yeast cells lacking multiple UBX proteins show severe phenotypes including cell death. These observations suggest that the single UBX proteins have critical, but overlapping functions (Decottignies et al, 2004; Schuberth et al, 2004; Buchberger, 2013). Similarly, in our experiments knockdown of p97 or Npl4 already caused a significant reduction in cell survival without further replication stress, while knockdown of the other analyzed cofactors did not. This observation stresses the importance of p97 and Npl4 for a myriad of pathways that are critical for cell survival, including cell cycle-related functions and functions in the protein quality control.

Taken together, there is evidence that p97 plays a role in DNA replication and the replication stress response. After p97 depletion, we observe reduced DNA synthesis,

DNA damage from S phase manifesting in mitosis, decreased cell survival and synthetic lethality with genotoxic agents. However, the exact function of p97 in replication and the replication stress response remains elusive.

3.3 The role of UBXD7

In the last part of this thesis, we aimed to investigate the novel p97 cofactor UBXD7 that was linked to DNA-related functions of p97. First, we analyzed the role of UBXD7 for diverse p97 substrate proteins. As a member of the family of UBA-UBX proteins, UBXD7 is able to bind to CRLs (Alexandru et al, 2008). Via its unique UIM domain, it binds to active, neddylated CRLs (Bandau et al, 2012; den Besten et al, 2012). Thereby, it directly links p97 to ubiquitin ligases. Moreover, p97-UBXD7 complexes bind to substrate proteins. So far, all identified UBXD7 substrates are nuclear proteins. These substrates include the CDC25A phosphatase which was identified as a substrate in this study, the hypoxia-inducible transcription factor HIF1α, the UV damage sensor DDB2, CSB which is required for the proteolytic release of RNA polymerase II, and, in yeast, the largest subunit of RNA polymerase II, Rpb1 (Alexandru et al, 2008; Verma et al, 2011; Puumalainen et al, 2014; He et al, 2016). However, the direct link of UBXD7 to p97 and to CRLs raised the question if UBXD7 is generally involved in CRL- and p97-dependent degradation both in the nucleus and in the cytoplasm.

To address this issue, we examined if UBXD7 participates in the turnover of a CRL- and p97-dependent substrate in the cytoplasm. For this purpose, we surveyed degradation of the cytosolic protein IκBα. Cytokine-induction prompts the CRL $SCF^{\beta TrCP}$ to ubiquitylate IκBα, leading to its proteasomal degradation with the help of $p97^{Ufd1\text{-}Npl4}$ (Li et al, 2014). Thus, IκBα is a cytosolic substrate of a CRL and p97. Immunoblot analysis revealed that, in contrast to $p97^{Ufd1\text{-}Npl4}$, UBXD7 is not involved IκBα degradation after TNFα induction (Fig. 3.1). Therefore, this indicates that UBXD7 is not required for the degradation of all CRL and p97 substrates. The finding that IκBα turnover is unaffected by UBXD7 is in line with the current view of UBXD7 acting exclusively in the nucleus. However, while two studies found overexpressed Flag-UBXD7 and GFP-UBXD7, respectively, localizing strictly to the nuclei of HeLa cells, a commercially available antibody from Millipore shows endogenous UBXD7 in the cytosol with the images being provided from the Alexandru group (Bandau et al, 2012; Raman et al, 2015). For this reason, we cannot exclude further functions of UBXD7 in the cytoplasm. Yet, Raman and colleagues performed systematic proteomics of the p97-UBXD adaptor network and identified several binding partners of UBXD7 that all localize to the nucleus (Raman et al, 2015). These binding partners include proteins

associated with TC-NER, other DDR proteins, and CRL components. It is unclear, if UBXD7 has a cytosolic counterpart overtaking its function in connecting p97 to CRLs in the cytoplasm.

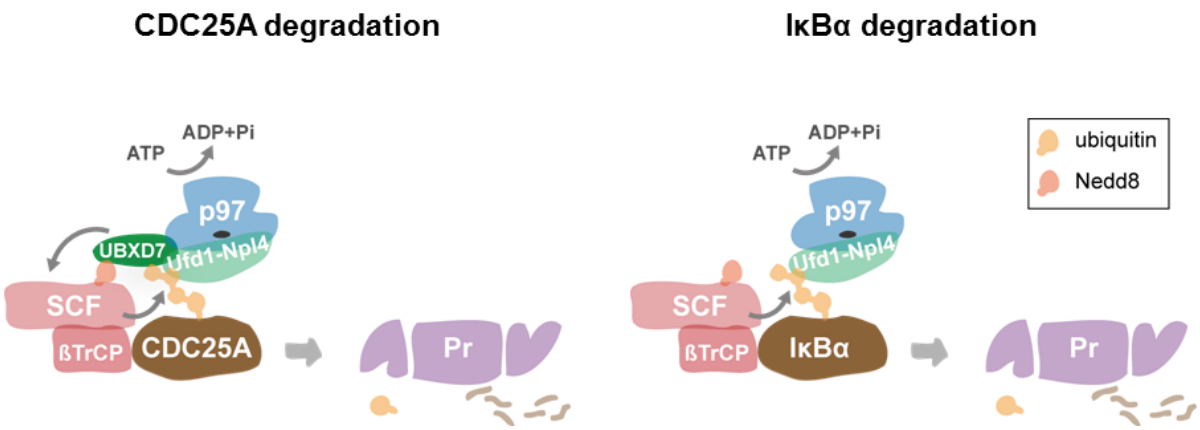

Figure 3.1: UBXD7 plays a role in CDC25A degradation, but not in IκBα degradation. CDC25A and IκBα are both ubiquitylated by $SCF^{\beta TrCP}$. After ubiquitylation, $p97^{Ufd1\text{-}Npl4}$ facilitates proteasomal degradation of both molecules. However, while UBXD7 is involved in CDC25A degradation, IκBα degradation is independent of UBXD7. Pr: proteasome.

In addition to studies on UBXD7 targets, we aimed to elucidate the relevance of the individual UBXD7 domains for its function. UBXD7 comprises an N-terminal ubiquitin-associated UBA domain, an ubiquitin-associating UAS domain, an ubiquitin-interacting motif (UIM) and a C-terminal UBX domain. The UBA domain is able to associate with ubiquitin, whereas the function of the UAS domain is unclear. The already mentioned UIM binds directly to the NEDD8 moiety of neddylated CRLs (Bandau et al, 2012; den Besten et al, 2012). However, it can also bind ubiquitin (Fisher et al, 2003). Interaction with p97 is mediated by the UBX domain.

To elucidate the contribution of the individual UBXD7 domains to its function, a detailed structure-function analysis of UBXD7-mediated degradation was performed. For this purpose, UBXD7 deletion mutants lacking the UBA, UAS or UIM domain, as well as a UBXD7 variant with a point-mutation known to abrogate p97-binding (P459G) were generated (Bandau et al, 2012). As the substrate for this experiment, the robust UBXD7 substrate DDB2 was chosen (Puumalainen et al, 2014). The UBXD7 variants were assayed for their ability to rescue DDB2 degradation, which is strictly UBXD7-dependent. We could show that the ΔUBA variant was able to almost completely rescue DDB2 degradation, whereas the ΔUAS mutant displayed only a partial rescue. In contrast, UBXD7_ΔUIM and UBXD7_P459G did not restore DDB2 degradation. These observations indicate that binding to neddylated CRLs via the UIM and binding to p97 via the UBX are essential for UBXD7 function, whereas the ability to directly

bind ubiquitylated substrates via the UBA is dispensable. The partial rescue of the UAS is difficult to explain, since its function is still unknown.

Bandau and colleagues found that a UBXD7 mutant lacking the UAS domain was able to interact with ubiquitin, p97 and CUL2 (Bandau et al, 2012). In contrast, den Besten and colleagues demonstrated that *in vivo* the ΔUAS variant is defective in CUL2-binding, which they did not observe *in vitro* (den Besten et al, 2012). Since we showed that the UBXD7_ΔUAS variant was only partially functional, this indicates that the UAS has a function in substrate degradation which still has to be explored.

The effect of the expression of the UBXD7_ΔUIM variant on the UBXD7 substrate HIF1α, which is ubiquitylated by CRL2 prior to proteasomal degradation, has already been investigated (Bandau et al, 2012). Previous experiments revealed that HIF1α levels decrease upon UBXD7 knockdown and increase upon UBXD7 overexpression, while the opposite is observed for knockdown or overexpression of p97 (Alexandru et al, 2008). As an explanation for this apparent paradox, it was proposed that lack of UBXD7 abolishes p97 recruitment to HIF1α, but allows the engagement of other proteasome targeting factors or the proteasome itself. Additionally, UBXD7 binding protects HIF1α from the association of these other proteasome targeting factors in p97-depleted cells. However, HIF1α accumulation upon UBXD7 overexpression was dependent on the UIM, as overexpression of the ΔUIM mutant did not affect HIF1α levels (Bandau et al, 2012). They could show that deletion of the UIM abolished the interaction with CUL2 and led to a complete loss of binding to non- or oligo-ubiquitylated HIF1α. Nonetheless, the ΔUIM mutant was still able to associate with poly-ubiquitylated HIF1α, most likely via the UBA domain. Consistently, deletion of the UIM led to a loss of function of UBXD7 in our experimental setting.

Furthermore, we could show that DDB2 turnover is independent of the UBA domain of UBXD7. Thus, direct binding of UBXD7 to ubiquitylated DDB2 via the UBA is dispensable. However, UBXD7_ΔUBA could still bind ubiquitin through its UIM. Additionally, UBXD7 indirectly interacts with the ubiquitylated substrate via its association with the CRL and p97. Alexandru and colleagues proposed that substrate binding to UBXD7 precedes the recruitment of $p97^{Ufd1\text{-}Npl4}$ and may even be a prerequisite for it (Alexandru et al, 2008). The basis for their suggestion was the observation that binding of UBXD7 to the substrate and the E3 ubiquitin ligase does not require $p97^{Ufd1\text{-}Npl4}$, whereas the interaction of $p97^{Ufd1\text{-}Npl4}$ with the substrate and E3 ubiquitin ligase depends on UBXD7. For this reason, they proposed a model that the UBA and UBX domains of UBXD7 bind intra- or intermolecularly, thereby maintaining UBXD7 in an inactive state. Only after UBXD7 binds to a ubiquitylated substrate via the UBA domain, the UBX domain would be set free to recruit the $p97^{Npl4\text{-}Ufd1}$ complex. In

contrast to their opinion that UBXD7 directly binds to ubiquitylated substrates via its UBA domain, we suggest that UBXD7 is recruited to the ubiquitylated substrate by its UIM associating with the neddylated CRL and therefore only indirectly interacts with the ubiquitylated substrate.

In a second step, $p97^{Ufd1\text{-}Npl4}$ is recruited to the ubiquitylated substrate. He and colleagues showed that p97 recruitment to sites of UV lesion is independent of UBXD7, indicating that p97 and UBXD7 are recruited to ubiquitin conjugates independent of each other (He et al, 2016). In contrast, p97 recruitment to sites of UV lesion was shown to depend on Ufd1 and Npl4 (Puumalainen et al, 2014). This indicates that p97 is recruited to ubiquitylated substrates via the ubiquitin binding domains of its ubiquitin adaptors. In the case of DDB2, this means that $p97^{Ufd1\text{-}Npl4}$ binds to ubiquitylated DDB2 via the UT3 and NZF domains of Ufd1 and Npl4, respectively. Consistent with this hypothesis, the UBA domain of UBXD7 is not critical for substrate degradation. However, it might support the interaction with the ubiquitylated substrate.

The UBXD7 interaction with p97 is mediated by its UBX domain and this interaction is essential for UBXD7 function. Surprisingly, a defect in p97-binding was shown to additionally impair ubiquitin-binding, whereas CUL2 interaction was largely unaffected (Bandau et al, 2008). Therefore, this indicates that binding to ubiquitylated substrates does neither occur directly via the UBA domain, nor indirectly via the CRL. In contrast, binding to ubiquitylated substrates would depend on p97-binding to the ubiquitylated substrate via Ufd1-Npl4.

Taken together, these data show that further experiments are required to clarify the contribution of the single UBXD7 domains to its function.

4 Material and Methods

4.1 Molecular biological methods

4.1.1 Cloning strategy

For the generation of a reporter cell line inducibly expressing GFP-CDC25A, GFP-CDC25A had to be cloned into the vector pcDNA5.0/FRT/TO (Thermo Scientific). We received CDC25A/pOPINE as a gift from Dr. Christian Ottmann, Chemical Genomics Centre, Dortmund, Germany. First, CDC25A was cloned from pOPINE into the vector pEGFP-C1 (Clontech). For this purpose, the coding sequence of CDC25A was amplified by polymerase chain reaction (PCR) with DNA primers carrying KpnI and BamHI restriction sites at the 5'- and 3'-end, respectively. After that, GFP-CDC25A was cloned from the GFP-CDC25A/pEGFP-C1 construct into the plasmid backbone pcDNA5.0/FRT/TO by PCR amplification of GFP-CDC25A with DNA primers introducing novel EcoRV and NotI restriction sites at the 5'- and 3'-end, respectively.

4.1.2 Polymerase chain reaction

The DNA primers for the PCR were designed with 15 to 20 nucleotides binding to the target sequence and one to three nucleotides overhang behind the restriction site. The length of the overhang was chosen according to the manufacturer's recommendations for the enzyme cutting the restriction site. The enzymes were purchased from New England Biolabs (NEB). The DNA primers were ordered from Metabion. The primer sequences are listed in Table 4.1.

Table 4.1: DNA primers used for PCR.

Target	Orientation	Sequence	$T_{annealing}$
CDC25A	forward	ATGGGTACCGAACTGGGCCCGGAGC	68 °C
	reverse	TGAGGATCCTTAGAGCTTCTTCAGACGAC	57 °C
GFP-CDC25A	forward	CGATATCGCCACCATGCTGAGC	53 °C
	reverse	AGCGGCCGCTTAGAGCTTCTTCAGACGAC	52 °C

The sequences of the DNA primers are given in 5' to 3' direction. The restriction sites are highlighted in red.

The PCR was carried out in 50 µl reactions, with the following components mixed in 0.2 ml PCR reaction tubes on ice:

10 µl 5x Phusion HF buffer

2 µl 10 mM dNTP mix (Invitrogen)

2 µl DNA-primer forward (100 pmol)

2 µl DNA-primer reverse (100 pmol)

10 ng DNA template
0.5 µl Phusion DNA Polymerase (2 U/µl; Thermo Scientific)
ad 50 µl ddH_2O
The target sequence was amplified with a TPersonal thermocycler (Biometra) using the standard PCR protocol described in Table 4.2.

Table 4.2: Standard PCR protocol.

	Temperature	Time	
First denaturation	98 °C	20 s	
Denaturation	98 °C	10 s	
Annealing	53/57 °C	30 s	27 cycles
Elongation	72 °C	1 min	
Final elongation	72 °C	9 min	

The annealing temperature was chosen according to the sequence of the DNA primers used for the PCR. The correct amplification of the PCR product was verified by agarose gel electrophoresis.

4.1.3 Agarose gel electrophoresis

The PCR mixture was mixed with 5x DNA loading buffer (NEB) and separated on a 1% TAE agarose gel supplemented with GelRed nucleic acid gel stain (Biotium). A 1 kb DNA ladder (NEB) served as a marker for size. Agarose gels were run in a chamber filled with TAE buffer for 1 h at a constant voltage of 100 V with the peQPOWER 300 power supply (Peqlab). After gel electrophoresis, the correct PCR product was cut out of the gel and purified with a PCR clean-up gel extraction kit (Macherey-Nagel). Then, the DNA concentration was determined photometrically with a BioPhotometer D30 (Eppendorf).

4.1.4 Restriction

The purified PCR product and the target backbone were cut with restriction endonucleases that target the newly introduced restriction sites of the PCR product. The restriction with two different enzymes was either carried out simultaneously or consecutively, depending on the manufacturer's recommendations for the respective restriction enzymes used. All restriction endonucleases were purchased from NEB.
The restriction was carried out for 1 h at 37 °C in 10 µl reactions containing the following components:

1 µg DNA
1 µl 10x NEB buffer (compatible to the enzyme used)
1 µl BSA
0.4 µl restriction enzyme (NEB)
ad 10 µl ddH_2O
After restriction, the mixtures were purified using a NucleoSpin Extract II Kit (Macherey-Nagel).

4.1.5 Ligation

To ligate the digested DNA fragment into the target vector, the digested vector was incubated with three times excess of the DNA insert. The ligation was carried out overnight at 16 °C in 20 µl reactions containing the following components:
150 ng DNA insert
50 ng plasmid vector
2 µl 10x ligase buffer
0.5 µl T4 DNA ligase (NEB)
ad 20 µl ddH_2O

4.1.6 Bacterial transformation

Chemically competent bacteria were transformed with the ligated plasmid constructs by heat shock. The bacteria used for transformation were *Escherichia coli* bacteria of the strain DH5α (genotype: *fhuA2 lac(del)U169 phoA glnV44 Φ80' lacZ(del)M15 gyrA96 recA1 relA1 endA1 thi-1 hsdR17*).
For transformation, 50 µl of DH5α bacteria was incubated with 10 µl of the ligation reaction for 20 min on ice. Then, the bacteria were placed in a 42 °C-water bath for 1 min and subsequently incubated on ice for 10 min. Bacteria transformed with plasmid DNA resistant against kanamycin (in this study the backbone pEGFP-C1) were incubated with 200 µl SOC medium for 30 min at 37 °C. After that, the bacteria were grown overnight at 37 °C on LB agar plates containing 50 µg/ml ampicillin (Diagonal) or 50 µg/ml kanamycin (Diagonal), depending on the resistance of the DNA plasmid.

4.1.7 Plasmid preparation (Mini prep)

Single colonies of the bacteria were picked and incubated with 2 ml LB medium supplemented with 50 µg/ml ampicillin or 50 µg/ml kanamycin overnight at 37 °C. Then, the plasmid DNA was purified using a Plasmid DNA Purification Kit (Macherey-Nagel). Insertion of the target fragment into the vector was confirmed by control restrictions.

4.1.8 Sequencing

The correct insertion of the target fragment into the vector was confirmed by sequencing. Sequencing reactions were carried out by GATC Biotech.

4.2 Cell culture

Cells were maintained at 37 °C and 5% CO_2. Dulbecco's Modified Eagle Medium (DMEM; PAN) supplemented with 10% fetal bovine serum (FBS; PAN, Lot No.: P280209) and 1% penicillin/streptomycin (PAN) was used as a cell culture medium for HeLa Kyoto or U2OS cells. U2OS-FRT-TO cells inducibly expressing GFP-CDC25A were maintained in DMEM supplemented with 10% tetracycline-free FBS (PAN, Lot No.: P040214TC), 1% penicillin/streptomycin, 130 µg/ml hygromycin B (PAN) and 4 µg/ml blasticidin S (Gibco). Expression of GFP-CDC25A was induced with 1 µg/ml doxycycline (Diagonal).

4.2.1 Generation of a GFP-CDC25A reporter cell line

To generate a reporter cell line inducibly expressing GFP-CDC25A, U2OS-FRT-TO cells carrying a single integrated FRT (Flp recombination target) site and a stably integrated tetracycline (Tet) repressor were used. The U2OS-FRT-TO cells were cultured in DMEM supplemented with 10% tetracycline-free FBS, 1% penicillin/streptomycin, 50 µg/ml zeocin (Invitrogen) and 4 µg/ml blasticidin S (Gibco). The cells were co-transfected with GFP-CDC25A/pcDNA5.0-FRT-TO and the pOG44 Flp-recombinase plasmid (Invitrogen) in a 1:9 ratio to achieve integration into the FRT site. Plasmids were transfected using Lipofectamine 2000 (Invitrogen) according to the manufacturer's instructions. After 24 h, cells were cultured in DMEM selection medium containing 10% tetracycline-free FBS, 1% penicillin/streptomycin, 130 µg/ml hygromycin B and 4 µg/ml blasticidin S, until single cell colonies were detectable. Single clones were picked and cultured separately.

4.2.2 RNA interference

RNA interference (RNAi) was carried out by transfection of cells with siRNA duplexes using the Lipofectamine RNAiMAX transfection reagent (Invitrogen). Cells were either seeded one day in advance (forward transfection) or at the same time as RNAi transfection (reverse transfection). The cells were transfected at 30 to 50% confluence with a final concentration of 10 nM siRNA. Transfection with Lipofectamine RNAiMAX transfection reagent was performed according to the manufacturer's instructions. All siRNAs were purchased from Microsynth. siRNA sequences are listed in Table 4.3. RNAi transfected cells were analyzed 48 or 72 h after transfection.

For a reverse transfection in a 6-well plate format, 1.2 µl of a 20 mM siRNA stock solution was diluted in 250 µl Opti-MEM I (Gibco). Separately, 2.4 µl of the Lipofectamine RNAiMAX transfection reagent was diluted in 250 µl Opti-MEM I, mixed briefly and added to the diluted siRNA. After 20 min incubation at room temperature, the transfection mixture was added to the wells, before the cells were seeded. For transfection in 12-well plates, half the volumes were used.

Table 4.3: siRNA oligonucleotides used for depletion.

Target	Oligo	Sequence	Source
-	siCtrl	UUCUCCGAACGUGUCACGUTT	Ritz et al., 2011
βTrCP1/2	siβTrCP1/2	GUGGAAUUUGUGGAACAUCTT	Busino et al., 2003
Chk1	siChk1 S1	AAGGGATAACCTCAAAATCTCTT	Carrassa et al., 2009
DVC1	siDVC1 S1	ACGAUGAGGUGGAUGAGUATT	Mosbech et al., 2012
	siDVC1 S2	UCAAGUACCACCUGUAUUATT	Mosbech et al., 2012
Luciferase	siluc	CGUACGCGGAAUACUUCGATT	Microsynth
Npl4	siNpl4 S1	CGUGGUGGAGGAUGAGAUUTT	Dobrynin et al., 2011
	siNpl4 S6	CGGAAGGUUGGCUGGAUAUUUTT	Li et al., 2014
p97	sip97 S2	AACAGCCAUUCUCAAACAGAATT	Qiagen, HS_VCP_7
	sip97 S6	GGAGUUCAAAGUGGUGGAAACAGAUTT	Invitrogen, HSS111264
PSMB5	siPSMB5	UUCUCCGAACGUGUCACGUTT	Li et al., 2014
Ufd1	siUfd1 S1	GGGCUACAAAGAACCCGAATT	Microsynth
	siUfd1 S2	GUGGCCACCUACUCCAAAUTT	Dobrynin et al., 2011
	siUfd1 S3	CUACAAAGAACCCGAAAGATT	Microsynth
	siUfd1 S4	ACAAAGAACCCGAAAGACATT	Microsynth
	siUfd1 S5	CUGGGCUACAAAGAACCCGAA	Qiagen, UFD1_L
	siUfd1 S6	CCCAAUCAAGCCUGGAGAUAUTT	Li et al., 2014
UBXD1	siUBXD1	CCAGGUGAGAAAGGAACUUTT	Ritz et al., 2011
UBXD7	siUBXD7 S1	CAGCUUGAAAGGAGUGUUUTT	Qiagen, Hs_KIAA0794_2
UBXD8	siUBXD8	GAAGUUAUUUCACUAAUAATT	Suzuki et al., 2012

4.2.3 Plasmid transfection

Plasmids were transfected using polyethylenimine (PEI). Reaction mixtures containing 2 µl PEI (10 mM stock, pH 7.0, Sigma), 2 µg DNA and 50 µl PBS (PAN) were incubated for 15 min and added dropwise onto cells with 60-80% confluency. Plasmids were expressed for 24 h.

4.2.4 Pharmacological treatments

To block protein synthesis, either 50 µg/ml was added to the cells. p97 function was inhibited by treatment with DBeQ (Sigma-Aldrich or BioCat), NMS-859 (Sigma-Aldrich), NMS-873 (Sigma-Aldrich), I8, I5, or I1. An information embargo bans us from revealing the full names and structures of the unpublished inhibitors I8, I5, and I1, which we received for testing. To block proteasomal degradation, cells were treated with 10 µM MG132 (Merck-Millipore). Replication stress was induced by treatment with either cisplatin (Teva), doxorubicin (Diagonal), or aphidicolin (Sigma-Aldrich). Since the p97 inhibitors and aphidicolin were dissolved in dimethyl sulfoxide (DMSO), DMSO served as control.

4.2.5 Irradiation

UV irradiation was carried out by use of the CL-1000 Ultraviolet Crosslinker (UVP). Cells were exposed to IR in a Cabinet X-Ray System (Philips MCN 165; 3 mm Al filter; 130 kV, 16 mA; dose-rate 1.2 Gy/min).

4.3 Cell-based assays

4.3.1 BrdU flow cytometry assay

Approximately 1 million HeLa cells were incubated with 30 µM BrdU for 15 min at 37 °C to pulse-label the cells. Then, the cells were washed twice with PBS, treated with trypsin and collected in reaction tubes. After cell counting, the cells were centrifuged for 5 min at 1500 rpm, the supernatant was removed and the cells were fixed with 1 ml 70% cold ethanol. The cells were again centrifuged for 5 min at 1500 rpm, the supernatant was removed and the cells were washed with 1 ml 0.9% NaCl. After that, the cells were again centrifuged for 5 min at 1500 rpm and the supernatant was removed. Next, the cells were incubated with 1 ml cold pepsin/HCl for 10 min at 37 °C. Subsequently, 3 ml ice-cold 0.9% NaCl was added and the suspension was centrifuged for 5 min at 1500 rpm and the supernatant was removed. Next, the pellet was resuspended in 1 ml 2 M HCl and incubated for 20 to 30 min at room temperature. Then, 3 ml 0.9% NaCl was added, the suspension was centrifuged for 5 min at 1500 rpm and the supernatant was removed. After that, the pellet was resuspended in 1 ml PBS-T, the suspension was centrifuged for 5 min at 1500 rpm and the supernatant was removed. Subsequently, the cells were incubated with 250 µl primary anti-BrdU antibody (BD, 347580) diluted 1:50 in PBS-T for 30 min. After another centrifugation step at 1500 rpm for 5 min, unbound primary antibody was removed by washing with 1 ml PBS-T-BSA (1%, Albumin fraction V, Applichem), the suspension was centrifuged for 5 min at 1500 rpm and the supernatant was removed. Then, the cells were

incubated with 250 µl secondary Alexa Fluor 488 goat anti-mouse antibody (Life Technologies, A-11029) diluted 1:200 in PBS-T-BSA (1%) for 30 min, the suspension was centrifuged at 1500 rpm for 5 min and the supernatant was removed. Next, the pellet was washed with 1 ml PBS-T-BSA (1%), the suspension was centrifuged for 5 min at 1500 rpm and the supernatant was removed. Finally, the pellet was resuspended in 1 ml PBS containing 25 µg/ml propidium iodide (Sigma) and 50 µg/ml RNAse A (Roche) and incubated for 15 min at 37 °C. After that, the suspension was analyzed by flow cytometry with a FACSCalibur (BD Biosciences). The measured intensities were evaluated with Kaluza Flow Cytometry Analysis software (Beckman Coulter). The Alexa Fluor 488 intensities were plotted against the PI intensities and the percentage of BrdU positive cells was determined. Additionally, to visualize the cell cycle distribution the counts were plotted against the PI intensities in histograms.

4.3.2 Radioresistant DNA synthesis assay

Approximately 0.1 to 0.15 million HeLa cells were cultured for 48 h in 25 cm^3 cell culture flasks and were irradiated with 10 Gy IR at 37 °C. Subsequently, they were brought to a warm room with a constant temperature of 37 °C and 5% CO_2. After specific time points, the cell culture medium was removed and 2 ml of prewarmed radioactive medium containing 0.3 µCi/ml ^{3}H-thymidine was added to the flasks for 15 min (pulse-labeling). Then, the radioactive medium was removed and the cells were washed with 2 ml cold PBS. After that, 1 ml trypsin was added to the cells and incubated for 3 min in the warm room. The cells were collected with 4 ml DMEM supplemented with 10% FBS and 1% penicillin/streptomycin in 15 ml Falcon tubes already placed in ice-water. After cell counting, the samples were poured on separate GF/A glass microfiber filters and the medium was aspirated with a vacuum pump. Then, 15 ml 10% trichloric acid was added onto each filter, incubated briefly and aspirated. Finally, 15 ml ddH_2O was added onto each filter, incubated briefly and aspirated. After that, each filter was placed into a separate scintillation vial and dried for a moment. Then, 0.5 ml 0.5 M NaOH was added into each vial. After incubation overnight at 65 °C, 0.5 ml 0.5 M HCl was added into each vial. Finally, 10 ml of liquid scintillation fluid was added into each vial, mixed briefly and ^{3}H-activity was measured using a liquid scintillation counter. The RDS assay was performed together with Dr. Aashish Soni at the Institute for Medical Radiation Biology at the University Hospital, Essen, run by Prof. Dr. George Iliakis.

4.3.3 Cell viability assay

The number of viable cells was determined with the CellTiter 96 AQueous One Solution Cell Proliferation Assay (Promega) in a 96-well plate format according to the manufacturer's instructions. This assay is based on the reduction of the tetrazolium salt MTS to its insoluble formazan. The quantity of formazan product as measured by the amount of 490 nm absorbance with a 96-well plate reader (SpectraMax Plus 384, Molecular Devices) is directly proportional to the number of viable cells in culture.

4.4 Biochemical methods

4.4.1 Preparation of cell extracts

For the preparation of cell extracts, all steps were carried out on ice to inhibit biochemical processes and preserve proteins. The cells were washed briefly with ice-cold PBS, before they were lysed in 50 µl extraction buffer supplemented with protease inhibitor (Roche, Complete EDTA-free) and, if necessary, phosphatase inhibitor (Roche, PhosSTOP), or 10 mM N-ethylmaleimide (Sigma-Aldrich) and PR619 (Abcam) to inhibit deubiquitylation. Cells were scraped from the bottom of the dishes they were cultured in using a cell scraper (BD Falcon) and transferred to reaction tubes. After incubation on ice for 15 min, the cell extracts were centrifuged for 15 min at 13300 rpm and 4 °C to remove nuclei and heavy membrane fragments. Protein concentration was determined using a BCA assay (Interchim) in a 96-well plate format. Cell extracts were frozen in liquid nitrogen and stored at -80 °C.

4.4.2 SDS-PAGE and Western blotting

Protein samples from cell extracts were separated according to their size by sodium dodecyl sulfate polyacrylamide gel electrophoresis (SDS-PAGE). Protein samples with a protein content of 30 to 50 µg were prepared. Samples were supplemented with 6x SDS loading buffer and boiled at 95 °C for 10 min. PageRuler Prestained Protein Ladder (Thermo Scientific) served as a marker for protein size. All SDS gels were casted with 10% polyacrylamide, except for the investigation of IκBα degradation, where gradient gels containing 5-15% polyacrylamide were used. 10% SDS gels are given in Table 4.4.

Table 4.4: Recipes for SDS gels.

	5% SDS gel	10% SDS gel	15% SDS gel
H_2O	5.37 ml	3.37 ml	1.37 ml
1 M Tris pH 8.8	4.5 ml	4.5 ml	4.5 ml
10% SDS	120 µl	120 µl	120 µl
30% PAA	2 ml	4 ml	6 ml
10% APS	60 µl	60 µl	60 µl
TEMED	6 µl	6 µl	6 µl

For SDS-PAGE, the Mini Trans-Blot system (Bio-Rad) was applied. The SDS running buffer contained Tris/glycine. Gels were run at a constant current of 20 mA per gel with an Electrophoresis Power Supply – EPS 601 (BioRad). To transfer the proteins from the gels onto nitrocellulose Hybond-C Extra (Amersham), either semi-dry or wet Western blotting was performed. For both, the gel was placed onto nitrocellulose and put between two double layers of Whatman filter paper, before the whole sandwich was soaked in blotting buffer. To avoid air bubbles, a plastic tube was rolled across the sandwich. For semi-dry blotting, the sandwich was put in a semi-dry Trans-blot SD transfer chamber (BioRad) and a constant current of 120 mA per gel was applied for 55 min to transfer the proteins from the gel onto the membrane. For wet blotting, the sandwich was placed in Mini Trans-Blot chambers (BioRad), the chamber was completely filled with a wet blot buffer and a constant current of 300 mA per gel was applied for 3 h at 4 °C for protein transfer. The membranes were stained with Ponceau-S dye to prove equal transfer. After destaining with 5% acetic acid and neutralization with PBS-T, the membranes were blocked in 10% fat free milk in PBS-T for 10 min. Membranes were washed three times for 5 min with PBS-T, before they were incubated with primary antibodies overnight at 4 °C or for 2 h at room temperature. Different primary antibodies were diluted to diverse concentrations in 3% BSA/PBS-T as described in Table 4.5. Membranes were washed again three times for 5 min with PBS-T and then incubated with secondary antibodies for 1 h at room temperature. HRP-coupled secondary antibodies were diluted to diverse concentrations in 3% BSA/PBS-T as detailed in Table 4.5. Finally, membranes were washed another three times for 5 min with PBS-T. To detect the membrane-bound secondary antibodies, membranes were briefly incubated with SuperSignal West Pico enhanced chemiluminescence (ECL) substrate (Thermo Scientific) or ECL Prime Western Blotting detection reagent (Amersham). Both solutions were prepared freshly according to the manufacturer's instructions. The light signals were detected on SUPER RX films (Fujifilm) and films were developed in a Cawomat 2000 IR (Cawo) developing machine.

Films were digitalized with an Epson Perfection V800 Photo film scanner (Epson). Digital images were quantified using either Bio1D analysis software (Vilber Lourmat) or TotalLabQuant (Cleaver Scientific).

Some of the membranes were stained with fluorophore-conjugated secondary antibodies. Importantly, in this case all washing steps were done with PBS instead of PBS-T. Moreover, blocking buffer and antibody dilutions were prepared with PBS and not PBS-T. The fluorescence signal was detected with the Odyssey CLx Imaging system (Li-Cor).

Table 4.5: Primary and secondary antibodies used for Western blotting.

Antigen	Species	Dilution	Source
α-tubulin	mouse	1:8000	Sigma-Aldrich, T5168
CDC25A	mouse	1:500	Thermo Scientific, Ab-1, Clone DCS-120
DDB2	mouse	1:200	Abcam, ab51017
GAPDH	mouse	1:20000	Sigma-Aldrich, G8795
HA	rabbit	1:1000	Sigma-Aldrich, H6908
IκBα	mouse	1:1000	Cell Signaling, 4814
Npl4	rabbit	1:500	H. Meyer, HME18, purified
p97	rabbit	1:2000	H. Meyer, HME8, serum
PSMB5	rabbit	1:1000	Abcam, ab3330
UBXD1	rabbit	1:10000	H. Meyer, E43, serum
UBXD7	sheep	1 µg/ml	G. Alexandru, S409D, serum
UBXD8	rabbit	1:1000	Novus Biologicals, NBP2-16381
Ufd1	mouse	1:500	C. Brasseur, 5E2, purified
HRP-anti mouse	goat	1:10000-1:20000	BioRad, 170-6516
HRP-anti rabbit	goat	1:10000-1:20000	BioRad, 170-6515
HRP-anti sheep	rabbit	1:10000-1:20000	Pierce, 31480
IRDye 800CW anti mouse	donkey	1:2500-1:20000	Li-Cor, 925-32212
IRDye 800CW anti rabbit	donkey	1:10000-1:15000	Li-Cor, 925-32213
IRDye800 anti goat	donkey	1:5000	Rockland antibodies, 605-732-125

4.5 Fluorescence microscopy

To visualize mitotic defects of mitotic or pre-mitotic origin, kinetochores were stained by immunofluorescence using a mixture of primary antibodies binding to kinetochores (CREST) and a fluorophore-conjugated secondary antibody. HeLa cells were seeded on sterile glass cover slips (0.18 mm in diameter, VWR) in 12-well plates. After siRNA

transfection for 48 h and further treatment with DMSO or 0.2 µM APH for 24 h, the cells were washed with PBS before fixation with 4% formaldehyde (PFA; Sigma-Aldrich) in PBS for 10 min. Following three washing steps with PBS for 5 min each, the cells were permeabilized with 0.1% Triton X-100 in PBS for 10 min. The cells were washed again three times with PBS for 5 min each and then blocked with 3% BSA (Applichem) in PBS for 30 min. After blocking, the cover slips were transferred into a wet chamber, where they were placed with the cell side down on drops of primary antibody on Parafilm (Bemis) and incubated for 90 min. The primary anti-centromere antibody (CREST, human, Antibody Inc., 15-234) was diluted 1:500 in 3% BSA in PBS. Following another three washing steps with PBS for 5 min each in 12-well plates, the cells were incubated with the secondary Alexa GAH594 antibody (Invitrogen) diluted 1:500 in 3% BSA in PBS in the wet chamber for 30 min. Then, the cells were washed for three times with PBS for 5 min each and washed once with ddH_2O to remove residual salts. After that, the cover slips were mounted on microscopy slides (Marienfeld) with the cell side down on drops of Mowiol (Calbiochem) solution, containing 0.5 µg/ml of the DNA dye DAPI. The microscopy slides were dried at room temperature and stored at 4 °C.
The counting of mitotic defects was performed on an inverted fluorescence microscope (Axio Observer Z1, Zeiss) using an x63, 1.4 NA objective. Images were taken with an inverted spinning-disc confocal microscope (Nikon Eclipse Ti equipped with a Yokogawa CSU X-1 spinning disk unit) using an x100, 1.49 NA objective. Images were acquired with an Andor iXon X3 EMCCD (electron multiplying charge coupled device) camera.

U2OS-FRT-TO cells inducibly expressing GFP-CDC25A were seeded on glass cover slips for fluorescence microscopy. One day later, they were induced with 1 µg/ml doxycycline for 24 h. After that, they were washed with PBS and fixed with 4% PFA for 10 min. Then, the cells were washed three times with PBS for 5 min each and permeabilized with 0.1% Triton X-100 in PBS for 10 min. Following three washing steps with PBS for 5 min each and a brief washing step with ddH_2O, the cover slips were mounted on microscopy slides with the cell side down on drops of Mowiol solution, containing 0.5 µg/ml DAPI. Again, the microscopy slides were dried at room temperature and stored at 4 °C.
Imaging was carried out with an inverted spinning-disc confocal microscope (Nikon Eclipse Ti equipped with a Yokogawa CSU X-1 spinning disk unit) using an x40, 0.94 NA objective. Images were acquired with an Andor iXon X3 EMCCD (electron

multiplying charge coupled device) camera. GFP intensity was quantified with CellProfiler software (Broad Institute).

4.6 Statistical analysis

Statistical analyses were performed in SigmaPlot software (Systat). Data were analyzed by unpaired, one-tailed Student's t-test or Mann-Whitney Rank sum test, depending on normality and equality of variances. Values of $p < 0.05$ (*), $p < 0.01$ (**), and $p < 0.001$ (***) were considered statistically significant.

4.7 Buffers and solutions

TAE buffer
40 mM Tris
20 mM acetic acid
1 mM EDTA
pH 8.3

SOC medium
0.5% yeast extract
2% tryptone
10 mM NaCl
2.5 mM KCl
10 mM $MgCl_2$
10 mM $MgSO_4$
20 mM glucose
pH7.0

LB medium
10 g/l peptone (Fluka)
10 g/l NaCl
5 g/l yeast extract (Applichem)
pH 7.0
for LB agar plates:
additional 20 g/l agar (Applichem)

PBS
10 mM Na_2HPO_4
2.17 mM NaH_2PO_4
154 mM NaCl
pH 7.4

Pepsin/HCl
5 g/l Pepsin
55 mM HCl

Extraction buffer
150 mM KCl
25 mM Tris, pH 7.4
5 mM $MgCl_2$
5% glycerol
1% Triton X-100
2 mM β-mercaptoethanol
pH 7.4

6x SDS loading buffer
0.35 M Tris, pH 6.8
30% glycerol
10% SDS
9.3% DTT
0.02% bromophenol blue

SDS running buffer

190 mM glycine

25 mM Tris

0. 1% SDS

pH 8.8

Blotting buffer

20% methanol

in SDS running buffer

Wet blot transfer buffer

0.192 mM glycine

20.5 mM Tris

0.04% SDS

pH 8.3

20% methanol

Ponceau-S

2 g/l Ponceau powder

0.05% acetic acid

PBS-T

0.05% Tween 20

in PBS

pH 7.4

Stripping buffer

7 M guanidinium chloride

50 mM glycine

pH 10.8

0.5 M EDTA

0.1 M KCl

20 mM β-mercaptoethanol

Mowiol

5 g Mowiol

20 ml PBS

stir overnight

add 10 ml glycerol (87%)

centrifuge 15 min at 17000 x g

add 0.5 µg/ml DAPI

PEI (10 mM stock)

45 mg PEI

8 ml H_2O

stir at 70 °C for 1h

pH 7.0

ad 10 ml dH_2O

steril filter

dilute 1:10 with dH_2O

5 References

Acquaviva C (2006) The anaphase-promoting complex/cyclosome: APC/C. *Journal of Cell Science* **119:** 2401–2404

Acs K, Luijsterburg MS, Ackermann L, Salomons FA, Hoppe T & Dantuma NP (2011) The AAA-ATPase VCP/p97 promotes 53BP1 recruitment by removing L3MBTL1 from DNA double-strand breaks. *Nature structural & molecular biology* **18:** 1345–1350

Alexandru G, Graumann J, Smith GT, Kolawa NJ, Fang R & Deshaies RJ (2008) UBXD7 binds multiple ubiquitin ligases and implicates p97 in HIF1alpha turnover. *Cell* **134:** 804–816

Altomare DA, Menges CW, Pei J, Zhang L, Skele-Stump KL, Carbone M, Kane AB & Testa JR (2009) Activated TNF-alpha/NF-kappaB signaling via down-regulation of Fas-associated factor 1 in asbestos-induced mesotheliomas from Arf knockout mice. *Proceedings of the National Academy of Sciences* **106:** 3420–3425

Anderson DJ, Le Moigne R, Djakovic S, Kumar B, Rice J, Wong S, Wang J, Yao B, Valle E, Kiss von Soly S, Madriaga A, Soriano F, Menon M, Wu ZY, Kampmann M, Chen Y, Weissman JS, Aftab BT, Yakes FM & Shawver L et al (2015) Targeting the AAA ATPase p97 as an Approach to Treat Cancer through Disruption of Protein Homeostasis. *Cancer Cell* **28:** 653–665

Anindya R, Aygün O & Svejstrup JQ (2007) Damage-Induced Ubiquitylation of Human RNA Polymerase II by the Ubiquitin Ligase Nedd4, but Not Cockayne Syndrome Proteins or BRCA1. *Molecular cell* **28:** 386–397

Aparicio T, Guillou E, Coloma J, Montoya G & Mendez J (2009) The human GINS complex associates with Cdc45 and MCM and is essential for DNA replication. *Nucleic acids research* **37:** 2087–2095

Aressy B, Jullien D, Cazales M, Marcellin M, Bugler B, Burlet-Schiltz O & Ducommun B (2014) A screen for deubiquitinating enzymes involved in the G 2 /M checkpoint identifies USP50 as a regulator of HSP90-dependent Wee1 stability. *Cell Cycle* **9:** 3839–3846

Arias EE & Walter JC (2007) Strength in numbers: Preventing rereplication via multiple mechanisms in eukaryotic cells. *Genes & Development* **21:** 497–518

Auner HW, Moody AM, Ward TH, Kraus M, Milan E, May P, Chaidos A, Driessen C, Cenci S, Dazzi F, Rahemtulla A, Apperley JF, Karadimitris A & Dillon N (2013) Combined inhibition of p97 and the proteasome causes lethal disruption of the secretory apparatus in multiple myeloma cells. *PloS one* **8:** e74415

Baboshina OV & Haas AL (1996) Novel Multiubiquitin Chain Linkages Catalyzed by the Conjugating Enzymes E2EPF and RAD6 Are Recognized by 26 S Proteasome Subunit 5. *Journal of Biological Chemistry* **271:** 2823–2831

Balakirev MY, Mullally JE, Favier A, Assard N, Sulpice E, Lindsey DF, Rulina AV, Gidrol X & Wilkinson KD (2015) Wss1 metalloprotease partners with Cdc48/Doa1 in processing genotoxic SUMO conjugates. *eLife* **4**

Bandau S, Knebel A, Gage ZO, Wood NT & Alexandru G (2012) UBXN7 docks on neddylated cullin complexes using its UIM motif and causes HIF1α accumulation. *BMC biology* **10:** 36

Banerjee S, Bartesaghi A, Merk A, Rao P, Bulfer SL, Yan Y, Green N, Mroczkowski B, Neitz RJ, Wipf P, Falconieri V, Deshaies RJ, Milne JLS, Huryn D, Arkin M & Subramaniam S (2016) 2.3 A resolution cryo-EM structure of human p97 and mechanism of allosteric inhibition. *Science* **351:** 871–875

Bartek J & Lukas J (2007) DNA damage checkpoints: From initiation to recovery or adaptation. *Current Opinion in Cell Biology* **19:** 238–245

Barthelme D & Sauer RT (2012) Identification of the Cdc48bullet20S Proteasome as an Ancient AAA+ Proteolytic Machine. *Science* **337:** 843–846

Barthelme D & Sauer RT (2013) Bipartite determinants mediate an evolutionarily conserved interaction between Cdc48 and the 20 S peptidase. *Proc Natl Acad Sci USA* **110:** 3327–3332

Bea S, Salaverria I, Armengol L, Pinyol M, Fernandez V, Hartmann EM, Jares P, Amador V, Hernandez L, Navarro A, Ott G, Rosenwald A, Estivill X & Campo E (2009) Uniparental disomies, homozygous deletions, amplifications, and target genes in mantle cell lymphoma revealed by integrative high-resolution whole-genome profiling. *Blood* **113:** 3059–3069

Bebeacua C, Forster A, McKeown C, Meyer HH, Zhang X & Freemont PS (2012) Distinct conformations of the protein complex p97-Ufd1-Npl4 revealed by electron cryomicroscopy. *Proceedings of the National Academy of Sciences* **109:** 1098–1103

Behrends C & Harper JW (2011) Constructing and decoding unconventional ubiquitin chains. *Nat Struct Mol Biol* **18:** 520–528

Bekker-Jensen S & Mailand N (2011) The ubiquitin- and SUMO-dependent signaling response to DNA double-strand breaks. *FEBS Letters* **585:** 2914–2919

Bell SP & Dutta A (2002) DNA replication in eukaryotic cells. *Annu. Rev. Biochem.* **71:** 333–374

Bergink S, Ammon T, Kern M, Schermelleh L, Leonhardt H & Jentsch S (2013) Role of Cdc48/p97 as a SUMO-targeted segregase curbing Rad51–Rad52 interaction. *Nat Cell Biol* **15:** 526–532

Beskow A, Grimberg KB, Bott LC, Salomons FA, Dantuma NP & Young P (2009) A Conserved Unfoldase Activity for the p97 AAA-ATPase in Proteasomal Degradation. *Journal of Molecular Biology* **394:** 732–746

Beuron F, Dreveny I, Yuan X, Pye VE, Mckeown C, Briggs LC, Cliff MJ, Kaneko Y, Wallis R, Isaacson RL, Ladbury JE, Matthews SJ, Kondo H, Zhang X & Freemont PS (2006) Conformational changes in the AAA ATPase p97–p47 adaptor complex. *EMBO J* **25:** 1967–1976

Bjørling-Poulsen M, Seitz G, Guerra B & Issinger O (2003) The pro-apoptotic FAS-associated factor 1 is specifically reduced in human gastric carcinomas. *Int J Oncol*

Blount JR, Burr AA, Denuc A, Marfany G, Todi SV & Menéndez-Arias L (2012) Ubiquitin-Specific Protease 25 Functions in Endoplasmic Reticulum-Associated Degradation. *PloS one* **7:** e36542

Boos D, Frigola J & Diffley JFX (2012) Activation of the replicative DNA helicase: Breaking up is hard to do. *Current Opinion in Cell Biology* **24:** 423–430

Bosu DR & Kipreos ET (2008) Cullin-RING ubiquitin ligases: Global regulation and activation cycles. *Cell Div* **3:** 7

Botuyan MV, Lee J, Ward IM, Kim J, Thompson JR, Chen J & Mer G (2006) Structural Basis for the Methylation State-Specific Recognition of Histone H4-K20 by 53BP1 and Crb2 in DNA Repair. *Cell* **127:** 1361–1373

Brandman O, Stewart-Ornstein J, Wong D, Larson A, Williams CC, Li G, Zhou S, King D, Shen PS, Weibezahn J, Dunn JG, Rouskin S, Inada T, Frost A & Weissman JS (2012) A Ribosome-Bound Quality Control Complex Triggers Degradation of Nascent Peptides and Signals Translation Stress. *Cell* **151:** 1042–1054

Branzei D & Foiani M (2010) Maintaining genome stability at the replication fork. *Nat Rev Mol Cell Biol* **11:** 208–219

Braun RJ & Zischka H (2008) Mechanisms of Cdc48/VCP-mediated cell death — from yeast apoptosis to human disease. *Biochimica et Biophysica Acta (BBA) - Molecular Cell Research* **1783:** 1418–1435

Bregman DB, Halaban R, van Gool AJ, Henning KA, Friedberg EC & Warren SL (1996) UV-induced ubiquitination of RNA polymerase II: a novel modification deficient in Cockayne syndrome cells. *Proceedings of the National Academy of Sciences of the United States of America* **93:** 11586–11590

Briggs LC, Baldwin GS, Miyata N, Kondo H, Zhang X & Freemont PS (2008) Analysis of Nucleotide Binding to P97 Reveals the Properties of a Tandem AAA Hexameric ATPase. *Journal of Biological Chemistry* **283:** 13745–13752

Bruderer RM, Brasseur C & Meyer HH (2004) The AAA ATPase p97/VCP Interacts with Its Alternative Co-factors, Ufd1-Npl4 and p47, through a Common Bipartite Binding Mechanism. *J. Biol. Chem.* **279:** 49609–49616

Buchberger A, Howard MJ, Proctor M & Bycroft M (2001) The UBX domain: A widespread ubiquitin-like module. *Journal of Molecular Biology* **307:** 17–24

Buchberger A (2010) Control of Ubiquitin Conjugation by Cdc48 and Its Cofactors. In *Conjugation and deconjugation of ubiquitin family modifiers,* Groettrup M (ed) pp. 17–30. Austin, Tex: Landes Bioscience

Buchberger A (2013) Roles of Cdc48 in regulated protein degradation in yeast. *Subcellular biochemistry* **66:** 195-222

Bug M & Meyer H (2012) Expanding into new markets – VCP/p97 in endocytosis and autophagy. *Journal of Structural Biology* **179:** 78–82

Burrell RA, McClelland SE, Endesfelder D, Groth P, Weller M, Shaikh N, Domingo E, Kanu N, Dewhurst SM, Gronroos E, Chew SK, Rowan AJ, Schenk A, Sheffer M, Howell M, Kschischo M, Behrens A, Helleday T, Bartek J & Tomlinson IP et al (2013) Replication stress links structural and numerical cancer chromosomal instability. *Nature* **494:** 492–496

Busino L, Donzelli M, Chiesa M, Guardavaccaro D, Ganoth D, Valerio Dorrello N, Hershko A, Pagano M & Draetta GF (2003) Degradation of Cdc25A by β-TrCP during S phase and in response to DNA damage. *Nature* **426:** 87–91

Cao K, Nakajima R, Meyer HH & Zheng Y (2003) The AAA-ATPase Cdc48/p97 Regulates Spindle Disassembly at the End of Mitosis. *Cell* **115:** 355–367

Caruso M, Jenna S, Bouchecareilh M, Baillie DL, Boismenu D, Halawani D, Latterich M & Chevet E (2008) GTPase-Mediated Regulation of the Unfolded Protein Response in Caenorhabditis elegans Is Dependent on the AAA+ ATPase CDC-48. *Molecular and Cellular Biology* **28:** 4261–4274

Centore RC, Yazinski SA, Tse A & Zou L (2012) Spartan/C1orf124, a reader of PCNA ubiquitylation and a regulator of UV-induced DNA damage response. *Molecular cell* **46:** 625–635

Cervi G, Magnaghi P, Asa D, Avanzi N, Badari A, Borghi D, Caruso M, Cirla A, Cozzi L, Felder E, Galvani A, Gasparri F, Lomolino A, Magnuson S, Malgesini B, Motto I, Pasi M, Rizzi S, Salom B & Sorrentino G et al (2014) Discovery of 2-(cyclohexylmethylamino)pyrimidines as a new class of reversible valosine containing protein inhibitors. *Journal of medicinal chemistry* **57:** 10443–10454

Chapman E, Fry AN & Kang M (2011) The complexities of p97 function in health and disease. *Mol. BioSyst.* **7:** 700–710

Chapman E, Maksim N, La Cruz F de & Clair J (2015) Inhibitors of the AAA+ Chaperone p97. *Molecules* **20:** 3027–3049

Cheng Y & Chen R (2010) The AAA-ATPase Cdc48 and cofactor Shp1 promote chromosome bi-orientation by balancing Aurora B activity. *Journal of Cell Science* **123:** 2025–2034

Chia WS, Chia DX, Rao F, Bar Nun S, Geifman Shochat S & Kursula I (2012) ATP Binding to p97/VCP D1 Domain Regulates Selective Recruitment of Adaptors to Its Proximal N-Domain. *PloS one* **7:** e50490

Cho I, Tsai P, Lake RJ, Basheer A, Fan H & Maizels N (2013) ATP-Dependent Chromatin Remodeling by Cockayne Syndrome Protein B and NAP1-Like Histone Chaperones Is Required for Efficient Transcription-Coupled DNA Repair. *PLoS Genet* **9:** e1003407

Choi AM, Ryter SW & Levine B (2013) Autophagy in Human Health and Disease. *N Engl J Med* **368:** 651–662

Chou T, Brown SJ, Minond D, Nordin BE, Li K, Jones AC, Chase P, Porubsky PR, Stoltz BM, Schoenen FJ, Patricelli MP, Hodder P, Rosen H & Deshaies RJ (2011) Reversible inhibitor of p97, DBeQ, impairs both ubiquitin-dependent and autophagic protein clearance pathways. *Proceedings of the National Academy of Sciences of the United States of America* **108:** 4834–4839

Chou T & Deshaies RJ (2011) Quantitative Cell-based Protein Degradation Assays to Identify and Classify Drugs That Target the Ubiquitin-Proteasome System. *J. Biol. Chem.* **286:** 16546–16554

Chou T, Li K, Frankowski KJ, Schoenen FJ & Deshaies RJ (2013) Structure-activity relationship study reveals ML240 and ML241 as potent and selective inhibitors of p97 ATPase. *ChemMedChem* **8:** 297–312

Chou T, Bulfer SL, Weihl CC, Li K, Lis LG, Walters MA, Schoenen FJ, Lin HJ, Deshaies RJ & Arkin MR (2014) Specific Inhibition of p97/VCP ATPase and Kinetic Analysis Demonstrate Interaction between D1 and D2 ATPase Domains. *Journal of Molecular Biology* **426:** 2886–2899

Citterio E (1998) Biochemical and Biological Characterization of Wild-type and ATPase-deficient Cockayne Syndrome B Repair Protein. *Journal of Biological Chemistry* **273:** 11844–11851

Citterio E, van den Boom V, Schnitzler G, Kanaar R, Bonte E, Kingston RE, Hoeijmakers JHJ & Vermeulen W (2000) ATP-Dependent Chromatin Remodeling by the Cockayne Syndrome B DNA Repair-Transcription-Coupling Factor. *Molecular and Cellular Biology* **20:** 7643–7653

Cohn MA, Kowal P, Yang K, Haas W, Huang TT, Gygi SP & D'Andrea AD (2007) A UAF1-Containing Multisubunit Protein Complex Regulates the Fanconi Anemia Pathway. *Molecular cell* **28:** 786–797

Coux O, Tanaka K & Goldberg AL (1996) Structure and Functions of the 20S and 26S Proteasomes. *Annu. Rev. Biochem.* **65:** 801–847

Craney A & Rape M (2013) Dynamic regulation of ubiquitin-dependent cell cycle control. *Current Opinion in Cell Biology* **25:** 704–710

Cukras S, Morffy N, Ohn T, Kee Y & Muzi-Falconi M (2014) Inactivating UBE2M Impacts the DNA Damage Response and Genome Integrity Involving Multiple Cullin Ligases. *PloS one* **9:** e101844

Dai R (1998) Involvement of Valosin-containing Protein, an ATPase Co-purified with Ikappa Balpha and 26 S Proteasome, in Ubiquitin-Proteasome-mediated Degradation of Ikappa Balpha. *Journal of Biological Chemistry* **273:** 3562–3573

Dantuma NP & Hoppe T (2012) Growing sphere of influence: Cdc48/p97 orchestrates ubiquitin-dependent extraction from chromatin. *Trends in cell biology* **22:** 483–491

Davis EJ, Lachaud C, Appleton P, Macartney TJ, Näthke I & Rouse J (2012) DVC1 (C1orf124) recruits the p97 protein segregase to sites of DNA damage. *Nature structural & molecular biology* **19:** 1093–1100

Decottignies A, Evain A & Ghislain M (2004) Binding of Cdc48p to a ubiquitin-related UBX domain from novel yeast proteins involved in intracellular proteolysis and sporulation. *Yeast* **21:** 127-139

DeHoratius C & Silver PA (1996) Nuclear transport defects and nuclear envelope alterations are associated with mutation of the Saccharomyces cerevisiae NPL4 gene. *Molecular Biology of the Cell* **7:** 1835–1855

Deichsel A, Mouysset J & Hoppe T (2009) The ubiquitin-selective chaperone CDC-48/p97, a new player in DNA replication. *Cell cycle* **8:** 185-190

De Laat WL, Jaspers NG, Hoeijmakers JH (1999) Molecular mechanism of nucleotide excision repair. *Genes & Development* **13:** 768-785

DeLaBarre B & Brunger AT (2003) Complete structure of p97/valosin-containing protein reveals communication between nucleotide domains. *Nat Struct Biol* **10:** 856–863

DeLaBarre B, Christianson JC, Kopito RR & Brunger AT (2006) Central Pore Residues Mediate the p97/VCP Activity Required for ERAD. *Molecular cell* **22:** 451–462

den Besten W, Verma R, Kleiger G, Oania RS & Deshaies RJ (2012) NEDD8 links cullin-RING ubiquitin ligase function to the p97 pathway. *Nature structural & molecular biology* **19:** 511-6, S1

Deshaies RJ & Joazeiro CA (2009) RING Domain E3 Ubiquitin Ligases. *Annu. Rev. Biochem.* **78:** 399–434

Dobrynin G, Popp O, Romer T, Bremer S, Schmitz MHA, Gerlich DW & Meyer H (2011) Cdc48/p97-Ufd1-Npl4 antagonizes Aurora B during chromosome segregation in HeLa cells. *Journal of Cell Science* **124:** 1571–1580

Donzelli M & Draetta GF (2003) Regulating mammalian checkpoints through Cdc25 inactivation. *EMBO Rep* **4:** 671–677

Dreveny I, Kondo H, Uchiyama K, Shaw A, Zhang X & Freemont PS (2004) Structural basis of the interaction between the AAA ATPase p97/VCP and its adaptor protein p47. *EMBO J* **23:** 1030–1039

Duda DM, Borg LA, Scott DC, Hunt HW, Hammel M & Schulman BA (2008) Structural Insights into NEDD8 Activation of Cullin-RING Ligases: Conformational Control of Conjugation. *Cell* **134:** 995–1006

El-Mahdy MA, Zhu Q, Wang Q, Wani G, Praetorius-Ibba M & Wani AA (2006) Cullin 4A-mediated Proteolysis of DDB2 Protein at DNA Damage Sites Regulates in Vivo Lesion Recognition by XPC. *Journal of Biological Chemistry* **281:** 13404–13411

Elsasser S & Finley D (2005) Delivery of ubiquitinated substrates to protein-unfolding machines. *Nat Cell Biol* **7:** 742–749

Ernst R, Mueller B, Ploegh HL & Schlieker C (2009) The Otubain YOD1 Is a Deubiquitinating Enzyme that Associates with p97 to Facilitate Protein Dislocation from the ER. *Molecular cell* **36:** 28–38

Esaki M & Ogura T (2010) ATP-bound form of the D1 AAA domain inhibits an essential function of Cdc48p/p97This paper is one of a selection of papers published in this special issue entitled 8th International Conference on AAA Proteins and has undergone the Journal's usual peer review process. *Biochem. Cell Biol.* **88:** 109–117

Ewens CA, Panico S, Kloppsteck P, McKeown C, Ebong I, Robinson C, Zhang X & Freemont PS (2014) The p97-FAF1 Protein Complex Reveals a Common Mode of p97 Adaptor Binding. *Journal of Biological Chemistry* **289:** 12077–12084

Fachinetti D, Bermejo R, Cocito A, Minardi S, Katou Y, Kanoh Y, Shirahige K, Azvolinsky A, Zakian VA & Foiani M (2010) Replication Termination at Eukaryotic Chromosomes Is Mediated by Top2 and Occurs at Genomic Loci Containing Pausing Elements. *Molecular cell* **39:** 595–605

Fang C, Gui L, Zhang X, Moen DR, Li K, Frankowski KJ, Lin HJ, Schoenen FJ & Chou T (2015) Evaluating p97 Inhibitor Analogues for Their Domain Selectivity and Potency against the p97-p47 Complex. *ChemMedChem* **10:** 52–56

Feng H, Zhong W, Punkosdy G, Gu S, Zhou L, Seabolt EK & Kipreos ET (1999) CUL-2 is required for the G1-to-S-phase transition and mitotic chromosome condensation in Caenorhabditis elegans. *Nature cell biology* **1:** 486–492

Fiebiger E (2004) Dissection of the Dislocation Pathway for Type I Membrane Proteins with a New Small Molecule Inhibitor, Eeyarestatin. *Molecular Biology of the Cell* **15:** 1635–1646

Fischer ES, Scrima A, Böhm K, Matsumoto S, Lingaraju GM, Faty M, Yasuda T, Cavadini S, Wakasugi M, Hanaoka F, Iwai S, Gut H, Sugasawa K & Thomä NH (2011) The Molecular Basis of CRL4DDB2/CSA Ubiquitin Ligase Architecture, Targeting, and Activation. *Cell* **147:** 1024–1039

Fisher RD, Wang B, Alam SL, Higginson DS, Robinson H, Sundquist WI & Hill CP (2003) Structure and ubiquitin binding of the ubiquitin-interacting motif. *Journal of Biological Chemistry* **278:** 28976-28984

Fox JT, Lee K & Myung K (2011) Dynamic regulation of PCNA ubiquitylation/deubiquitylation. *FEBS Letters* **585:** 2780–2785

Fradet-Turcotte A, Canny MD, Escribano-Díaz C, Orthwein A, Leung CCY, Huang H, Landry M, Kitevski-LeBlanc J, Noordermeer SM, Sicheri F & Durocher D (2013) 53BP1 is a reader of the DNA-damage-induced H2A Lys 15 ubiquitin mark. *Nature* **499:** 50–54

Franz A, Orth M, Pirson PA, Sonneville R, Blow JJ, Gartner A, Stemmann O & Hoppe T (2011) CDC-48/p97 coordinates CDT-1 degradation with GINS chromatin dissociation to ensure faithful DNA replication. *Molecular cell* **44:** 85–96

Franz A, Pirson PA, Pilger D, Halder S, Achuthankutty D, Kashkar H, Ramadan K & Hoppe T (2016) Chromatin-associated degradation is defined by UBXN-3/FAF1 to safeguard DNA replication fork progression. *Nature communications* **7:** 10612

Friedberg EC, Lehmann AR & Fuchs RP (2005) Trading Places: How Do DNA Polymerases Switch during Translesion DNA Synthesis? *Molecular cell* **18:** 499–505

Fröhlich KU, Fries HW, Rüdiger M, Erdmann R, Botstein D & Mecke D (1991) Yeast cell cycle protein CDC48p shows full-length homology to the mammalian protein VCP and is a member of a protein family involved in secretion, peroxisome formation, and gene expression. *The Journal of cell biology* **114:** 443-453

Fu X, Ng C, Feng D & Liang C (2003) Cdc48p is required for the cell cycle commitment point at Start via degradation of the G1-CDK inhibitor Far1p. *J Cell Biol* **163:** 21–26

Fujii K, Kitabatake M, Sakata T & Ohno M (2012) 40S subunit dissociation and proteasome-dependent RNA degradation in nonfunctional 25S rRNA decay. *The EMBO Journal* **31:** 2579–2589

Fujita K, Nakamura Y, Oka T, Ito H, Tamura T, Tagawa K, Sasabe T, Katsuta A, Motoki K, Shiwaku H, Sone M, Yoshida C, Katsuno M, Eishi Y, Murata M, Paul Taylor J, Wanker EE, Kono K, Tashiro S & Sobue G et al (2013) A functional deficiency of TERA/VCP/p97 contributes to impaired DNA repair in multiple polyglutamine diseases. *Nat Comms* **4:** 1816

Galanty Y, Belotserkovskaya R, Coates J & Jackson SP (2012) RNF4, a SUMO-targeted ubiquitin E3 ligase, promotes DNA double-strand break repair. *Genes & Development* **26:** 1179–1195

Gambus A, Jones RC, Sanchez-Diaz A, Kanemaki M, van Deursen F, Edmondson RD & Labib K (2006) GINS maintains association of Cdc45 with MCM in replisome progression complexes at eukaryotic DNA replication forks. *Nat Cell Biol* **8:** 358–366

Geigl JB, Obenauf AC, Schwarzbraun T & Speicher MR (2008) Defining ‘chromosomal instability‘. *Trends in genetics* **24:** 64-69

Ghosal G, Leung JW, Nair BC, Fong K & Chen J (2012) Proliferating cell nuclear antigen (PCNA)-binding protein C1orf124 is a regulator of translesion synthesis. *The Journal of biological chemistry* **287:** 34225–34233

Gibbs-Seymour I, Oka Y, Rajendra E, Weinert BT, Passmore LA, Patel KJ, Olsen JV, Choudhary C, Bekker-Jensen S & Mailand N (2015) Ubiquitin-SUMO circuitry controls activated fanconi anemia ID complex dosage in response to DNA damage. *Molecular cell* **57:** 150–164

Goldberg AL (2012) Development of proteasome inhibitors as research tools and cancer drugs. *The Journal of cell biology* **199:** 583–588

Groisman R, Polanowska J, Kuraoka I, Sawada J, Saijo M, Drapkin R, Kisselev AF, Tanaka K & Nakatani Y (2003) The Ubiquitin Ligase Activity in the DDB2 and CSA Complexes Is Differentially Regulated by the COP9 Signalosome in Response to DNA Damage. *Cell* **113:** 357–367

Groisman R (2006) CSA-dependent degradation of CSB by the ubiquitin-proteasome pathway establishes a link between complementation factors of the Cockayne syndrome. *Genes & Development* **20:** 1429–1434

Groll M, Ditzel L, Löwe J, Stock D, Bochtler M, Bartunik HD & Huber R (1997) Structure of 20S proteasome from yeast at 2.4Å resolution. *Nature* **386:** 463–471

Haglund K & Dikic I (2005) Ubiquitylation and cell signaling. *EMBO J* **24:** 3353–3359

Haines DS (2010) p97-Containing Complexes in Proliferation Control and Cancer: Emerging Culprits or Guilt by Association? *Genes & Cancer* **1:** 753–763

Hannich JT, Lewis A, Kroetz MB, Li S, Heide H, Emili A & Hochstrasser M (2005) Defining the SUMO-modified Proteome by Multiple Approaches in Saccharomyces cerevisiae. *J. Biol. Chem.* **280:** 4102–4110

Hänzelmann P, Buchberger A & Schindelin H (2011) Hierarchical binding of cofactors to the AAA ATPase p97. *Structure (London, England : 1993)* **19:** 833–843

Harreman M, Taschner M, Sigurdsson S, Anindya R, Reid J, Somesh B, Kong SE, Banks CAS, Conaway RC, Conaway JW & Svejstrup JQ (2009) Distinct ubiquitin ligases act sequentially for RNA polymerase II polyubiquitylation. *Proceedings of the National Academy of Sciences* **106:** 20705–20710

Havens CG & Walter JC (2009) Docking of a Specialized PIP Box onto Chromatin-Bound PCNA Creates a Degron for the Ubiquitin Ligase CRL4Cdt2. *Molecular cell* **35:** 93–104

He J, Zhu Q, Wani G, Sharma N & Wani AA (2016) VCP/p97 Segregase Mediates Proteolytic Processing of CSB in Damaged Chromatin. *The Journal of biological chemistry*

Heinemeyer W, Fischer M, Krimmer T, Stachon U & Wolf DH (1997) The Active Sites of the Eukaryotic 20 S Proteasome and Their Involvement in Subunit Precursor Processing. *Journal of Biological Chemistry* **272:** 25200–25209

Heo J, Livnat-Levanon N, Taylor EB, Jones KT, Dephoure N, Ring J, Xie J, Brodsky JL, Madeo F, Gygi SP, Ashrafi K, Glickman MH & Rutter J (2010) A Stress-Responsive System for Mitochondrial Protein Degradation. *Molecular cell* **40:** 465–480

Hershko A & Ciechanover A (1998) THE UBIQUITIN SYSTEM. *Annu. Rev. Biochem.* **67:** 425–479

Hidalgo A, Baudis M, Petersen I, Arreola H, Piña P, Vázquez-Ortiz G, Hernández D, González J, Lazos M, López R, Pérez C, García J, Vázquez K, Alatorre B & Salcedo M (2005). *BMC cancer* **5:** 77

Higa LA, Banks D, Wu M, Kobayashi R, Sun H & Zhang H (2006) L2DTL/CDT2 interacts with the CUL4/DDB1 complex and PCNA and regulates CDT1 proteolysis in response to DNA damage. *Cell cycle* **5:** 1675-1680

Hodskinson MR, Silhan J, Crossan GP, Garaycoechea JI, Mukherjee S, Johnson CM, Schärer OD & Patel KJ (2014) Mouse SLX4 Is a Tumor Suppressor that Stimulates the Activity of the Nuclease XPF-ERCC1 in DNA Crosslink Repair. *Molecular cell* **54:** 472–484

Hsieh M, Chen R & Polymenis M (2011) Cdc48 and Cofactors Npl4-Ufd1 Are Important for G1 Progression during Heat Stress by Maintaining Cell Wall Integrity in Saccharomyces cerevisiae. *PloS one* **6:** e18988

Hu J, McCall CM, Ohta T & Xiong Y (2004) Targeted ubiquitination of CDT1 by the DDB1–CUL4A–ROC1 ligase in response to DNA damage. *Nat Cell Biol* **6:** 1003–1009

Huang TT, Nijman SM, Mirchandani KD, Galardy PJ, Cohn MA, Haas W, Gygi SP, Ploegh HL, Bernards R & D'Andrea AD (2006) Regulation of monoubiquitinated PCNA by DUB autocleavage. *Nat Cell Biol* **8:** 341–347

Hubbers CU, Clemen CS, Kesper K, Boddrich A, Hofmann A, Kamarainen O, Tolksdorf K, Stumpf M, Reichelt J, Roth U, Krause S, Watts G, Kimonis V, Wattjes MP, Reimann J, Thal DR, Biermann K, Evert BO, Lochmuller H & Wanker EE et al (2007) Pathological consequences of VCP mutations on human striated muscle. *Brain* **130:** 381–393

Huibregtse JM, Yang JC & Beaudenon SL (1997) The large subunit of RNA polymerase II is a substrate of the Rsp5 ubiquitin-protein ligase. *Proceedings of the National Academy of Sciences* **94:** 3656-3661

Huyton T, Pye VE, Briggs LC, Flynn TC, Beuron F, Kondo H, Ma J, Zhang X & Freemont PS (2003) The crystal structure of murine p97/VCP at 3.6Å. *Journal of Structural Biology* **144:** 337–348

Hwang BJ, Ford JM, Hanawalt PC & Chu G (1999) Expression of the p48 xeroderma pigmentosum gene is p53-dependent and is involved in global genomic repair. *Proceedings of the National Academy of Sciences* **96:** 424–428

Hwang W, Artan M, Seo M, Lee D, Nam HG & Lee SV (2015) Inhibition of elongin C promotes longevity and protein homeostasis via HIF-1 in C. elegans. *Aging Cell* **14:** 995–1002

Ilves I, Petojevic T, Pesavento JJ & Botchan MR (2010) Activation of the MCM2-7 Helicase by Association with Cdc45 and GINS Proteins. *Molecular cell* **37:** 247–258

Indig FE, Partridge JJ, Kobbe Cv, Aladjem MI, Latterich M & Bohr VA (2004) Werner syndrome protein directly binds to the AAA ATPase p97/VCP in an ATP-dependent fashion. *Journal of Structural Biology* **146:** 251–259

Isaacson RL, Pye VE, Simpson P, Meyer HH, Zhang X, Freemont PS & Matthews S (2007) Detailed Structural Insights into the p97-Npl4-Ufd1 Interface. *Journal of Biological Chemistry* **282:** 21361–21369

Ishiai M, Kitao H, Smogorzewska A, Tomida J, Kinomura A, Uchida E, Saberi A, Kinoshita E, Kinoshita-Kikuta E, Koike T, Tashiro S, Elledge SJ & Takata M (2008) FANCI phosphorylation functions as a molecular switch to turn on the Fanconi anemia pathway. *Nat Struct Mol Biol* **15:** 1138–1146

Jackson SP & Bartek J (2009) The DNA-damage response in human biology and disease. *Nature* **461:** 1071–1078

Jagannathan M, Nguyen T, Gallo D, Luthra N, Brown GW, Saridakis V & Frappier L (2013) A Role for USP7 in DNA Replication. *Molecular and Cellular Biology* **34:** 132–145

Jain S, Diefenbach, Zain J & O'Connor (2011) Emerging role of carfilzomib in treatment of relapsed and refractory lymphoid neoplasms and multiple myeloma. *CE:* 43

Jin J, Arias EE, Chen J, Harper JW & Walter JC (2006) A Family of Diverse Cul4-Ddb1-Interacting Proteins Includes Cdt2, which Is Required for S Phase Destruction of the Replication Factor Cdt1. *Molecular cell* **23:** 709–721

Johnson ES, Ma PCM, Ota IM & Varshavsky A (1995) A Proteolytic Pathway That Recognizes Ubiquitin as a Degradation Signal. *Journal of Biological Chemistry* **270:** 17442–17456

Johnson JO, Mandrioli J, Benatar M, Abramzon Y, van Deerlin VM, Trojanowski JQ, Gibbs JR, Brunetti M, Gronka S, Wuu J, Ding J, McCluskey L, Martinez-Lage M, Falcone D, Hernandez DG, Arepalli S, Chong S, Schymick JC, Rothstein J & Landi F et al (2010) Exome Sequencing Reveals VCP Mutations as a Cause of Familial ALS. *Neuron* **68:** 857–864

Joo W, Xu G, Persky NS, Smogorzewska A, Rudge DG, Buzovetsky O, Elledge SJ & Pavletich NP (2011) Structure of the FANCI-FANCD2 Complex: Insights into the Fanconi Anemia DNA Repair Pathway. *Science* **333:** 312–316

Ju J, Fuentealba RA, Miller SE, Jackson E, Piwnica-Worms D, Baloh RH & Weihl CC (2009) Valosin-containing protein (VCP) is required for autophagy and is disrupted in VCP disease. *J Cell Biol* **187:** 875–888

Ju JS & Weihl CC (2010) Inclusion body myopathy, Paget's disease of the bone and fronto-temporal dementia: A disorder of autophagy. *Human Molecular Genetics* **19:** R38-R45

Juhasz S, Balogh D, Hajdu I, Burkovics P, Villamil MA, Zhuang Z & Haracska L (2012) Characterization of human Spartan/C1orf124, an ubiquitin-PCNA interacting regulator of DNA damage tolerance. *Nucleic acids research* **40:** 10795–10808

Kamiuchi S, Saijo M, Citterio E, Jager M de, Hoeijmakers JHJ & Tanaka K (2002) Translocation of Cockayne syndrome group A protein to the nuclear matrix: Possible relevance to transcription-coupled DNA repair. *Proceedings of the National Academy of Sciences* **99:** 201–206

Kamura T (1999) Rbx1, a Component of the VHL Tumor Suppressor Complex and SCF Ubiquitin Ligase. *Science* **284:** 657–661

Kanemori Y, Uto K & Sagata N (2005) Beta-TrCP recognizes a previously undescribed nonphosphorylated destruction motif in Cdc25A and Cdc25B phosphatases. *Proceedings of the National Academy of Sciences* **102:** 6279–6284

Kapetanaki MG, Guerrero-Santoro J, Bisi DC, Hsieh CL, Rapic-Otrin V & Levine AS (2006) The DDB1-CUL4ADDB2 ubiquitin ligase is deficient in xeroderma pigmentosum group E and targets histone H2A at UV-damaged DNA sites. *Proceedings of the National Academy of Sciences* **103:** 2588–2593

Kelly AE, Sampath SC, Maniar TA, Woo EM, Chait BT & Funabiki H (2007) Chromosomal Enrichment and Activation of the Aurora B Pathway Are Coupled to Spatially Regulate Spindle Assembly. *Developmental Cell* **12:** 31–43

Kern M, Fernandez-Sáiz V, Schäfer Z & Buchberger A (2009) UBXD1 binds p97 through two independent binding sites. *Biochemical and biophysical research communications* **380:** 303–307

Kim HC & Huibregtse JM (2009) Polyubiquitination by HECT E3s and the Determinants of Chain Type Specificity. *Molecular and Cellular Biology* **29:** 3307–3318

Kim H & D'Andrea AD (2012) Regulation of DNA cross-link repair by the Fanconi anemia/BRCA pathway. *Genes & Development* **26:** 1393–1408

Kim MS, Machida Y, Vashisht AA, Wohlschlegel JA, Pang Y & Machida YJ (2013) Regulation of error-prone translesion synthesis by Spartan/C1orf124. *Nucleic acids research* **41:** 1661–1668

Kimonis VE, Fulchiero E, Vesa J & Watts G (2008) VCP disease associated with myopathy, Paget disease of bone and frontotemporal dementia: Review of a unique disorder. *Biochimica et Biophysica Acta (BBA) - Molecular Basis of Disease* **1782:** 744–748

Kirchner P, Bug M & Meyer H (2013) Ubiquitination of the N-terminal Region of Caveolin-1 Regulates Endosomal Sorting by the VCP/p97 AAA-ATPase. *Journal of Biological Chemistry* **288:** 7363–7372

Klein Douwel D, Boonen RA, Long DT, Szypowska AA, Räschle M, Walter JC & Knipscheer P (2014) XPF-ERCC1 Acts in Unhooking DNA Interstrand Crosslinks in Cooperation with FANCD2 and FANCP/SLX4. *Molecular cell* **54:** 460–471

Kloppsteck P, Ewens CA, Förster A, Zhang X & Freemont PS (2012) Regulation of p97 in the ubiquitin–proteasome system by the UBX protein-family. *Biochimica et Biophysica Acta (BBA) - Molecular Cell Research* **1823:** 125–129

Knipscheer P, Raschle M, Smogorzewska A, Enoiu M, Ho TV, Scharer OD, Elledge SJ & Walter JC (2009) The Fanconi Anemia Pathway Promotes Replication-Dependent DNA Interstrand Cross-Link Repair. *Science* **326:** 1698–1701

Köhler A, Cascio P, Leggett DS, Woo KM, Goldberg AL & Finley D (2001) The Axial Channel of the Proteasome Core Particle Is Gated by the Rpt2 ATPase and Controls Both Substrate Entry and Product Release. *Molecular cell* **7:** 1143–1152

Kondo H, Rabouille C, Newman R, Levine TP, Pappin D, Freemont P & Warren G (1997) p47 is a cofactor for p97-mediated membrane fusion. *Nature* **388:** 75–78

Kops GJ, Weaver BA & Cleveland DW (2005) On the road to cancer: Aneuploidy and the mitotic checkpoint. *Nat Rev Cancer* **5:** 773–785

Kothe M, Ye Y, Wagner JS, Luca HE de, Kern E, Rapoport TA & Lencer WI (2005) Role of p97 AAA-ATPase in the Retrotranslocation of the Cholera Toxin A1 Chain, a Non-ubiquitinated Substrate. *Journal of Biological Chemistry* **280:** 28127–28132

Kottemann MC & Smogorzewska A (2013) Fanconi anaemia and the repair of Watson and Crick DNA crosslinks. *Nature* **493:** 356–363

Kress E, Schwager F, Holtackers R, Seiler J, Prodon F, Zanin E, Eiteneuer A, Toya M, Sugimoto A, Meyer H, Meraldi P & Gotta M (2013) The UBXN-2/p37/p47 adaptors of CDC-48/p97 regulate mitosis by limiting the centrosomal recruitment of Aurora A. *J Cell Biol* **201:** 559–575

Kunz BA, Straffon AF & Vonarx EJ (2000) DNA damage-induced mutation: Tolerance via translesion synthesis. *Mutation Research/Fundamental and Molecular Mechanisms of Mutagenesis* **451:** 169–185

La Spada AR & Taylor JP (2010) Repeat expansion disease: Progress and puzzles in disease pathogenesis. *Nat Rev Genet* **11:** 247–258

Lampson MA, Renduchitala K, Khodjakov A & Kapoor TM (2004) Correcting improper chromosome–spindle attachments during cell division. *Nat Cell Biol* **6:** 6–237

Laney JD (2003) Ubiquitin-dependent degradation of the yeast Mat 2 repressor enables a switch in developmental state. *Genes & Development* **17:** 2259–2270

Larsen CN & Finley D (1997) Protein Translocation Channels in the Proteasome and Other Proteases. *Cell* **91:** 431–434

Lessel D, Vaz B, Halder S, Lockhart PJ, Marinovic-Terzic I, Lopez-Mosqueda J, Philipp M, Sim JCH, Smith KR, Oehler J, Cabrera E, Freire R, Pope K, Nahid A, Norris F, Leventer RJ, Delatycki MB, Barbi G, Ameln S von & Högel J et al (2014) Mutations in SPRTN cause early onset hepatocellular carcinoma, genomic instability and progeroid features. *Nature genetics* **46:** 1239–1244

Li J & Baker MD (2000) Formation and repair of heteroduplex DNA on both sides of the double-strand break during mammalian gene targeting. *Journal of Molecular Biology* **295:** 505-516

Li W, Bengtson MH, Ulbrich A, Matsuda A, Reddy VA, Orth A, Chanda SK, Batalov S, Joazeiro CAP & Ploegh H (2008) Genome-Wide and Functional Annotation of Human E3 Ubiquitin Ligases Identifies MULAN, a Mitochondrial E3 that Regulates the Organelle's Dynamics and Signaling. *PloS one* **3:** e1487

Li M & Zhang P (2009) The function of APC/CCdh1 in cell cycle and beyond. *Cell Div* **4:** 2

Li JM, Wu H, Zhang W, Blackburn MR & Jin J (2014) The p97-UFD1L-NPL4 protein complex mediates cytokine-induced IkappaBalpha proteolysis. *Molecular and Cellular Biology* **34:** 335-347

Liu C, Li X, Thompson D, Wooding K, Chang T, Tang Z, Yu H, Thomas PJ & DeMartino GN (2006) ATP Binding and ATP Hydrolysis Play Distinct Roles in the Function of 26S Proteasome. *Molecular cell* **24:** 39–50

Liu Y, Soetandyo N, Lee J, Liu L, Xu Y, Clemons WM & Ye Y (2014) USP13 antagonizes gp78 to maintain functionality of a chaperone in ER-associated degradation. *eLife* **3:** 804

Livingstone M, Ruan H, Weiner J, Clauser KR, Strack P, Jin S, Williams A, Greulich H, Gardner J, Venere M, Mochan TA, DiTullio RA Jr, Moravcevic K, Gorgoulis VG, Burkhardt A & Halazonetis TD (2005) Valosin-containing protein phosphorylation at Ser784 in response to DNA damage. *Cancer Research* **65:** 7533-7540

Livnat-Levanon N & Glickman MH (2011) Ubiquitin–Proteasome System and mitochondria — Reciprocity. *Biochimica et Biophysica Acta (BBA) - Gene Regulatory Mechanisms* **1809:** 80–87

Livneh Z, Ziv O & Shachar S (2010) Multiple two-polymerase mechanisms in mammalian translesion DNA synthesis. *Cell cycle* **9:** 729-735

Löbrich M & Jeggo PA (2007) The impact of a negligent G2/M checkpoint on genomic instability and cancer induction. *Nat Rev Cancer* **7:** 861–869

Lowe J, Stock D, Jap B, Zwickl P, Baumeister W & Huber R (1995) Crystal structure of the 20S proteasome from the archaeon T. acidophilum at 3.4 A resolution. *Science* **268:** 533–539

Machida Y, Kim MS & Machida YJ (2012) Spartan/C1orf124 is important to prevent UV-induced mutagenesis. *Cell cycle (Georgetown, Tex.)* **11:** 3395–3402

Maculins T, Nkosi PJ, Nishikawa H & Labib K (2015) Tethering of SCF(Dia2) to the Replisome Promotes Efficient Ubiquitylation and Disassembly of the CMG Helicase. *Current biology : CB* **25:** 2254–2259

Madsen L, Seeger M, Semple CA & Hartmann-Petersen R (2009) New ATPase regulators—p97 goes to the PUB. *The International Journal of Biochemistry & Cell Biology* **41:** 2380–2388

Maerki S, Olma MH, Staubli T, Steigemann P, Gerlich DW, Quadroni M, Sumara I & Peter M (2009) The Cul3–KLHL21 E3 ubiquitin ligase targets Aurora B to midzone microtubules in anaphase and is required for cytokinesis. *J Cell Biol* **187:** 791–800

Magnaghi P, D'Alessio R, Valsasina B, Avanzi N, Rizzi S, Asa D, Gasparri F, Cozzi L, Cucchi U, Orrenius C, Polucci P, Ballinari D, Perrera C, Leone A, Cervi G, Casale E, Xiao Y, Wong C, Anderson DJ & Galvani A et al (2013) Covalent and allosteric inhibitors of the ATPase VCP/p97 induce cancer cell death. *Nature chemical biology* **9:** 548–556

Mahon C, Krogan N, Craik C & Pick E (2014) Cullin E3 Ligases and Their Rewiring by Viral Factors. *Biomolecules* **4:** 897–930

Maia AR, Garcia Z, Kabeche L, Barisic M, Maffini S, Macedo-Ribeiro S, Cheeseman IM, Compton DA, Kaverina I & Maiato H (2012) Cdk1 and Plk1 mediate a CLASP2 phospho-switch that stabilizes kinetochore-microtubule attachments. *The Journal of cell biology* **199:** 285-301

Mallette FA, Mattiroli F, Cui G, Young LC, Hendzel MJ, Mer G, Sixma TK & Richard S (2012) RNF8- and RNF168-dependent degradation of KDM4A/JMJD2A triggers 53BP1 recruitment to DNA damage sites. *The EMBO Journal* **31:** 1865–1878

Malumbres M & Barbacid M (2005) Mammalian cyclin-dependent kinases. *Trends in biochemical sciences* **30:** 630–641

Maric M, Maculins T, Piccoli G de & Labib K (2014) Cdc48 and a ubiquitin ligase drive disassembly of the CMG helicase at the end of DNA replication. *Science (New York, N.Y.)* **346:** 1253596

Maskey RS, Kim MS, Baker DJ, Childs B, Malureanu LA, Jeganathan KB, Machida Y, van Deursen JM & Machida YJ (2014) Spartan deficiency causes genomic instability and progeroid phenotypes. *Nature communications* **5:** 5744

Mattiroli F, Vissers JH, van Dijk WJ, Ikpa P, Citterio E, Vermeulen W, Marteijn JA & Sixma TK (2012) RNF168 Ubiquitinates K13-15 on H2A/H2AX to Drive DNA Damage Signaling. *Cell* **150:** 1182–1195

McIntosh D & Blow JJ (2012) Dormant Origins, the Licensing Checkpoint, and the Response to Replicative Stresses. *Cold Spring Harbor Perspectives in Biology* **4:** a012955-a012955

Meerang M, Ritz D, Paliwal S, Garajova Z, Bosshard M, Mailand N, Janscak P, Hübscher U, Meyer H & Ramadan K (2011) The ubiquitin-selective segregase VCP/p97 orchestrates the response to DNA double-strand breaks. *Nature cell biology* **13:** 1376–1382

Melixetian M, Klein DK, Sørensen CS & Helin K (2009) NEK11 regulates CDC25A degradation and the IR-induced G2/M checkpoint. *Nat Cell Biol* **11:** 1247–1253

Meselson M & Stahl FW (1958) The replication of DNA. *Cold Spring Harb Symp Quant Biol* **23:** 9-12

Metzger MB, Hristova VA & Weissman AM (2012) HECT and RING finger families of E3 ubiquitin ligases at a glance. *Journal of Cell Science* **125:** 531–537

Meyer HH, Shorter JG, Seemann J, Pappin D & Warren G (2000) A complex of mammalian Ufd1 and Npl4 links the AAA-ATPase, p97, to ubiquitin and nuclear transport pathways. *The EMBO Journal* **19:** 2181–2192

Meyer HH (2002) Direct binding of ubiquitin conjugates by the mammalian p97 adaptor complexes, p47 and Ufd1-Npl4. *The EMBO Journal* **21:** 5645–5652

Meyer HH (2005) Golgi reassembly after mitosis: The AAA family meets the ubiquitin family. *Biochimica et Biophysica Acta (BBA) - Molecular Cell Research* **1744:** 108–119

Meyer H, Bug M & Bremer S (2012) Emerging functions of the VCP/p97 AAA-ATPase in the ubiquitin system. *Nat Cell Biol* **14:** 117–123

Min J, Allali-Hassani A, Nady N, Qi C, Ouyang H, Liu Y, MacKenzie F, Vedadi M & Arrowsmith CH (2007) L3MBTL1 recognition of mono- and dimethylated histones. *Nat Struct Mol Biol* **14:** 1229–1230

Moir D, Stewart SE, Osmond BC & Botstein D (1982) Cold-sensitive cell-division-cycle mutants of yeast: isolation, properties, and pseudoreversion studies. *Genetics* **100:** 547-563.

Moreno SP, Bailey R, Campion N, Herron S & Gambus A (2014) Polyubiquitylation drives replisome disassembly at the termination of DNA replication. *Science (New York, N.Y.)* **346:** 477–481

Mosbech A, Gibbs-Seymour I, Kagias K, Thorslund T, Beli P, Povlsen L, Nielsen SV, Smedegaard S, Sedgwick G, Lukas C, Hartmann-Petersen R, Lukas J, Choudhary C, Pocock R, Bekker-Jensen S & Mailand N (2012) DVC1 (C1orf124) is a DNA damage-targeting p97 adaptor that promotes ubiquitin-dependent responses to replication blocks. *Nature structural & molecular biology* **19:** 1084–1092

Mouysset J, Deichsel A, Moser S, Hoege C, Hyman AA, Gartner A & Hoppe T (2008) Cell cycle progression requires the CDC-48UFD-1/NPL-4 complex for efficient DNA replication. *Proceedings of the National Academy of Sciences of the United States of America* **105:** 12879–12884

Moyer SE, Lewis PW & Botchan MR (2006) Isolation of the Cdc45/Mcm2-7/GINS (CMG) complex, a candidate for the eukaryotic DNA replication fork helicase. *Proceedings of the National Academy of Sciences* **103:** 10236–10241

Nadeau M, Rico C, Tsoi M, Vivancos M, Filimon S, Paquet M & Boerboom D (2015) Pharmacological targeting of valosin containing protein (VCP) induces DNA damage and selectively kills canine lymphoma cells. *BMC cancer* **15:** 479

Nie M, Aslanian A, Prudden J, Heideker J, Vashisht AA, Wohlschlegel JA, Yates JR & Boddy MN (2012) Dual Recruitment of Cdc48 (p97)-Ufd1-Npl4 Ubiquitin-selective Segregase by Small Ubiquitin-like Modifier Protein (SUMO) and Ubiquitin in SUMO-targeted Ubiquitin Ligase-mediated Genome Stability Functions. *Journal of Biological Chemistry* **287:** 29610–29619

Nishitani H, Sugimoto N, Roukos V, Nakanishi Y, Saijo M, Obuse C, Tsurimoto T, Nakayama KI, Nakayama K, Fujita M, Lygerou Z & Nishimoto T (2006) Two E3 ubiquitin ligases, SCF-Skp2 and DDB1-Cul4, target human Cdt1 for proteolysis. *EMBO J* **25:** 1126–1136

Nishiyama A, Frappier L & Mechali M (2011) MCM-BP regulates unloading of the MCM2-7 helicase in late S phase. *Genes & Development* **25:** 165–175

Niwa H, Ewens CA, Tsang C, Yeung HO, Zhang X & Freemont PS (2012) The Role of the N-Domain in the ATPase Activity of the Mammalian AAA ATPase p97/VCP. *Journal of Biological Chemistry* **287:** 8561–8570

Noi K, Yamamoto D, Nishikori S, Arita-Morioka K, Kato T, Ando T & Ogura T (2013) High-Speed Atomic Force Microscopic Observation of ATP-Dependent Rotation of the AAA+ Chaperone p97. *Structure* **21:** 1992–2002

Nurse P (2000) A Long Twentieth Century of the Cell Cycle and Beyond. *Cell* **100:** 71–78

Nyberg KA, Michelson RJ, Putnam CW & Weinert TA (2002) Toward Maintaining the Genome: DNA Damage and Replication Checkpoints. *Annu. Rev. Genet.* **36:** 617–656

O'Connell MJ (1997) Chk1 is a wee1 kinase in the G2 DNA damage checkpoint inhibiting cdc2 by Y15 phosphorylation. *The EMBO Journal* **16:** 545–554

Ohh M, Park CW, Ivan M, Hoffman MA, Kim TY, Huang LE, Pavletich N, Chau V & Kaelin WG (2000) Ubiquitination of hypoxia-inducible factor requires direct binding to the beta-domain of the von Hippel-Lindau protein. *Nature cell biology* **2:** 423-427

Olzmann JA, Richter CM & Kopito RR (2013) Spatial regulation of UBXD8 and p97/VCP controls ATGL-mediated lipid droplet turnover. *Proceedings of the National Academy of Sciences* **110:** 1345–1350

Ossareh-Nazari B, Bonizec M, Cohen M, Dokudovskaya S, Delalande F, Schaeffer C, van Dorsselaer A & Dargemont C (2010) Cdc48 and Ufd3, new partners of the ubiquitin protease Ubp3, are required for ribophagy. *EMBO Rep* **11:** 548–554

Pacek M, Tutter AV, Kubota Y, Takisawa H & Walter JC (2006) Localization of MCM2-7, Cdc45, and GINS to the Site of DNA Unwinding during Eukaryotic DNA Replication. *Molecular cell* **21:** 581–587

Park S, Isaacson R, Kim HT, Silver PA & Wagner G (2005) Ufd1 Exhibits the AAA-ATPase Fold with Two Distinct Ubiquitin Interaction Sites. *Structure* **13:** 995–1005

Partridge JJ, Lopreiato JO Jr, Latterich M & Indig FE (2003) DNA damage modulates nucleolar interaction of the Werner protein with the AAA ATPase p97/VCP. *Molecular Biology of the Cell* **14:** 4221-4229

Parzych K, Chinn TM, Chen Z, Loaiza S, Porsch F, Valbuena GN, Kleijnen MF, Karadimitris A, Gentleman E, Keun HC & Auner HW (2015) Inadequate fine-tuning of protein synthesis and failure of amino acid homeostasis following inhibition of the ATPase VCP/p97. *Cell death & disease* **6:** e2031

Patil M, Pabla N & Dong Z (2013) Checkpoint kinase 1 in DNA damage response and cell cycle regulation. *Cell. Mol. Life Sci.* **70:** 4009–4021

Pause A, Lee S, Worrell RA, Chen DY, Burgess WH, Linehan WM & Klausner RD (1997) The von Hippel-Lindau tumor-suppressor gene product forms a stable complex with human CUL-2, a member of the Cdc53 family of proteins*. Proceedings of the National Academy of Sciences* **94:** 2156-2161

Peng J, Schwartz D, Elias JE, Thoreen CC, Cheng D, Marsischky G, Roelofs J, Finley D & Gygi SP (2003) A proteomics approach to understanding protein ubiquitination. *Nat Biotech* **21:** 921–926

Peters JM, Franke WW & Kleinschmidt JA (1994) Distinct 19 S and 20 S subcomplexes of the 26 S proteasome and their distribution in the nucleus and the cytoplasm. *J. Biol. Chem.* **269:** 7709–7718

Petroski MD & Deshaies RJ (2005) Function and regulation of cullin–RING ubiquitin ligases. *Nat Rev Mol Cell Biol* **6:** 9–20

Polucci P, Magnaghi P, Angiolini M, Asa D, Avanzi N, Badari A, Bertrand J, Casale E, Cauteruccio S, Cirla A, Cozzi L, Galvani A, Jackson PK, Liu Y, Magnuson S, Malgesini B, Nuvoloni S, Orrenius C, Sirtori FR & Riceputi L et al (2013) Alkylsulfanyl-1,2,4-triazoles, a new class of allosteric valosine containing protein inhibitors. Synthesis and structure-activity relationships. *Journal of medicinal chemistry* **56:** 437–450

Prakash S (2002) Translesion DNA synthesis in eukaryotes: A one- or two-polymerase affair. *Genes & Development* **16:** 1872–1883

Prakash S, Johnson RE & Prakash L (2005) Eukaryotic translesion synthesis DNA polymerases: Specificity of structure and function. *Annu. Rev. Biochem.* **74:** 317–353

Puumalainen M, Lessel D, Rüthemann P, Kaczmarek N, Bachmann K, Ramadan K & Naegeli H (2014) Chromatin retention of DNA damage sensors DDB2 and XPC through loss of p97 segregase causes genotoxicity. *Nat Comms* **5**

Pye VE, Beuron F, Keetch CA, McKeown C, Robinson CV, Meyer HH, Zhang X & Freemont PS (2007) Structural insights into the p97-Ufd1-Npl4 complex. *Proceedings of the National Academy of Sciences* **104:** 467–472

Ramadan K, Bruderer R, Spiga FM, Popp O, Baur T, Gotta M & Meyer HH (2007) Cdc48/p97 promotes reformation of the nucleus by extracting the kinase Aurora B from chromatin. *Nature* **450:** 1258–1262

Ramadan K (2012) p97/VCP- and Lys48-linked polyubiquitination form a new signaling pathway in DNA damage response. *Cell cycle (Georgetown, Tex.)* **11:** 1062–1069

Raman M, Havens CG, Walter JC & Harper JW (2011) A genome-wide screen identifies p97 as an essential regulator of DNA damage-dependent CDT1 destruction. *Molecular cell* **44:** 72–84

Raman M, Sergeev M, Garnaas M, Lydeard JR, Huttlin EL, Goessling W, Shah JV & Harper JW (2015) Systematic proteomics of the VCP-UBXD adaptor network identifies a role for UBXN10 in regulating ciliogenesis. *Nature cell biology* **17:** 1356-1369

Ramanathan HN & Ye Y (2011) Revoking the Cellular License to Replicate: Yet Another AAA Assignment. *Molecular cell* **44:** 3–4

Rape M, Hoppe T, Gorr I, Kalocay M, Richly H & Jentsch S (2001) Mobilization of Processed, Membrane-Tethered SPT23 Transcription Factor by CDC48UFD1/NPL4, a Ubiquitin-Selective Chaperone. *Cell* **107:** 667–677

Reyes-Turcu FE, Ventii KH & Wilkinson KD (2009) Regulation and Cellular Roles of Ubiquitin-Specific Deubiquitinating Enzymes. *Annu. Rev. Biochem.* **78:** 363–397

Richly H, Rape M, Braun S, Rumpf S, Hoege C & Jentsch S (2005) A Series of Ubiquitin Binding Factors Connects CDC48/p97 to Substrate Multiubiquitylation and Proteasomal Targeting. *Cell* **120:** 73–84

Riemer A, Dobrynin G, Dressler A, Bremer S, Soni A, Iliakis G & Meyer H (2014) The p97-Ufd1-Npl4 ATPase complex ensures robustness of the G2/M checkpoint by facilitating CDC25A degradation. *Cell cycle (Georgetown, Tex.)* **13:** 919–927

Ritz D, Vuk M, Kirchner P, Bug M, Schütz S, Hayer A, Bremer S, Lusk C, Baloh RH, Lee H, Glatter T, Gstaiger M, Aebersold R, Weihl CC & Meyer H (2011) Endolysosomal sorting of ubiquitylated caveolin-1 is regulated by VCP and UBXD1 and impaired by VCP disease mutations. *Nat Cell Biol* **13:** 1116–1123

Rothballer A, Tzvetkov N & Zwickl P (2007) Mutations in p97/VCP induce unfolding activity. *FEBS Letters* **581:** 1197–1201

Rotin D & Kumar S (2009) Physiological functions of the HECT family of ubiquitin ligases. *Nat Rev Mol Cell Biol* **10:** 398–409

Rouiller I, DeLaBarre B, May AP, Weis WI, Brunger AT, Milligan RA & Wilson-Kubalek EM (2002) Conformational changes of the multifunction p97 AAA ATPase during its ATPase cycle. *Nat Struct Biol* **9:** 950–957

Rumpf S & Jentsch S (2006) Functional Division of Substrate Processing Cofactors of the Ubiquitin-Selective Cdc48 Chaperone. *Molecular cell* **21:** 261–269

Rumpf S, Lee SB, Jan LY & Jan YN (2011) Neuronal remodeling and apoptosis require VCP-dependent degradation of the apoptosis inhibitor DIAP1. *Development* **138:** 1153–1160

Saha A & Deshaies RJ (2008) Multimodal Activation of the Ubiquitin Ligase SCF by Nedd8 Conjugation. *Molecular cell* **32:** 21–31

Saifee NH & Zheng N (2008) A Ubiquitin-like Protein Unleashes Ubiquitin Ligases. *Cell* **135:** 209–211

Sale JE, Lehmann AR & Woodgate R (2012) Y-family DNA polymerases and their role in tolerance of cellular DNA damage. *Nat Rev Mol Cell Biol* **13:** 141–152

Sancar A, Lindsey-Boltz LA, Ünsal-Kaçmaz K & Linn S (2004) Molecular mechanisms of DNA repair and the DNA damage checkpoints. *Annu. Rev. Biochem.* **73:** 39–85

Sasagawa Y, Otani M, Higashitani N, Higashitani A, Sato K, Ogura T & Yamanaka K (2009) Caenorhabditis elegans p97 controls germline-specific sex determination by controlling the TRA-1 level in a CUL-2-dependent manner. *Journal of Cell Science* **122:** 3663–3672

Sasagawa Y, Higashitani A, Urano T, Ogura T & Yamanaka K (2012) CDC-48/p97 is required for proper meiotic chromosome segregation via controlling AIR-2/Aurora B kinase localization in Caenorhabditis elegans. *Journal of Structural Biology* **179:** 104–111

Schuberth C, Richly H, Rumpf S & Buchberger A (2004) Shp1 and Ubx2 are adaptors of Cdc48 involved in ubiquitin-dependent protein degradation. *EMBO Rep* **5:** 818-824

Schuberth C & Buchberger A (2008) UBX domain proteins: Major regulators of the AAA ATPase Cdc48/p97. *Cell. Mol. Life Sci.* **65:** 2360–2371

Sclafani RA & Holzen TM (2007) Cell Cycle Regulation of DNA Replication. *Annu. Rev. Genet.* **41:** 237–280

Scrima A, Konícková R, Czyzewski BK, Kawasaki Y, Jeffrey PD, Groisman R, Nakatani Y, Iwai S, Pavletich NP & Thomä NH (2008) Structural basis of UV DNA-damage recognition by the DDB1-DDB2 complex. *Cell* **135:** 1213–1223

Shcherbik N & Haines DS (2007) Cdc48pNpl4p/Ufd1p Binds and Segregates Membrane-Anchored/Tethered Complexes via a Polyubiquitin Signal Present on the Anchors. *Molecular cell* **25:** 385–397

Shiloh Y (2001) ATM and ATR: Networking cellular responses to DNA damage. *Current Opinion in Genetics & Development* **11:** 71–77

Shiyanov P, Nag A & Raychaudhuri P (1999) Cullin 4A Associates with the UV-damaged DNA-binding Protein DDB. *Journal of Biological Chemistry* **274:** 35309–35312

Silverman JS, Skaar JR & Pagano M (2012) SCF ubiquitin ligases in the maintenance of genome stability. *Trends in biochemical sciences* **37:** 66–73

Skaar JR, Pagan JK & Pagano M (2009) SnapShot: F Box Proteins I. *Cell* **137:** 1160-1160.e1

Smith DM, Kafri G, Cheng Y, Ng D, Walz T & Goldberg AL (2005) ATP Binding to PAN or the 26S ATPases Causes Association with the 20S Proteasome, Gate Opening, and Translocation of Unfolded Proteins. *Molecular cell* **20:** 687–698

Smith DM, Chang S, Park S, Finley D, Cheng Y & Goldberg AL (2007) Docking of the Proteasomal ATPases' Carboxyl Termini in the 20S Proteasome's α Ring Opens the Gate for Substrate Entry. *Molecular cell* **27:** 731–744

Song C, Wang Q, Song C & Rogers TJ (2015) Valosin-containing protein (VCP/p97) is capable of unfolding polyubiquitinated proteins through its ATPase domains. *Biochemical and biophysical research communications* **463:** 453–457

Soucy TA, Smith PG & Rolfe M (2009) Targeting NEDD8-Activated Cullin-RING Ligases for the Treatment of Cancer. *Clinical Cancer Research* **15:** 3912–3916

Sowa ME, Bennett EJ, Gygi SP & Harper JW (2009) Defining the Human Deubiquitinating Enzyme Interaction Landscape. *Cell* **138:** 389–403

Stewart S (2005) Destruction Box-Dependent Degradation of Aurora B Is Mediated by the Anaphase-Promoting Complex/Cyclosome and Cdh1. *Cancer Research* **65:** 8730–8735

Stingele J, Schwarz MS, Bloemeke N, Wolf PG & Jentsch S (2014) A DNA-Dependent Protease Involved in DNA-Protein Crosslink Repair. *Cell* **158:** 327–338

Stingele J, Habermann B & Jentsch S (2015) DNA-protein crosslink repair: proteases as DNA repair enzymes. *Trends in biochemical sciences* **40:** 67–71

Sugasawa K, Okuda Y, Saijo M, Nishi R, Matsuda N, Chu G, Mori T, Iwai S, Tanaka K, Tanaka K & Hanaoka F (2005) UV-Induced Ubiquitylation of XPC Protein Mediated by UV-DDB-Ubiquitin Ligase Complex. *Cell* **121:** 387–400

Sumara I, Quadroni M, Frei C, Olma MH, Sumara G, Ricci R & Peter M (2007) A Cul3-Based E3 Ligase Removes Aurora B from Mitotic Chromosomes, Regulating Mitotic Progression and Completion of Cytokinesis in Human Cells. *Developmental Cell* **12:** 887–900

Svejstrup JQ (2002) Mechanisms of transcription-coupled DNA repair. *Nat. Rev. Mol. Cell Biol.* **3:** 21–29

Tanaka A, Cleland MM, Xu S, Narendra DP, Suen D, Karbowski M & Youle RJ (2010) Proteasome and p97 mediate mitophagy and degradation of mitofusins induced by Parkin. *J Cell Biol* **191:** 1367–1380

Tanaka S & Araki H (2013) Helicase Activation and Establishment of Replication Forks at Chromosomal Origins of Replication. *Cold Spring Harbor Perspectives in Biology* **5:** a010371-a010371

Tang J, Erikson RL & Liu X (2006) Checkpoint kinase 1 (Chk1) is required for mitotic progression through negative regulation of polo-like kinase 1 (Plk1). *Proceedings of the National Academy of Sciences* **103:** 11964–11969

Thrower JS (2000) Recognition of the polyubiquitin proteolytic signal. *The EMBO Journal* **19:** 94–102

Tonddast-Navaei S & Stan G (2013) Mechanism of Transient Binding and Release of Substrate Protein during the Allosteric Cycle of the p97 Nanomachine. *J. Am. Chem. Soc.* **135:** 14627–14636

Tresse E, Salomons FA, Vesa J, Bott LC, Kimonis V, Yao TP, Dantuma NP & Taylor JP (2010) VCP/p97 is essential for maturation of ubiquitin-containing autophagosomes and this function is impaired by mutations that cause IBMPFD. *Autophagy* **6:** 217-227

Trusch F, Matena A, Vuk M, Koerver L, Knævelsrud H, Freemont PS, Meyer H & Bayer P (2015) The N-terminal Region of the Ubiquitin Regulatory X (UBX) Domain-containing Protein 1 (UBXD1) Modulates Interdomain Communication within the Valosin-containing Protein p97. *J. Biol. Chem.* **290:** 29414–29427

Uchiyama K (2002) VCIP135, a novel essential factor for p97/p47-mediated membrane fusion, is required for Golgi and ER assembly in vivo. *The Journal of cell biology* **159:** 855–866

Valle CW, Min T, Bodas M, Mazur S, Begum S, Tang D & Vij N (2011) Critical role of VCP/p97 in the pathogenesis and progression of non-small cell lung carcinoma. *PloS one* **6:** e29073

Verhoef LG, Heinen C, Selivanova A, Halff EF, Salomons FA & Dantuma NP (2008) Minimal length requirement for proteasomal degradation of ubiquitin-dependent substrates. *The FASEB Journal* **23:** 123–133

Verma R, Oania R, Graumann J & Deshaies RJ (2004) Multiubiquitin Chain Receptors Define a Layer of Substrate Selectivity in the Ubiquitin-Proteasome System. *Cell* **118:** 99–110

Verma R, Oania R, Fang R, Smith GT & Deshaies RJ (2011) Cdc48/p97 mediates UV-dependent turnover of RNA Pol II. *Molecular cell* **41:** 82–92

Verma R, Oania RS, Kolawa NJ & Deshaies RJ (2013) Cdc48/p97 promotes degradation of aberrant nascent polypeptides bound to the ribosome. *eLife* **2:** 4114

Vij N (2008) AAA ATPase p97/VCP: Cellular functions, disease and therapeutic potential. *Journal of Cellular and Molecular Medicine* **12:** 2511–2518

Vilenchik MM & Knudson AG (2011) Endogenous DNA double-strand breaks: Production, fidelity of repair, and induction of cancer. *Proceedings of the National Academy of Sciences* **100:** 12871–12876

Voges D, Zwickl P & Baumeister W (1999) THE 26S PROTEASOME: A Molecular Machine Designed for Controlled Proteolysis. *Annu. Rev. Biochem.* **68:** 1015–1068

Vong QP (2005) Chromosome Alignment and Segregation Regulated by Ubiquitination of Survivin. *Science* **310:** 1499–1504

Wakasugi M, Kawashima A, Morioka H, Linn S, Sancar A, Mori T, Nikaido O & Matsunaga T (2002) DDB Accumulates at DNA Damage Sites Immediately after UV Irradiation and Directly Stimulates Nucleotide Excision Repair. *J. Biol. Chem.* **277:** 1637–1640

Wang Q, Song C & Li CH (2003) Hexamerization of p97-VCP is promoted by ATP binding to the D1 domain and required for ATPase and biological activities. *Biochemical and biophysical research communications* **300:** 253–260

Wang Y, Satoh A, Warren G & Meyer HH (2004) VCIP135 acts as a deubiquitinating enzyme during p97–p47-mediated reassembly of mitotic Golgi fragments. *J Cell Biol* **164:** 973–978

Wang H, Zhai L, Xu J, Joo H, Jackson S, Erdjument-Bromage H, Tempst P, Xiong Y & Zhang Y (2006) Histone H3 and H4 Ubiquitylation by the CUL4-DDB-ROC1 Ubiquitin Ligase Facilitates Cellular Response to DNA Damage. *Molecular cell* **22:** 383–394

Wang Q, Li L & Ye Y (2008) Inhibition of p97-dependent protein degradation by Eeyarestatin I. *The Journal of biological chemistry* **283:** 7445–7454

Wang Q, Mora-Jensen H, Weniger MA, Perez-Galan P, Wolford C, Hai T, Ron D, Chen W, Trenkle W, Wiestner A & Ye Y (2009) ERAD inhibitors integrate ER stress with an epigenetic mechanism to activate BH3-only protein NOXA in cancer cells. *Proceedings of the National Academy of Sciences of the United States of America* **106:** 2200–2205

Wang Q, Shinkre BA, Lee J, Weniger MA, Liu Y, Chen W, Wiestner A, Trenkle WC & Ye Y (2010) The ERAD inhibitor Eeyarestatin I is a bifunctional compound with a membrane-binding domain and a p97/VCP inhibitory group. *PloS one* **5:** e15479

Wang J, Qian J, Hoeksema MD, Zou Y, Espinosa AV, Rahman SMJ, Zhang B & Massion PP (2013) Integrative genomics analysis identifies candidate drivers at 3q26-29 amplicon in squamous cell carcinoma of the lung. *Clinical cancer research : an official journal of the American Association for Cancer Research* **19:** 5580–5590

Watanabe N, Arai H, Iwasaki J, Shiina M, Ogata K, Hunter T & Osada H (2005) Cyclin-dependent kinase (CDK) phosphorylation destabilizes somatic Wee1 via multiple pathways. *Proceedings of the National Academy of Sciences* **102:** 11663–11668

Watson JD & Crick FH (1953) Molecular structure of nucleic acids. A structure for deoxyribose nucleic acid. *Nature* **171:** 737-8.

Watts GD, Wymer J, Kovach MJ, Mehta SG, Mumm S, Darvish D, Pestronk A, Whyte MP & Kimonis VE (2004) Inclusion body myopathy associated with Paget disease of bone and frontotemporal dementia is caused by mutant valosin-containing protein. *Nature genetics* **36:** 377-381

Weihl CC, Pestronk A & Kimonis VE (2009) Valosin-containing protein disease: Inclusion body myopathy with Paget's disease of the bone and fronto-temporal dementia. *Neuromuscular Disorders* **19:** 308–315

Wilcox AJ & Laney JD (2009) A ubiquitin-selective AAA-ATPase mediates transcriptional switching by remodelling a repressor–promoter DNA complex. *Nat Cell Biol* **11:** 1481–1486

Wild P & Dikic I (2010) Mitochondria get a Parkin' ticket. *Nat Cell Biol* **12:** 104–106

Wilson MD, Harreman M, Taschner M, Reid J, Walker J, Erdjument-Bromage H, Tempst P & Svejstrup JQ (2013) Proteasome-Mediated Processing of Def1, a Critical Step in the Cellular Response to Transcription Stress. *Cell* **154:** 983–995

Wittschieben BO (2005) DDB1-DDB2 (Xeroderma Pigmentosum Group E) Protein Complex Recognizes a Cyclobutane Pyrimidine Dimer, Mismatches, Apurinic/Apyrimidinic Sites, and Compound Lesions in DNA. *Journal of Biological Chemistry* **280:** 39982–39989

Xie Y, Rubenstein EM, Matt T & Hochstrasser M (2010) SUMO-independent in vivo activity of a SUMO-targeted ubiquitin ligase toward a short-lived transcription factor. *Genes & Development* **24:** 893–903

Xu B & Kastan MB (2004) Analyzing cell cycle checkpoints after ionizing radiation. *Methods in molecular biology* **281:** 283-292

Xu S, Peng G, Wang Y, Fang S & Karbowski M (2011) The AAA-ATPase p97 is essential for outer mitochondrial membrane protein turnover. *Molecular Biology of the Cell* **22:** 291–300

Yamanaka K, Sasagawa Y & Ogura T (2012) Recent advances in p97/VCP/Cdc48 cellular functions. *Biochimica et Biophysica Acta (BBA) - Molecular Cell Research* **1823:** 130–137

Yardimci H, Loveland AB, Habuchi S, van Oijen AM & Walter JC (2010) Uncoupling of Sister Replisomes during Eukaryotic DNA Replication. *Molecular cell* **40:** 834–840

Yardimci H & Walter JC (2014) Prereplication-complex formation: A molecular double take? *Nat Struct Mol Biol* **21:** 20–25

Ye Y, Meyer HH & Rapoport TA (2003) Function of the p97–Ufd1–Npl4 complex in retrotranslocation from the ER to the cytosol. *J Cell Biol* **162:** 71–84

Ye Y (2006) Diverse functions with a common regulator: Ubiquitin takes command of an AAA ATPase. *Journal of Structural Biology* **156:** 29–40

Yeh JI, Levine AS, Du S, Chinte U, Ghodke H, Wang H, Shi H, Hsieh CL, Conway JF, van Houten B & Rapic-Otrin V (2012) Damaged DNA induced UV-damaged DNA-binding protein (UV-DDB) dimerization and its roles in chromatinized DNA repair. *Proceedings of the National Academy of Sciences* **109:** E2737-E2746

Yeung HO, Kloppsteck P, Niwa H, Isaacson RL, Matthews S, Zhang X & Freemont PS (2008) Insights into adaptor binding to the AAA protein p97. *Biochm. Soc. Trans.* **36:** 62–67

Yeung HO, Forster A, Bebeacua C, Niwa H, Ewens C, McKeown C, Zhang X & Freemont PS (2014) Inter-ring rotations of AAA ATPase p97 revealed by electron cryomicroscopy. *Open Biology* **4:** 130142

Zhang X, Zhang H & Wang Y (2013) Phosphorylation regulates VCIP135 function in Golgi membrane fusion during the cell cycle. *Journal of Cell Science* **127:** 172–181

Zhang J & Walter JC (2014) Mechanism and regulation of incisions during DNA interstrand cross-link repair. *DNA repair* **19:** 135–142

Zhang J, Wan L, Dai X, Sun Y & Wei W (2014) Functional characterization of Anaphase Promoting Complex/Cyclosome (APC/C) E3 ubiquitin ligases in tumorigenesis. *Biochimica et Biophysica Acta (BBA) - Reviews on Cancer* **1845:** 277–293

Zheng N, Schulman BA, Song L, Miller JJ, Jeffrey PD, Wang P, Chu C, Koepp DM, Elledge SJ, Pagano M, Conaway RC, Conaway JW, Harper JW & Pavletich NP (2002) Structure of the Cul1–Rbx1–Skp1–F boxSkp2 SCF ubiquitin ligase complex. *Nature* **416:** 703–709

Zhong W, Feng H, Santiago FE & Kipreos ET (2003) CUL-4 ubiquitin ligase maintains genome stability by restraining DNA-replication licensing. *Nature* **423:** 885–889

Zhou H, Wang J, Yao B, Wong S, Djakovic S, Kumar B, Rice J, Valle E, Soriano F, Menon M, Madriaga A, Kiss von Soly S, Kumar A, Parlati F, Yakes FM, Shawver L, Le Moigne R, Anderson DJ, Rolfe M & Wustrow D (2015) Discovery of a First-in-Class, Potent, Selective, and Orally Bioavailable Inhibitor of the p97 AAA ATPase (CB-5083). *Journal of medicinal chemistry* **58:** 9480–9497

Zhu Q, Wani G, Wang Q, El-mahdy M, Snapka RM & Wani AA (2005) Deubiquitination by proteasome is coordinated with substrate translocation for proteolysis in vivo. *Experimental Cell Research* **307:** 436–451

Acknowledgements

I want to thank…

Prof. Dr. Hemmo Meyer for the opportunity to write my PhD thesis in his laboratory, for providing all resources and for scientific input which helped me to graduate.

the whole Meyer group for a fun time in- and outside the lab. Special thanks to everyone who helped me with experimental methods and software problems or provided me with scientific input.

the GRK1739 for the special training, the extra money and the enjoyable social events.

Ich danke…

meinen Eltern Dr. Raymund und Evelyn Dressler, die mich auf jede erdenkliche Weise bedingungslos unterstützt haben.

meinen Geschwistern Verena und Marius für ihr offenes Ohr und ihre humorvolle, aufbauende Art.

Thomas Petrik für seinen Rat bei Gestaltungs- und Formatierungsfragen und seinen moralischen Beistand.

Danke, liebe Familie, dass ihr immer an mich geglaubt habt.

Curriculum Vitae

Der Lebenslauf ist in der Online-Version aus Gründen des Datenschutzes nicht enthalten.

Der Lebenslauf ist in der Online-Version aus Gründen des Datenschutzes nicht enthalten.

Der Lebenslauf ist in der Online-Version aus Gründen des Datenschutzes nicht enthalten.

Declarations

Erklärung:

Hiermit erkläre ich, gem. § 6 Abs. 2, f der Promotionsordnung der Math.-Nat. Fakultäten zur Erlangung des Dr. rer. nat., dass ich das Arbeitsgebiet, dem das Thema „The AAA-ATPase p97 and its cofactors in regulatory degradation of substrate proteins after DNA damage or replication stress“ zuzuordnen ist, in Forschung und Lehre vertrete und den Antrag von Alina Dressler befürworte.

Essen, den _____ _____

Unterschrift eines Mitglieds
der Universität Duisburg-Essen

Erklärung:

Hiermit erkläre ich, gem. § 7 Abs. 2, c und e der Promotionsordnung der Math.-Nat. Fakultäten zur Erlangung des Dr. rer. nat., dass ich die vorliegende Dissertation selbständig verfasst und mich keiner anderen als der angegebenen Hilfsmittel bedient habe und alle wörtlich oder inhaltlich übernommenen Stellen als solche gekennzeichnet habe.

Essen, den _____ _____

Unterschrift der Doktorandin

Erklärung:

Hiermit erkläre ich, gem. § 7 Abs. 2, d und f der Promotionsordnung der Math.-Nat. Fakultäten zur Erlangung des Dr. rer. nat., dass ich keine anderen Promotionen bzw. Promotionsversuche in der Vergangenheit durchgeführt habe, dass diese Arbeit von keiner anderen Fakultät abgelehnt worden ist, und dass ich die Dissertation nur in diesem Verfahren einreiche.

Essen, den _____ _____

Unterschrift des Doktoranden